

# Aberrant Ras/MAPK signaling in skeletal development

by

Simona Nedelcu

B.S. Biology  
California Institute of Technology, 2007

Submitted to the Department of Biology in Partial Fulfillment of the Requirements  
for the Degree of

DOCTOR OF PHILOSOPHY

at the

MASSACHUSETTS INSTITUTE OF TECHNOLOGY

September 2013

© 2013 Massachusetts Institute of Technology. All rights reserved

Signature of Author \_\_\_\_\_  
Department of Biology  
July 30<sup>th</sup>, 2013

Certified by \_\_\_\_\_  
Jacqueline A. Lees  
Professor of Biology  
Thesis Supervisor

Accepted by \_\_\_\_\_  
Stephen P. Bell  
Professor of Biology  
Chairman, Graduate Committee

# Aberrant Ras/MAPK signaling in skeletal development

## ABSTRACT

The Mitogen-activated protein kinase (MAPK) signaling pathway has been studied intensively in the context of neoplastic transformation. Other studies have focused on the roles of this pathway during development and have modeled syndromes, such as Noonan Syndrome (NS), that are caused by aberrant germline Ras/MAPK signaling. One hallmark of these developmental syndromes is a defect in the skeletal development of the patients. However, the *in vivo* role of MAPK signaling during bone development is still controversial, with some studies supporting a positive role of the MAPK pathway during this process, and others arguing for a suppressive role. To analyze in depth the bone defects caused by aberrant K-ras/MAPK signaling during development and to understand how bone mass is regulated via K-ras/MAPK control of osteoblast differentiation we have generated two novel mouse models. Specifically, to investigate how hyperactive K-ras affects skeletal development when expressed in a spatial and temporal specific manner we activated K-ras<sup>G12D</sup> at various stages during limb development, either in all mesenchymal lineages (*Prx1-Cre;K-ras<sup>G12D</sup>* mutants), or specifically in the osteoblasts (*Osx1-Cre;K-ras<sup>G12D</sup>*). The *Prx1-Cre;K-ras<sup>G12D</sup>* mutant mice display greatly shortened and thickened bones that mirror the defects found in patients with NS. We determined that this bone defect appears during embryogenesis around E14.5 and is distinguished by impairment in formation of the bone collar. Furthermore, we describe a treatment strategy that rescues the skeletal phenotype, and identify a narrow developmental time window, where *in utero* treatment with MEK inhibitor is sufficient to completely rescue the bone phenotype. The *Osx1-Cre;K-ras<sup>G12D</sup>* mutant mice allowed us to activate expression of hyperactive K-ras in the osteoblast population at different times during the development of the organism. Using this model, we defined two time windows when expression of active K-ras results in opposing bone phenotypes in the mutant mice. In the first time window (approximately between E11.5 and E14.5) induction of active K-ras<sup>G12D</sup> in osteoblast precursors impairs terminal differentiation and leads to profound bone loss. In the second time window, activation of K-ras<sup>G12D</sup> at birth acts to promote osteoblast differentiation and consequently long bone mineralization. Taken together, our data has revealed a critical involvement of K-ras/MAPK signaling in osteoblast differentiation during skeletal development, in embryogenesis and after birth. They also show how the MAPK pathway can be modulated chemically to rescue the skeletal defects seen in a mouse model for NS. These findings yield insight into diseases of the bone, including both developmental syndromes caused by aberrant MAPK activation, such as NS, and diseases characterized by an imbalance in the bone mass, such as osteoporosis.

Thesis Supervisor: Jacqueline A. Lees

Title: Professor of Biology

## SIMONA NEDELCO

Koch Institute of Integrative Cancer Research, MIT  
Dr. Jacqueline Lees Laboratory  
56 Linnaean St, Cambridge, MA 02138  
[tescu@mit.edu](mailto:tescu@mit.edu), 857-499-0050

### EDUCATION

- Massachusetts Institute of Technology, Cambridge, MA 2008 – Present
- PhD candidate in Biology, Department of Biology,
- California Institute of Technology, Pasadena, CA 2004 – 2007
- BS with Honors, Biology

### RESEARCH EXPERIENCE

- Professor Jacqueline A. Lees, MIT, Cambridge, MA June 09 – Aug 13
- PhD Candidate
  - Thesis Title: Aberrant Ras/MAPK signaling in skeletal development
- Professor Robert H. Horvitz, MIT, Cambridge, MA July 07 – Aug 08
- Research Technician
  - Project: Identification of genes that control aging in *C. elegans*
- Professor Paul H. Patterson, Caltech, Pasadena, CA Jan 06 – June 07
- Undergraduate Research Fellow
  - Project: IKK $\gamma$  and mutant huntingtin regulation of Pleiotrophin expression in neuronal models of Huntington's Disease
- Professor Henry A. Lester, Caltech, Pasadena, CA March 05 – Dec 05
- Undergraduate Research Fellow
  - Project: Electrophysiology and fluorescence studies of the muscle nicotinic receptors

### PUBLICATIONS

Hilgendorf KI, Leshchiner ES, **Nedelcu S**, Maynard MA, Calo E, Ianari A, Walensky LD, Lees JA. "The retinoblastoma protein induces apoptosis directly at the mitochondria." *Genes Dev.* 2013 May 1; 27(9): 1003-15.

Berdichevsky A, **Nedelcu S**, Boulias K, Bishop N, Guarente L, and Horvitz RH. "3-Ketoacyl thiolase delays aging of *C. elegans* and is required for longevity mediated by sir-2.1" *PNAS* 2010 Nov 2; 107(44): 18927-32

Calo E, Quintero JA, Danielian PS, **Nedelcu S**, Berman SD and Lees JA. "Rb regulates fate choice and lineage commitment *in vivo*". *Nature* 2010 Aug 26; 466(7310): 1110-4.

Khoshnan A, Ko J, **Tescu S\***, Brundin P, Patterson PH. "IKKalpha and IKKbeta regulation of DNA damage-induced cleavage of huntingtin", *PLoS One*. 2009 Jun 2; 4(6): e5768.

\*Publications before July 2009 appear under my maiden name: Simona Tescu

## PRESENTATIONS

Nedelcu S, Lees JA. Activation of MAPK signaling pathway disrupts normal bone development in mice. Colrain Meeting, Colrain, MA (2012) *Oral Presentation*

Nedelcu S, Lees JA. Stage-Specific Effects of Activating Oncogenic K-ras on Mesenchymal Development and Tumorigenesis. Mechanisms and Models of Cancer, Cold Spring Harbor (2012) *Poster Presentation*

Nedelcu S, Lees JA. Consequences of activating oncogenic K-ras during bone development. Koch Institute Focus Seminar Series, Cambridge, MA (2011) *Oral Presentation*

Nedelcu S, Lees JA. Effects of Activating Oncogenic K-ras During Skeletal Formation and Mesenchymal Lineage Specification. Koch Institute Retreat, MA (2011) *Poster Presentation*

Nedelcu S, Stanciu M, Calo E, Lees JA. Understanding the Mechanisms of Osteosarcoma Formation and Metastasis. Ludwig Retreat, MIT Endicott House, MA (2011) *Poster Presentation*

## TEACHING EXPERIENCE

Introduction to Genetics, Genomics and Evolution (Life Sciences 1b), Harvard University	Spring 12, 13
Chemistry, Molecular Biology, and Cell Biology (Life Sciences 1a), Harvard University	Fall 11, 12
Principles of Human Disease (7.27), MIT	Spring 2012
Undergraduate Biochemistry – Head TA (7.05), MIT	Spring 2010
Undergraduate Biochemistry (7.05), MIT	Spring 2008

## **AWARDS**

Koch Graduate Fellowship Award, MIT	2011 – 2012
Gene Brown-Merck Teaching Award, MIT	July 2010
Lester Wolfe Graduate Fellowship, MIT	2009 – 2011
Graduate Education in Medical Sciences (GEMS) Fellow, HST, MIT	2009 – 2011
Praecis Presidential Graduate Fellow, MIT	2008 – 2009

## **EXTRACURRICULAR/ LEADERSHIP ACTIVITIES**

Graduate Resident Tutor in Pforzheimer House, Harvard	2011 – Present
BioREF (with certificate in mediation training), MIT	2010 – 2013
Romanian Student Association President, MIT	2009 – 2011
Academics, Research and Careers Committee Co-Chair, Graduate Student Council, MIT	2010 – 2011
Diversity Task Force Co-Chair, Graduate Student Council, MIT	2009 – 2010

## ACKNOWLEDGEMENTS

I have numerous people to thank for their support, friendship, and mentorship during my graduate work. I would like to express my gratitude to...

...my thesis advisor, Jackie for constant support and guidance. Since day one she has been very enthusiastic about instilling a love for science in me. I am grateful for the time and energy she spent guiding and teaching me how to think, write and communicate more clearly, and how to do better science. She has been an incredible mentor and teacher, and I am grateful to have completed my PhD studies in her laboratory.

...my committee meeting members, Tyler Jacks and Mike Hemman for their guidance and helpful advice over the years during my committee meetings, and for always keeping me on track with my project.

...Prof. Kronenberg, for opening the doors to his lab to me to help me navigate through the world of bone research, for allowing me to join his lab meetings and for always offering great advice. Also, I would like to thank him for agreeing to participate in my thesis defense.

...my lab mates for being my family away from home. I would especially want to thank Tiziana Parisi and Keren Hilgendorf, not only being great lab mates, but also for being the best friends somebody could ask for.

...my family, for loving and supporting me unconditionally, even from 6k miles away.

...my high school chemistry professor, for instilling in me a passion for science and encouraging me to participate in chemistry Olympiads. If it weren't for my participation and awards in these contests, I could have not come to US to study.

...my husband, for always supporting me and believing in me. Going together through graduate school was challenging, but it brought us even closer. Now, I can't wait to see what our next chapter of life together will bring.

## **DEDICATION**

I dedicate this thesis to my mother.

I live to honor your memory.

# TABLE OF CONTENTS

<b>ABSTRACT</b> .....	2
<b>CURRICULUM VITAE</b> .....	3
<b>ACKNOWLEDGEMENTS</b> .....	6
<b>DEDICATION</b> .....	7
<b>TABLE OF CONTENTS</b> .....	8
<b>CHAPTER 1: Introduction</b> .....	10
I. Bone Development.....	11
1. Anatomy and function of the skeleton.....	11
2. Mechanisms of bone formation.....	12
3. Cell lineages involved in bone development.....	16
4. Major signaling pathways involved in bone development.....	21
II. The Ras Oncogenes.....	25
1. Discovery.....	25
2. Ras proteins and the GTPase cycle.....	27
3. Ras downstream signaling pathways – MAPK pathway.....	29
III. MAPK Signaling.....	33
1. MAPK signaling during development – human syndromes.....	33
2. Modeling Noonan Syndrome using animal models .....	39
3. MAPK signaling pathway in skeletal development.....	41
References.....	46
<b>CHAPTER 2: Expression of K-ras<sup>G12D</sup> in mesenchymal lineages leads to Noonan-specific bone defects in mice, which are rescued by treatment with MEK inhibitors</b> .....	57
2.1 Abstract.....	58
2.2 Introduction.....	60
2.3 Results.....	62
2.4 Discussion.....	74
2.5 Supplemental Figures.....	77
2.6 Methods.....	79
2.7 References.....	82
2.8 Acknowledgements.....	85
<b>CHAPTER 3: Expression of K-ras<sup>G12D</sup> in the osteoblast lineage differentially affects osteoblast differentiation in a time-dependent manner</b> .....	86
3.1 Abstract.....	87

3.2 Introduction.....	88
3.3 Results.....	91
3.4 Discussion.....	104
3.5 Supplemental Figures.....	108
3.6 Methods.....	109
3.7 References.....	112
3.8 Acknowledgements.....	115
<b>CHAPTER 4: Discussion.....</b>	<b>116</b>
4.1 Identification of a critical developmental time period during bone development specifically affected by aberrant MAPK signaling.....	119
4.2 K-ras <sup>G12D</sup> activation leads to divergent bone phenotypes when expressed in all mesenchymal lineages versus exclusively in the osteoblast lineage...	122
4.3 K-ras <sup>G12D</sup> activation leads to divergent bone phenotypes when expressed in the osteoblast lineage during development versus after birth.....	124
4.4 K-ras <sup>G12D</sup> affects the fate of osteoblast differentiation in an <i>in vitro</i> setting.....	125
4.5. Generation of novel mouse models to study Noonan Syndrome associated bone defects and potential treatment strategies.....	128
4.6 References.....	130
<b>APPENDIX A: Rb regulates fate choice and lineage commitment <i>in vivo</i>.....</b>	<b>132</b>
<b>APPENDIX B: The retinoblastoma protein induces apoptosis directly at the mitochondria.....</b>	<b>161</b>

# **CHAPTER 1**

## **Introduction**

This thesis presents two novel mouse models in which a constitutive mutation of K-ras is expressed at various stages during limb development. These models are used to investigate how K-ras<sup>G12D</sup> affects skeletal development when expressed in a spatial and temporal specific manner. In this introduction I will review general aspects of bone development, a complex process in which various cell types and several signaling pathways are carefully coordinated to regulate the normal growth of the skeleton. I will also describe the major players and signaling pathways that coordinate bone growth with particular focus on the role of the Ras/ MAPK signaling pathway. Finally, I will discuss developmental syndromes, and mouse models for these diseases, which are caused by abnormal activation of the MAPK pathway during development. In particular I will describe Noonan Syndrome because this thesis describes the generation and analysis of a mouse strain that models the bone defects arising in this disease.

## **PART I. BONE DEVELOPMENT**

### **I.1. Anatomy and function of the skeleton**

The skeleton is a complex organ, consisting of more than 200 skeletal elements, two kinds of tissues (cartilage and bone) and 3 types of cells (chondrocytes, osteoblasts and osteoclasts). The skeleton provides support, offers body shape and, by acting as a protective case, prevents damage of vital organs such as the brain and the spinal cord. Bones are part of specialized joint structures, which work in conjunction with many associated muscles to control specific movements.

They also function as a reservoir for inorganic ions, such as calcium and phosphate, and are important for maintaining blood calcium levels (Harada and Rodan, 2003).

There are two major kinds of bones: cortical bone, making up about 80% of the skeleton, and trabecular or spongy bone, which accounts for the remaining 20%. The cortical bone is thick, solid, and is located on the surface of long bones, such as the femur or tibia. It is also present in flat bones, such as the bones of the skull and the ribs. Its main function is to support body weight and protect internal organs. In contrast, the trabecular bone is localized at the end of the bones that bear weight. It is soft and it is found in vertebrae and the ends (epiphyses) of the long bones. It contains the bone marrow, where hematopoiesis occurs.

Chemically, bones are made up of both inorganic and organic materials. The organic matrix is mainly composed of collagen, the most abundant protein in the body, which forms approximately 10% of the adult bone. Collagen provides flexibility to the skeleton. The mineral component of bones is hydroxyapatite (~65%), an insoluble salt of calcium and phosphorus that represents the inorganic component of the mineralized bone matrix. Bones also contain water (25%) and small amounts of magnesium, sodium and bicarbonate.

## **I.2. Mechanisms of bone formation**

The first step in skeletal formation is skeletal morphogenesis, the process through which Prx expressing mesenchymal progenitors migrate from the cranial neural crest, somites and lateral plate mesoderm to the location of future bones (Zelzer and Olsen, 2003). At these locations mesenchymal progenitors exclude

blood vessels and form cell condensations in the respective matrices, collectively termed the 'membranous skeleton' (Figure 1A).

In mammalian organisms, bone formation occurs through two distinct mechanisms: intramembranous and endochondral ossification. The latter mechanism is used for most bones in the body including all axial and appendicular skeletal elements, such as the long bones, ribs and vertebrae. During this process, condensed mesenchymal precursors give rise to both chondrocytes and osteoblasts. More specifically, the cells located at the center of these mesenchymal condensations will differentiate into chondrocytes and start proliferating (Figure 1B) (Karsenty et al., 2009). These immature proliferative cells secrete a matrix rich in type II collagen (Col2), and form a cartilaginous template that is gradually replaced by bone. Chondrocytes at the center of the template stop proliferating, enlarge and subsequently mature into postmitotic hypertrophic chondrocytes that will undergo apoptosis (Figure 1C). These postmitotic, hypertrophic chondrocytes secrete a matrix rich in type X collagen (ColX) and mineralize the matrix that surrounds them. The death of hypertrophic chondrocytes is followed by vascular invasion and recruitment of Osterix (Osx) expressing osteoblasts (Figure 1D). This results in the formation of a new area of mineralization, the primary spongiosa (PS), in the shaft of long bones where invading osteoblasts secrete an osteoid matrix to form trabecular bone and hematopoietic cells to create bone marrow (Figure 1E). At this location Osx expressing osteoblasts differentiate into committed osteoblasts, which express Col1. These Col1 expressing osteoblasts further differentiate into Osetocalcin (OC) expressing osteoblasts, which will further differentiate to

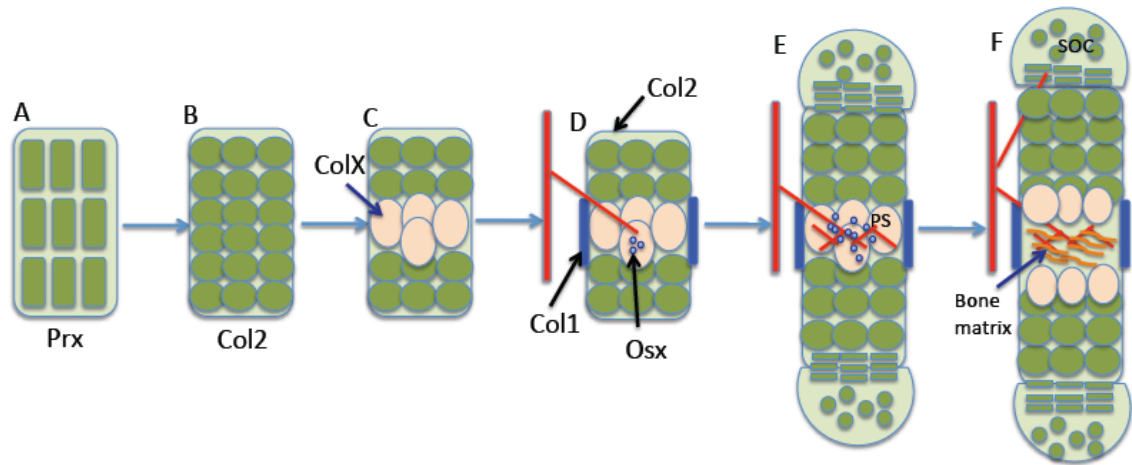


**Figure 1. Schematic representation of endochondral bone formation.** Adapted from Karsenty et al.,(2009). (A) Mesenchymal cells condense and (B) then become Col2 positive chondrocytes, (C) Chondrocytes at the centre of the condensation stop proliferating, become hypertrophic and express ColX (shown in pink). (D) Perichondrial cells adjacent to hypertrophic chondrocytes become Col1 positive osteoblasts, which form the bone collar. (E) Hypertrophic chondrocytes direct the formation of mineralized matrix, attract blood vessels, and undergo apoptosis. (F) Osteoblasts of primary spongiosa accompany vascular invasion, forming the primary spongiosa (ps). Chondrocytes continue to proliferate, lengthening the bone. At the end of the bone, the secondary ossification centre (soc) forms through cycles of chondrocyte hypertrophy, vascular invasion and osteoblast activity.

mature osteoblasts. Some markers that characterize the final stages of osteoblast differentiation are ALP (Alkaline Phosphatase) and BSP (Bone Sialo-Protein).

Concurrently, the cells at the periphery of the chondrocyte template will become the perichondrium (Kronenberg, 2007). The perichondrial cells have specific functions during endochondral ossification. First, they are able to differentiate into either chondrocytes or osteoblasts, which will migrate to the trabecular and cortical bone. Second, they signal back and forth with the underlying cartilage. This specific signaling between the chondrocytes and perichondrial cells causes Col2 expressing chondrocytes to differentiate and mature at the perichondrium into Col1 expressing osteoblasts, which will specifically form the bone collar (Maes et al., 2010) (Figure 1D). As bones grow in size, the secondary ossification centers (SOC) form, usually in the epiphysis of long bones. These regions form through cycles of chondrocyte hypertrophy, vascular invasion and osteoblast activity (Figure 1F). In the long bones, chondrocytes continue to proliferate and cartilage matrix is deposited, causing the bone to grow in length. This process, which starts in embryogenesis, is completed usually at puberty.

The alternate bone differentiation mechanism, intramembranous ossification is used for the cranial flat bones of the skull (frontal, parietal, occipital, and temporal bones) and the clavicles. In this process, condensed mesenchymal precursors differentiate directly into osteoblasts, without a cartilage intermediate. Like endochondral ossification, this process initiates *in utero*, but is completed after birth. Once bones have formed during embryonic development, either through endochondral or intramembranous ossification, they continue to be actively

remodeled after birth during periods of growth or bone repair. This involves a tightly regulated interplay between the activities of chondrocytes, osteoblasts and osteoclasts, the three cell lineages involved in bone development.

### **I.3. Cell lineages involved in bone development**

Three key players are involved in bone formation: osteoblasts and chondrocytes, which originate from common mesenchymal progenitors and osteoclasts, which are of hematopoietic origin (Kronenberg, 2003; Zelzer and Olsen, 2003).

#### Chondrocytes

Early during endochondral ossification, mesenchymal progenitors differentiate into chondrocytes. This process is critically dependent upon the transcription factor Sox9 (Figure 2), which binds, and activates the transcription of chondrocyte-specific genes (Bell et al., 1997; Zelzer and Olsen, 2003). Sox9 belongs to a large family of transcription factors, which also includes Sox5 and Sox6. These two Sox family members also play important roles in chondrocyte differentiation. In particular, they actively cooperate to regulate the expression of cartilage-specific components encountered in the extracellular matrix – such as type II collagen (Col2a1). Consistent with this, Sox 5, 6 and 9 form complexes with other nuclear proteins in chondrocytes and are also co-expressed at sites of chondrogenesis (Zhou et al., 1998). Furthermore, in Sox5- and Sox6-null mice the chondrocytes of the growth plate are unable to differentiate into hypertrophic chondrocytes (Lefebvre et al., 1998). Also, inactivation of Sox9 in limb buds prior to

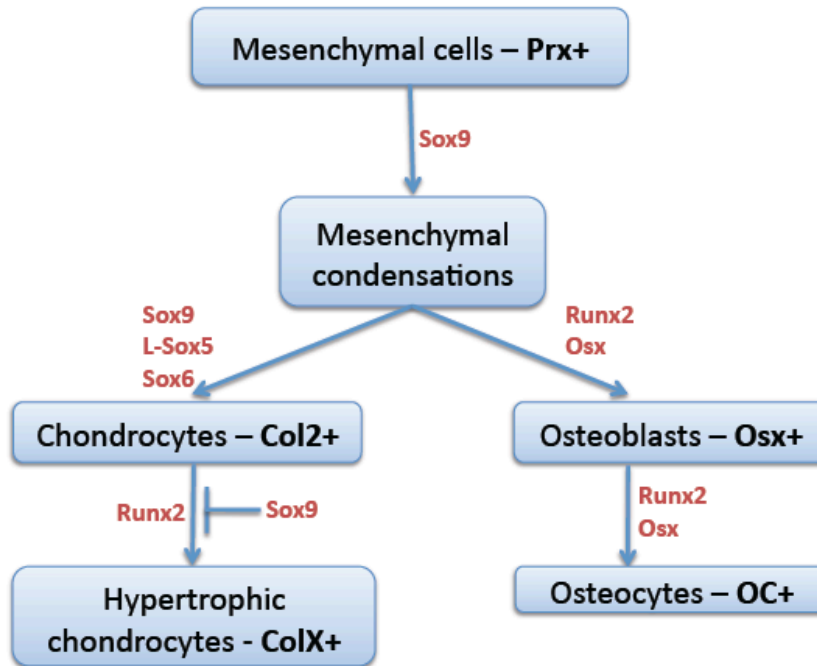


**Figure 2. Differentiation factors involved in chondrocytic and osteoblastic differentiation.** Adapted from (Zelzer and Olsen, 2003). Mesenchymal precursors, which express Prx, form mesenchymal condensations at the location of the future bones. The cells of these condensations will differentiate either into Col2 expressing chondrocytes under the control of Sox9, Sox6 and Sox5, or into Osx expressing osteoblasts. The Col2 chondrocytes will differentiate into ColX expressing hypertrophic chondrocytes in the presence of Runx2 and Sox9 inhibits this process. The Osx osteoblasts will differentiate into Osteocalcin (OC) expressing mature osteocytes, capable of secreting mineralized matrix.

the formation of mesenchymal condensations causes complete absence of both cartilage and bone (Akiyama et al., 2002).

Additionally, RUNX2, a transcription factor that was first identified through its role in osteoblast has also been linked to later stages of chondrocyte differentiation. Runx2 is required for chondrocytes to exit the cell cycle and become hypertrophic, since Runx2-deficient mice lack hypertrophic chondrocytes in their limbs (Kim et al., 1999). Runx2 positively regulates maturation to hypertrophic chondrocyte, while Sox9 negatively regulates this process (Figure 2).

Other important factors involved in proper chondrocyte differentiation are the signaling molecules Indian Hedgehog (Ihh) and Parathyroid hormone-related protein (PTHrP). These will be discussed in more detail in Section 1.4 of this introduction.

### Osteoblasts

Osteoblasts originate from mesenchymal progenitor cells and go through several stages of differentiation to become mineralizing mature osteoblasts. Different proteins are expressed at different stages of osteoblast differentiation and are therefore used as markers to study the dynamics of osteoblast differentiation from osteoblast progenitors to mature osteoblasts (Figure 2). Early in development, osteoblast progenitors express RUNX2. This promotes differentiation, resulting in the formation of *Osx*-expressing osteoblast precursors that commit to an osteoblastic fate through expression of alkaline phosphatase (ALP) and type I collagen (Col1). Mid-stage markers of osteoblast differentiation are osteopontin

(OPN) and osteonectin, while the late stage marker osteocalcin (OC) is expressed specifically by mature osteoblasts. Osteocytes, the most abundant bone cells (95%) in adult bone, are the terminal stage of osteoblast differentiation and they are embedded deep within the bone matrix during bone formation (Franz-Odenaal et al., 2006; Fulzele et al., 2012). These cells are important for regulating bone remodeling, due to their ability to secrete RANKL, which promotes osteoclast differentiation (Xiong et al., 2011) and also expression of sclerostin, a suppressor of osteoblast proliferation (Winkler et al., 2003).

Runx2 is the earliest transcription factor absolutely required for the differentiation of mesenchymal progenitors into osteoblasts (Figure 2). Runx2 regulates the expression of several osteoblast specific proteins, such as osteocalcin, alkaline phosphatase and type I collagen (Ducy et al., 1997; Lee et al., 2007). Interestingly, overexpression of Runx2 in other cell types *in vitro*, such as fibroblasts or myoblasts, is sufficient to induce the expression of osteoblast specific markers (Ducy, 2000). Conversely, deletion of Runx2 in mice prevents expression of early or late osteoblast markers and formation of mature bone tissue (Ducy et al., 1997). As noted above, these *Runx2* null mice also lack hypertrophic chondrocytes, despite other types of chondrocytes being present (Komori et al., 1997; Otto et al., 1997). Taken together, these observations prove that Runx2 is a critical factor required for proper osteoblast differentiation.

Osterix1 (OSX1) is the other transcription factor known to be essential for osteoblast differentiation (Figure 2). *Osx1*-null mice do not express any bone-specific markers (Nakashima et al., 2002). However, it was shown by *in situ*

hybridization analysis that *Osx*-null mice express *Runx2*. At the same time *Runx2*-null mice do not express *Osx*, indicating that *Osx* acts downstream *Runx2* in the osteoblast differentiation lineage (Nakashima et al., 2002). As *Runx2* has a role in both chondrocytic and osteoblastic differentiation, *Osterix* is likely the factor that provides specificity in osteoblastic differentiation. *Osx* expression is highly specific to the osteoblast lineage, but low-level expression has been detected in chondrocytes *in vivo* (Nakashima et al., 2002; Rodda and McMahon, 2006; Yagi et al., 2003). In an *in vitro* setting, *Osx* is sufficient to induce expression of osteoblast markers (Tai et al., 2004).

Importantly, normal cartilage development is required for proper osteoblast differentiation. This is supported by *in vivo* mouse studies showing that mutation of chondrocyte specific factors, such as *Ihh*, cause defects in osteoblasts differentiation. *In vivo* bone development is also negatively impacted when mutations are introduced into *Ihh*. Specifically, *Ihh*-null mice exhibit severe dwarfism in axial and appendicular skeletal elements and do not form endochondral bones (St-Jacques et al., 1999); (Long et al., 2004; Rodda and McMahon, 2006).

### Osteoclasts

Osteoclasts originate from the hematopoietic lineage, specifically from mature monocytes and macrophages, and their role is to release specific enzymes that can lyse adjacent bone. The balance between osteoblast activity (which build bone) and osteoclast activity (which destroy it) is crucial for maintaining bone density and regulating proper bone remodeling. Notably, osteoblasts can influence osteoclast differentiation in either a positive or negative manner, through secretion

of regulatory factors, such as CSF-1, RANKL and Osteoprotegerin (OPG). CSF-1 and RANKL play a promoting role via activation of osteoclast specific genes. OPG is a receptor for RANKL that acts to sequester it, and thereby inhibits osteoclast formation (Simonet et al., 1997). Animal studies have shown that mice without CSF-1 or the receptor for RANKL are unable to make osteoclasts (Kong et al., 1999; Yoshida et al., 1990) and they develop osteopetrosis. In cartilage, RUNX2 promotes expression of RANKL, the key ligand driving osteoclast differentiation. Hyperactive osteoclasts are responsible for many adult skeletal diseases, including osteoporosis, rheumatoid arthritis and periodontal disease (Rodan and Martin, 2000). Reduced osteoclast activity leads to diseases where excessive bone fills out the bone marrow cavity, such as osteopetrosis.

#### **I.4. Major signaling pathways involved in bone development**

Several major signaling pathways are important for bone development, including the Indian Hedgehog (Ihh)/Parathyroid hormone-related protein (PTHrP), the fibroblast growth factor (FGF) and the bone morphogenetic protein (BMP) pathways (Kronenberg, 2003). In general, these pathways function to coordinate proper chondrocyte and osteoblast differentiation. The Ihh/PTHrP and the FGF pathways will be discussed in more detail in the next section.

##### Indian hedgehog/ Parathyroid hormone-related protein signaling

Ihh and PTHrP signaling is complex, involving crosstalk and both negative and positive feedback loops (Figure 3). Perichondrial cells and chondrocytes at the end of long bones secrete PTHrP. (Figure 3.1). PTHrP acts on receptors found on

proliferating chondrocytes and keeps the cells in a proliferative state and delays their secretion of Ihh (Kronenberg, 2003; St-Jacques et al., 1999). Ihh is produced by cells that fail to receive enough PTHrP to suppress its expression. Ihh acts on its own receptor found on proliferating chondrocytes, and it stimulates their continuous proliferation and prevents differentiation to hypertrophic chondrocytes (Figure 3.2). Ihh also acts on chondrocytes at the end of the long bones and stimulates their production of PTHrP (Figure 3.3). Importantly, Ihh signals to perichondrial cells immediately adjacent to the prehypertrophic and hypertrophic cells, and it directs them to move away from the chondrocyte pathway and differentiate to osteoblasts. These osteoblasts end up forming the bone collar (Figure 3.4). *In vivo* studies have shown that Ihh-null mice exhibit severe dwarfism in axial and appendicular skeletal elements and do not form endochondral bones (St-Jacques et al., 1999). Null mutations of PTHrP or its receptor decreases the number of proliferating growth plate chondrocytes and increases the size of the hypertrophic zone (Lanske et al., 1996).

#### Fibroblast growth factor (FGF) signaling

FGF signaling has an important role in chondrocyte proliferation and differentiation. The mechanism by which this signaling pathway works is complex and still not fully understood. This is mainly due to the fact that various

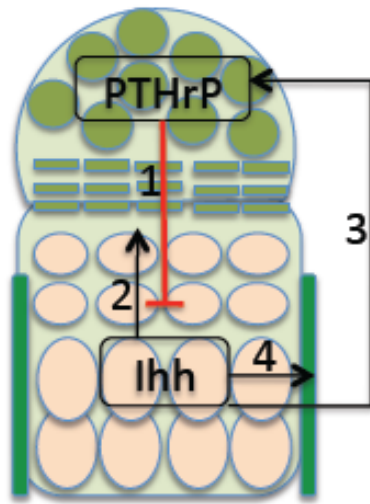


**Figure 3. Indian hedgehog (Ihh)/parathyroid hormone-related protein (PTHrP) negative-feedback loop.** Adapted from Kronenberg (2003). (1) Chondrocytes at the end of long bones secrete PTHrP. PTHrP acts on receptors found on proliferating chondrocytes to keep them in a proliferative state. (2) Ihh is produced by cells that fail to receive enough PTHrP to suppress its expression. Ihh acts on its own receptor found on proliferating chondrocytes, stimulates their continuous proliferation and prevents their differentiation to hypertrophic chondrocytes. (3) Ihh also acts on chondrocytes at the end of the long bones and stimulates their production of PTHrP. (4) Ihh signals to perichondrial cells immediately adjacent to the prehypertrophic and hypertrophic cells, and it directs them to differentiate to osteoblasts.

members of the FGF family, and also many FGF receptors, are expressed early in bone development and these have overlapping functions. Early during endochondral bone development, FGFR-2 is expressed in the condensing mesenchyme. *In vitro* studies in mesenchymal cell lines showed that FGFs stimulate expression of Sox9, the transcription factor essential for early stage chondrocyte differentiation (Figure 2). Thus, expression of FGFR-2 early in the limb mesenchyme is thought to induce the expression of Sox-9. At late times in development, proliferating chondrocytes express FGFR-3, while pre-hypertrophic and hypertrophic chondrocytes express FGFR-2. FGF signaling through FGFR-3 was studied in more depth and shown to have a negative effect on chondrocyte proliferation. This conclusion is based on the finding that activating mutations in FGFR-3 decrease the proliferation rate of chondrocytes, partially through the JAK-STAT1 pathway (Sahni et al., 1999). Notably, *Fgfr3* null mice show an increase in the rate of chondrocyte proliferation and expansion of chondrocyte columns (Colvin et al., 1996; Deng et al., 1996). Concomitantly, FGF signaling partially works through regulating the *Ihh*/ PTHrP negative loop, by suppressing *Ihh* expression and inducing a decrease in chondrocyte proliferation (Naski et al., 1998; Ornitz and Marie, 2002).

## **PART II. THE RAS ONCOGENES**

Proper cellular proliferation is essential for normal development and growth of organisms. Tight regulation of the cell cycle machinery, through various intracellular and extracellular signals, is very important for cells to know when to divide, or stop dividing, under the right conditions (Hanahan and Weinberg, 2000). In cancer, this regulation is disrupted and tumor cancer cells proliferate excessively. Mutations in the mitogenic signaling pathways, such as in members of the RAS family, are some of the most common mutations in cancer and result in an uncoupling of cell cycle regulation from extracellular cues. Given the importance of these proteins in proliferation and tumorigenesis, it is not surprising that their deregulation also has profound effects on normal development. RASopathies are a group of developmental disorders caused by germline mutations in components of the Ras/MAPK pathway that result in increased signaling. These will be discussed in further detail in Part III of this introduction.

This thesis presents two novel mouse models in which a constitutive mutation of K-ras is expressed at various stages during limb development. These models are used to investigate how K-ras<sup>G12D</sup> affects skeletal development when expressed in a spatial and temporal specific manner.

### **II. 1. Discovery**

Initially, the Ras genes were discovered as the transforming sequences from the genomes of Harvey and Kirsten rat sarcoma viruses (Chien et al., 1979; Ellis et al., 1981). Independently, the same sequences, cloned from various cancer cells lines

(Pulciani et al., 1982; Shih and Weinberg, 1982) or isolated from chemically treated cells (Shih et al., 1981) were identified as inducers of transformation of NIH 3T3 cells. Soon after, it was realized that the sequences in the two different contexts, viruses (viral Ras genes) and cancer cells, are homologous (Parada et al., 1982). This led to the discovery of the 3 members of the *Ras* family: *H-Ras*, *K-Ras* and lastly *N-ras* (Capon et al., 1983; Johnson et al., 2001).

Further work has shown that a single point mutation in these genes can transform the normal cellular gene into an oncogene (Tabin et al., 1982; Taparowsky et al., 1982). *RAS* genes represent frequent mutational targets in cancer and have been shown to be mutated in ~30% of human tumors (Johnson et al., 2001). Interestingly, mutations in the *RAS* genes are not randomly distributed among the different isoforms, and the majority of mutations occur in *K-RAS*, especially in lung, pancreas and colon tumors (Bos, 1989; Johnson et al., 2001). It is clear that mutations in different members of the Ras family lead to different tumor types (Karnoub and Weinberg, 2008).

*H-ras* and *N-ras* are dispensable for development, both individually and in combination (Janssen et al., 2005). *K-ras* encodes two splice variants with *KRASA* expressed in a tissue specific and developmentally restricted fashion and *KRASB* being ubiquitously expressed. Mice with a homozygous null mutation in *K-ras* are not viable and die during embryogenesis due to a wide spectrum of defects (cardiac, liver, neurological and hematopoietic defects), indicating that *K-ras* is essential for embryonic development (Tuveson et al., 2004).

## II.2. Ras proteins and the GTPase cycle

Early studies identified Ras proteins as small 21kD proteins localized to the cell membrane. These could both bind GTP, and hydrolyze it, proof of an internal GTP-ase activity (Shih et al., 1980). Soon after, these proteins were classified as small G-proteins (Hurley et al., 1984) that function as molecular switches in controlling the signaling from membrane receptors to intracellular effector cascades. They are regulated by binding to either GTP (in their ON state) or to GDP (in their OFF state; Figure 4). Following the discovery that the mitogenic signaling molecule, induces GTP binding (Kamata and Feramisco, 1984), it was concluded that the intracellular effector cascades controlled by Ras proteins were involved in cell proliferation, differentiation, and apoptosis.

Subsequent studies and the discovery of many other players helped to establish the precise mechanism by which mitogenic signals are transmitted from the cell membrane to the cell machinery and a complex GTP-GDP cycle was described (Figure 4; McCormick, 1993). Upon binding of mitogenic ligands to growth factor receptors, the intracellular domains of these receptors bind adaptor proteins (GRB2), which recruit guanine nucleotide exchange factors (GEFs, such as SOS) to the plasma membrane. This brings these in close proximity to the Ras proteins, which are tethered in the membrane, allowing interaction and to release GDP and bind GTP, which results in their activation and the activation of downstream pathways. This stimulates the Ras proteins as described in more detail below. The inactivation of the GTP-bound Ras proteins occurs through the hydrolysis of GTP to GDP, catalyzed by GTPase-activating proteins (GAPs)

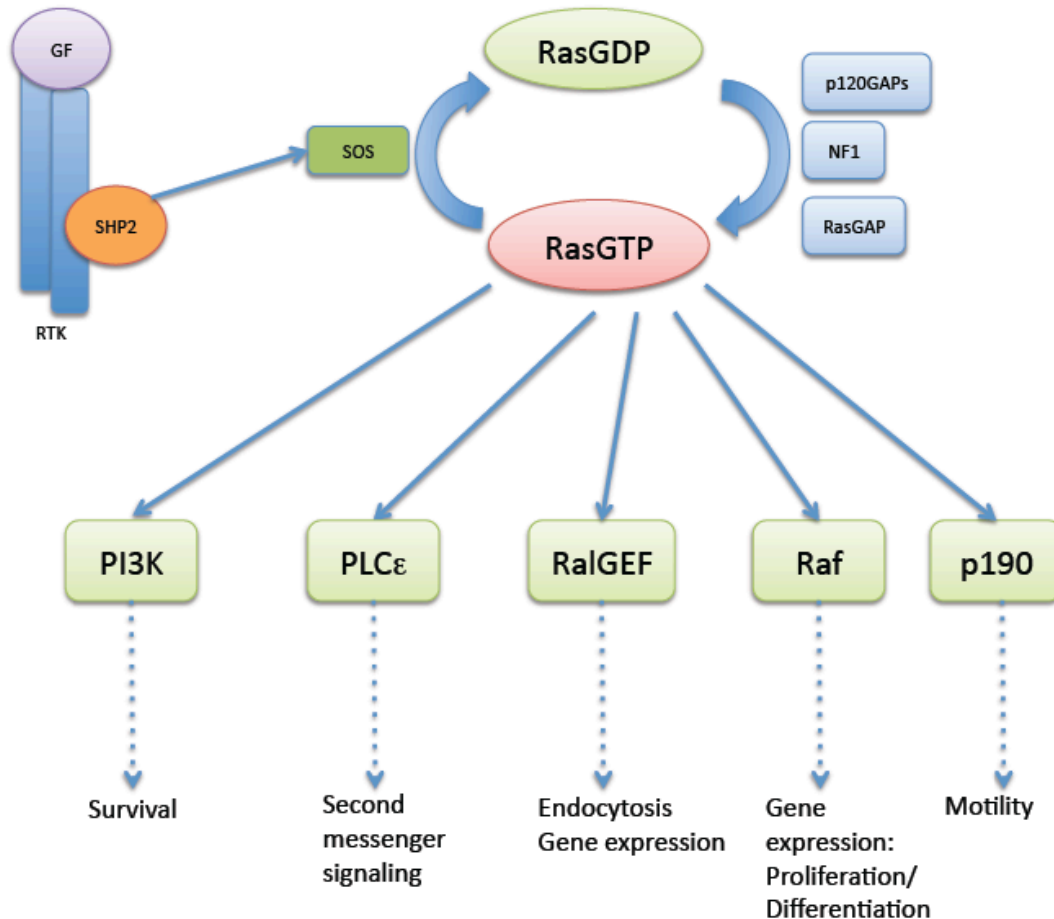


**Figure 4. Ras complex downstream signaling networks.** Adapted from Karnoub and Weinberg (2008). The MAPK signaling pathway controls downstream effectors critically involved in cell proliferation, differentiation, motility, apoptosis and senescence. The binding of GTP to Ras protein locks it in an active state, which enables interactions with multiple downstream effectors. A slow intrinsic GTPase activity leads to Ras inactivation and signal termination. This ON-OFF cycle is tightly controlled by GTPase-activating proteins (GAPs – p120GAP or NF1) and guanine-nucleotide exchange factors (GEFs – SOS).

GF=Growth Factor, RTK=Receptor Tyrosine Kinase.

including p210GAP and NF1 (Cawthon et al., 1990; Karnoub and Weinberg, 2008; Martin et al., 1990).

Not surprisingly, mutations that disrupt the GTP-GDP cycle of Ras proteins have been shown to be oncogenic. More specifically, these mutations cause an inhibition or reduction of the intrinsic GTPase activity or suppress their interaction with GAPs. This results in deregulated activation of the Ras proteins - often in the absence of appropriate upstream signaling - by increasing the ratio of the active GTP-bound state relative to the GDP-bound inactive state. The most common oncogenic point mutations in the Ras genes are found in codons 12, 13 and 61 (Clark et al., 1985; Der et al., 1986; Trahey and McCormick, 1987). These mutations lock Ras protein in a constitutively active form, by preventing it from releasing the bound GTP.

### **II.3. Ras downstream signaling pathways - MAPK pathway**

Ras downstream effectors can have a multitude of biological functions. Since growth factors such as EGF can stimulate Ras activity, it was concluded that one of the most important roles for Ras proteins is their role in mitogenic signaling (Mulcahy et al., 1985). Subsequently, it became clear that Ras activates a multitude of downstream signaling pathways, and has numerous roles including controlling cell cycle and differentiation (MAPK pathway), cell survival (PI3K pathway), cell signaling (PLC $\epsilon$ ), endocytosis (Ral-GEF) and many others (Karnoub and Weinberg, 2008; Figure 4). It is important to understand how Ras can execute all these

downstream functions, as this can shed more light on the role of these proteins in development and cancer.

I will further focus my discussion on the MAPK pathway, because this is most relevant to this thesis project. The Mitogen Activated Protein Kinase (MAPK) pathway is one of the best-characterized downstream signaling pathways of the Ras proteins. The Ras/MAPK pathway transduces extracellular signals in the form of growth factors and small molecules to the intracellular environment.

Active Ras leads to the activation of the Raf family of kinases: A-Raf, B-Raf and/or C-Raf. Raf, first identified as an oncogene (Vojtek et al., 1993), becomes localized to the plasma membrane and initiates activation of the MAPK signaling cascade (Figure 4). In this cascade, Raf kinase phosphorylates MEK1/2 (MAPK kinases), which then phosphorylate and activate ERK1/2 kinases (Hagemann and Blank, 2001). ERK1/2 are the ultimate effectors and exert their function on a large number of downstream molecules including nuclear factors, transcription factors, membrane proteins, and protein kinases. All these molecules control vital cellular functions including cell cycle progression, differentiation, and cell growth (Yoon and Seger, 2006).

Some of the better-characterized downstream ERK effectors are the Ets, ELK and AP-1 (c-Fos-c-Jun) complex of transcription factors. Activation of these transcription factors leads to increased expression of cell cycle genes, such as cyclin D1 (Hitomi and Stacey, 1999), supporting the role of Ras as a mitogenic protein. The MAPK pathway can have other outputs as well, such as the p38 pathway and the Jun N-terminal kinase (JNK) pathway, with roles related to stress responses. Notably,

Ras can direct distinct outputs and have different effects depending on which MAPK pathways it activates.

ERK targets several core regulators of osteoblast differentiation. It phosphorylates the RUNX2 transcription factor and positively regulates early osteoblast differentiation *in vivo* (Ge et al., 2007; Xiao et al., 2000; Figure 5). Furthermore, active ERK, via its association with RUNX2, binds to the osteoblast specific promoters osteocalcin (*Ocn*) and bone sialoprotein (*Bsp*) (Li et al., 2009). Besides RUNX2, ERK also activates RSK2 (Dalby et al., 1998), which phosphorylates ATF4, a pro-collagen gene transcriptional regulator of late-stage osteoblasts (Yang et al., 2004; Figure 5).

Given that Ras has a direct role in cellular transformation and during development, an important question becomes which of its downstream signaling pathways are critical for its tumorigenic functions, versus its various developmental roles. The complexity of Ras signaling underscores the importance of focusing on specific cell types when studying the Ras effector pathways.

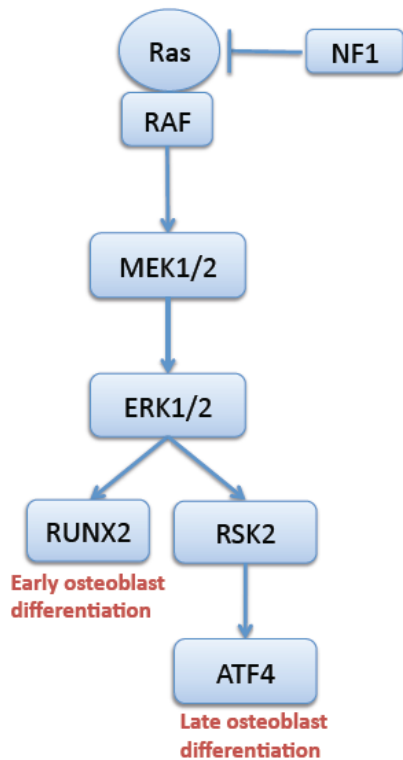


**Figure 5. MAPK (ERK) pathway in osteoblast differentiation.** Adapted from (Greenblatt et al., 2013) During early osteoblast differentiation, ERK phosphorylates RUNX2 to increase its transcriptional activity and induce osteoblast differentiation. Later in osteoblast differentiation, ERK activates the kinase RSK2, which in turn phosphorylates and activates ATF4.

## **PART III. MAPK SIGNALING**

The role of MAPK signaling both during embryonic development, as well as during skeletal differentiation has been actively investigated. However, a clear understanding of its effects in these two settings is still not available. This thesis describes two mouse models that allow us to study and further investigate the effects of activating the MAPK pathway during embryonic development, specifically in the skeletal lineage.

### **III.1. MAPK signaling during development – human syndromes**

MAPK signaling has been shown to play an important role during embryonic development, as well as during postnatal development in various model organisms, including mice, zebrafish and drosophila (Furthauer et al., 2004; Gabay et al., 1997). Particularly in zebrafish, FGF signaling through the MAPK pathway is important for early embryo patterning (Curran and Grainger, 2000). In mice, it was shown that ERK signaling is active during mouse embryogenesis, and ERK phosphorylation can be detected in the neural crest, peripheral nervous system and early structures, which will later become ear, eye, heart and blood vessels (Corson et al., 2003). Other transgenic mouse models with mutations in the genes of the Ras/MAPK pathway further elucidated the essential role that these genes play during development (Galabova-Kovacs et al., 2006; Johnson et al., 1997).

In humans, the RASopathies, a group of developmental disorders caused by germline mutations in genes encoding components of the Ras/MAPK pathway

(Figure 6) clearly illustrates the important role of this pathway during normal development. Some described RASopathies are Noonan, LEOPARD, gingival fibromatosis 1, neurofibromatosis 1, capillary malformation-arteriovenous malformation, Costello, autoimmune lymphoproliferative (ALPS), cardio-facio-cutaneous and Legius syndromes (Tidyman and Rauen, 2009). These are caused by constitutive active mutations in different members of the MAPK pathway that result in increased signaling. Some MAPK pathway members are seen in multiple syndromes, while others appear highly syndrome specific (Figure 6).

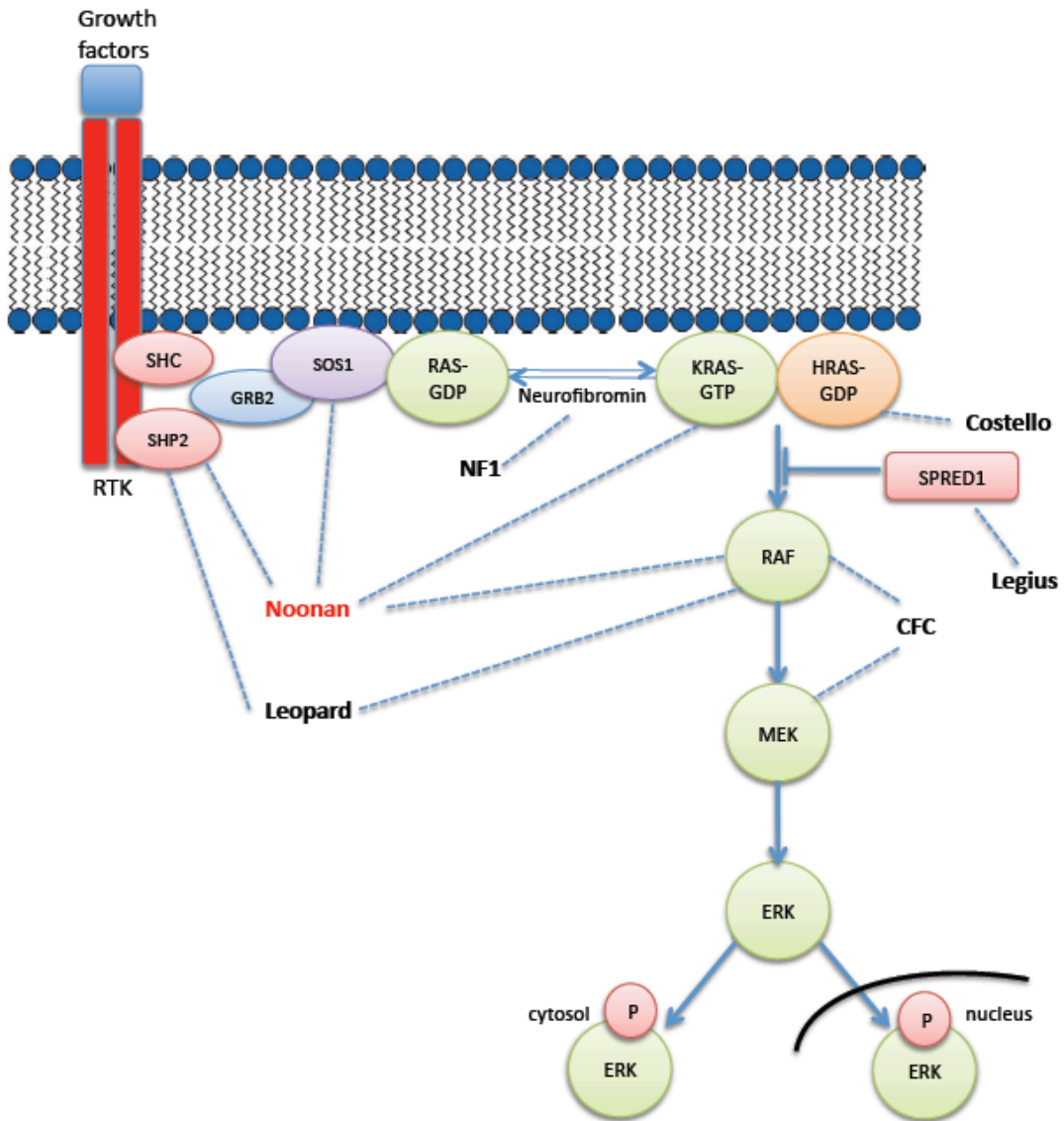


**Figure 6. Ras/ MAPK signaling pathway and associated developmental syndromes.** Adapted from Tidyman and Rauen, (2009). The blue dotted lines indicate specific components of the Ras/MAPK pathway whose germline mutations in its respective components is associated with Noonan, LEOPARD, neurofibromatosis 1, Costello, cardio-facio-cutaneous and Legius syndromes.

Although the various syndromes each display some unique symptoms, they also have some overlapping defects. Frequently observed defects include characteristic craniofacial dysmorphism, cardiac malformations, cutaneous, musculoskeletal and ocular abnormalities, neurocognitive impairment and, in some syndromes, predisposition to certain malignancies (Tidyman and Rauen, 2009).

It should be noted that the common germline mutations that result in RASopathies differ from the somatic mutations commonly found in cancer. For example, the V600E oncogenic mutation in B-RAF is not seen in Cardio-Facial-Cutaneous Syndrome, and the most common oncogenic mutations in K-RAS are not encountered in patients with Noonan Syndrome (Mercer et al., 2005). Instead, the Rasopathy mutations are typically weaker acting mutations. The most likely explanation is that the cancer causing somatic mutations are too strong to be compatible with embryonic viability (Tuveson et al., 2004). Interestingly, patients with RASopathies do have a mild predisposition to cancer. For example, Noonan patients are prone to develop cancers of the blood, more specifically myeloproliferative diseases, which typically resolve but sometimes develop into leukemia (Johannes et al., 1995; Side and Shannon, 1997).

### Noonan syndrome

Noonan Syndrome (NS) is an autosomal dominant disorder that affects 1/1000 to 1/2500 newborns. Patients with NS have specific craniofacial features, short stature, skeletal abnormalities, congenital cardiac abnormalities, neurocognitive delay and a predisposition to cancer (Shaw et al., 2007).

Activating germline mutations in *PTPN11* (Tartaglia et al., 2001), *KRAS* (Schubbert

et al., 2006), *SOS1* (Roberts et al., 2007; Tartaglia et al., 2007) and *RAF1* (Pandit et al., 2007; Razzaque et al., 2007) have all been linked to NS. *PTPN11* missense mutations are responsible for 50% of NS cases. *PTPN11* encodes for protein SHP2, a non-receptor protein tyrosine phosphatase, which contains an N-terminal SH2 domain, a C-terminal SH2 domain and catalytic protein tyrosine phosphatase (PTP) domain. The majority of NS-causing mutations in *PTPN11* are in residues involved in the interaction between the N-SH2 and PTP domains. This interaction inhibits the catalytic function of SHP2 and causes increased signaling down the Ras/MAPK pathway (Keilhack et al., 2005). *SOS1* missense mutations are responsible for 12% of Noonan cases. *SOS1* encodes for the SOS1 protein, a Ras-GEF, responsible for the conversion of Ras from the GDP-bound form to the GTP-bound form. The majority of *SOS1* mutations are in residues responsible for stabilizing the protein in an inhibited conformation. They result in a gain-of-function *SOS1* and a subsequent increase in the active form of Ras and increased Ras/MAPK pathway signaling (Roberts et al., 2007). 3-5% of NS cases are caused by mutations in *RAF1*, which encodes a serine/threonine kinase that is a downstream effector of Ras. The NS mutations result in a gain-of-function phenotype for Ras (Pandit et al., 2007). *KRAS* mutations account for about 2% of the NS cases. These mutations cause an increase in the GTP-bound form of *KRAS* and thus increased signaling down the Ras/MAPK pathway either by reducing the intrinsic GAP activity of the *KRAS* protein or by affecting the interaction of *KRAS* with guanine nucleotides (Schubbert et al., 2006).

Studying and understanding the consequences of deregulating the Ras/MAPK pathway during development using various model organisms will shed

light on the role that this pathway plays during embryonic and postnatal human development. In the next section I will describe the efforts that have been done to model Noonan Syndrome (NS) using various model organisms. Furthermore, my thesis describes a novel mouse model for NS, which allows us to study in more depth the skeletal defects associated with this syndrome.

### **III. 2. Modeling Noonan syndrome using animal models**

Previous efforts to model RASopathies have been carried out in both fish and mice. Specific mutations encountered in Noonan Syndrome have been expressed in either the germline or a cell specific manner to generate animal models that recapitulate symptoms of patients with RASopathies. While these models have recapitulated the cardiac abnormalities and cranio-facial deformities of NS patients, they have not offered a good model to study the limb abnormalities of these patients. With the mouse model I have generated in my thesis I am specifically modeling the skeletal defects found in patients with NS. Furthermore, other studies have shown that treatment with MEK inhibitors exclusively during embryonic development can rescue the cardiac defects associated with NS. In my thesis, I identify a defined period during embryonic development when giving MEK inhibitors can fully rescue the bone phenotype.

In the next section I will summarize the existing literature on some of the animals that have been developed to model the Noonan syndrome.

## Germline mutations

Araki et al, 2004 have generated a mouse model for Noonan Syndrome containing a germline heterozygous D61G mutation in *Ptpn11*, one of the genes known to cause NS when mutated. Their model recapitulates the short stature and craniofacial abnormalities of NS patients, as well some of the heart defects seen in patients that include atrial and atrioventricular septal defects, thinning of ventricular wall and hypertrophy of atrioventricular and outflow tract valves (Araki et al., 2004). The same group later analyzed the mechanisms underlying the cardiac defects and showed that they are caused by Shp2 expression specifically in the endocardium, but not in the myocardium or neural crest. The D61G mutation results in an increased MAPK activation and affects the endocardial to mesenchymal transformation of endocardial cells (Araki et al., 2009).

In another germline model, researchers have generated mice with a specific *Sos* mutation. These mice exhibited NS-associated phenotypes, such as growth delay, facial dysmorphia, hematological and cardiac abnormalities (Chen et al., 2010) The MAPK pathway, as well as Rac and Stat3, were found to be active in the mutant hearts. Importantly, symptoms were rescued by prenatal administration of a MEK inhibitor, demonstrating that this signaling pathway might represent a promising therapeutic target for NS. Wu et al, 2011, use generated a NS mouse model with a germline mutation in Raf. These mice had short stature, craniofacial and hematological abnormalities and these defects were rescued by postnatal treatment with MEK inhibitors (Wu et al., 2011b)

### Spatial and temporal restricted mutations

A more restricted approach has been used by Nakamura et al., 2007, who expressed the SHP2 protein with a Q79R mutation selectively in cardiomyocytes in a time restricted manner, during gestation or after birth. They saw that the mutation caused a heart defect (ventricular septal defect), only when expressed during embryonic development. They further showed that activation of the ERK pathway is both necessary and sufficient for the mutant effects caused by the Q79R mutation, since the expression of mutant SHP2 in an ERK 1/2 null background rescued the mutant phenotype. This study suggested that ERK pathway modulation could have important implications for the treatment of congenital cardiac defects (Nakamura et al., 2007). The same group showed in a subsequent study that repression of pERK activity using a MAPK/ERK kinase inhibitor administered during embryonic development rescues the NS specific phenotypes caused by expression of the mutant SHP2 protein specifically in neural crest cells (Nakamura et al., 2009).

### **III. 3. MAPK signaling pathway in skeletal development**

In the previous part I have discussed how deregulation of the MAPK pathway results in developmental defects in various model organisms. The open question still remains what is the molecular basis of these defects. My thesis investigates the molecular basis of the skeletal defects caused by a constitutive active K-ras mutation expressed either in mesenchymal progenitors and subsequent lineages, or in osteoblast precursors. Here I will summarize the literature to date on various studies investigating the effects of increased MAPK signaling at various stages of

skeletal development.

Increased signaling through the MAPK pathway is commonly encountered in many cancers and is usually correlated with increased and unrestrained proliferation. However, in the context of bone development the effects of the MAPK pathway on cell proliferation and differentiation are less clear. Thus, a thorough analysis of the importance of MAPK signaling pathways in osteoblasts and chondrocytes is essential to understand how bone mass is regulated.

Various *in vitro* and *in vivo* studies suggest a key role of the MAPK signaling pathway in osteogenesis. However, the physiological role of the MAPK pathway in osteoblasts remains controversial, with some studies supporting a stimulatory role in osteoblast differentiation and others proposing that this pathway is actually inhibitory. Several studies have shown that the MAPK-ERK pathway regulates bone formation by osteoblasts (Ge et al., 2007; Greenblatt et al., 2010; Zou et al., 2011). Expression of a dominant-negative form of MEK1 in osteoblasts results in low bone mineralization, especially in the clavicle and the calvaria (Ge et al., 2007). Furthermore, mice with a germline deletion of Erk1 and also a conditional deletion of Erk2 in the limb mesenchyme display reduced bone mineralization, proving the necessity of ERK activity for proper osteoblast functioning (Matsushita et al., 2009).

*In vivo* deletion of NF1 (a Ras inhibitor) in late stage osteoblasts, using the Ocn promoter to express Cre recombinase, shows increased RSK2 phosphorylation and ATF4 expression, and an increase in bone mass (Elefteriou et al., 2006).

Treatment with ERK inhibitors rescued these defects, supporting the idea that ERK is critical for regulating RSK2 and ATF4 expression and its activation leads to

increased collagen synthesis and bone matrix deposition. Surprisingly, deleting NF1 in osteochondral progenitors, using the Col2 promoter to express Cre, causes reduced bone mass and impaired osteoblast differentiation (Wang et al., 2011; Wu et al., 2011a). *In vitro* studies further showed that osteoprogenitors collected from NF1 deficient mice exhibited lower induction of osteoblast differentiation (Kolanczyk et al., 2007; Yu et al., 2005). The contradictory results observed in these two NF1-deficient models argue that NF1 and subsequently, the MAPK pathway exert different effects at different stages of osteoblast differentiation. Additionally, the data suggests that ectopic ERK activation has different effects when targeting Runx2 (in early differentiation) versus RSK2/ ATF4 (in late differentiation). In conclusion, Ras-MAPK signaling is essential for the commitment of multipotent progenitors to an osteoblast cell fate, but it can antagonize further osteogenic differentiation (Ge et al., 2007; Nakamura et al., 2009; Schindeler and Little, 2006).

MAPK pathway also plays an important role in chondrocyte differentiation during skeletal development (Hill et al., 2005; Rodda and McMahon, 2006). In other differentiating systems, such as muscle and fat, ERK-MAPK signaling has been shown to control stem cells/progenitor lineage decisions. In fat, ERK1 phosphorylates PPAR $\gamma$  and inhibits its activity, blocking adipogenesis as a result (Adams et al., 1997). In *X. laevis* muscle differentiation, MAPK increases the levels of XMyoD, a master regulator of muscle differentiation (Zetser et al., 2001). Consequently, in the context of chondrogenesis, MAPK pathway is also believed to play a role in controlling progenitor/stem cell lineage decisions.

Interestingly, mice with the MAPK pathway activated selectively in

osteochondral progenitors, either by a constitutive active mutation in MEK1 or by constitutively active FGF3, display chondrodysplasia (short limbs). Activating the MAPK pathway in osteochondral progenitors leads to an increase in the levels of Sox9, a master regulator of chondrocyte differentiation, which keeps chondrocytes in a pre-hypertrophic state. As a result, the limbs are short due to a reduction of the hypertrophic zone (Murakami et al., 2000). In these mice, the chondrocyte hypertrophy is inhibited, but interestingly there is no effect on chondrocyte proliferation (Murakami et al., 2004; Murakami et al., 2000). Furthermore, mice with a deletion of Erk1 and Erk2 in the limb mesenchyme cannot clear hypertrophic chondrocytes (Matsushita et al., 2009), suggesting that MAPK-ERK is a fundamental pathway for the regulation of Runx2 activity in chondrocytes.

*In vitro*, increased activity of the MEK-ERK cascade has been reported to be a positive regulator of cartilage markers in cultured costal chondrocytes (Murakami et al., 2000), but a negative regulator of cartilage markers in the embryonic limb mesenchyme (Bobick and Kulyk, 2004). Furthermore, other studies have shown that the MEK/ERK pathway functions as a negative regulator of chondrocyte differentiation in micromass cultures prepared from frontonasal mesenchyme of stage 24/25 chick embryos (Bobick and Kulyk, 2006). In contrast, the MEK/ERK cascade acts as a positive regulator of chondrogenesis in the mesenchyme of the stage 24/25 mandibular arch, as well as in the frontonasal mesenchyme of the stage 28/29 embryos.

In conclusion, studies from the literature suggest that MAPK pathway may either activate or repress chondrocyte and osteoblast development depending on

the stage at which it is activated in the osteo-chondrogenic differentiation program. Specifically, it seems likely that uncommitted multipotent progenitors, committed osteoprogenitors, mature osteoblasts, and cells derived from other lineages respond differently to identical stimuli, thereby explaining some of the apparent conflict in the literature.

Based on the two mouse models I have generated, in which constitutive K-ras is expressed in a spatial and temporal specific manner during skeletal development, this thesis addresses two issues. The first is the nature of the skeletal defects encountered in patients with NS. This is important since limited information exists in the literature regarding the defects in bone mineralization seen in NS (Choudhry et al., 2012). The second is the effect that Ras/MAPK activation has on osteoblast and chondrocyte differentiation, and how this varies depending on the developmental stage at which K-ras mutation is activated.

## REFERENCES

- Adams, M., M.J. Reginato, D. Shao, M.A. Lazar, and V.K. Chatterjee. 1997. Transcriptional activation by peroxisome proliferator-activated receptor gamma is inhibited by phosphorylation at a consensus mitogen-activated protein kinase site. *J Biol Chem.* 272:5128-32.
- Akiyama, H., M.C. Chaboissier, J.F. Martin, A. Schedl, and B. de Crombrughe. 2002. The transcription factor Sox9 has essential roles in successive steps of the chondrocyte differentiation pathway and is required for expression of Sox5 and Sox6. *Genes Dev.* 16:2813-28.
- Araki, T., G. Chan, S. Newbigging, L. Morikawa, R.T. Bronson, and B.G. Neel. 2009. Noonan syndrome cardiac defects are caused by PTPN11 acting in endocardium to enhance endocardial-mesenchymal transformation. *Proc Natl Acad Sci U S A.* 106:4736-41.
- Araki, T., M.G. Mohi, F.A. Ismat, R.T. Bronson, I.R. Williams, J.L. Kutok, W. Yang, L.I. Pao, D.G. Gilliland, J.A. Epstein, and B.G. Neel. 2004. Mouse model of Noonan syndrome reveals cell type- and gene dosage-dependent effects of Ptpn11 mutation. *Nat Med.* 10:849-57.
- Bell, D.M., K.K. Leung, S.C. Wheatley, L.J. Ng, S. Zhou, K.W. Ling, M.H. Sham, P. Koopman, P.P. Tam, and K.S. Cheah. 1997. SOX9 directly regulates the type-II collagen gene. *Nat Genet.* 16:174-8.
- Bobick, B.E., and W.M. Kulyk. 2004. The MEK-ERK signaling pathway is a negative regulator of cartilage-specific gene expression in embryonic limb mesenchyme. *J Biol Chem.* 279:4588-95.
- Bobick, B.E., and W.M. Kulyk. 2006. MEK-ERK signaling plays diverse roles in the regulation of facial chondrogenesis. *Exp Cell Res.* 312:1079-92.
- Bos, J.L. 1989. ras oncogenes in human cancer: a review. *Cancer Res.* 49:4682-9.
- Capon, D.J., P.H. Seeburg, J.P. McGrath, J.S. Hayflick, U. Edman, A.D. Levinson, and D.V. Goeddel. 1983. Activation of Ki-ras2 gene in human colon and lung carcinomas by two different point mutations. *Nature.* 304:507-13.
- Cawthon, R.M., R. Weiss, G.F. Xu, D. Viskochil, M. Culver, J. Stevens, M. Robertson, D. Dunn, R. Gesteland, P. O'Connell, and et al. 1990. A major segment of the neurofibromatosis type 1 gene: cDNA sequence, genomic structure, and point mutations. *Cell.* 62:193-201.
- Chen, P.C., H. Wakimoto, D. Conner, T. Araki, T. Yuan, A. Roberts, C. Seidman, R. Bronson, B. Neel, J.G. Seidman, and R. Kucherlapati. 2010. Activation of

- multiple signaling pathways causes developmental defects in mice with a Noonan syndrome-associated *Sos1* mutation. *J Clin Invest.* 120:4353-65.
- Chien, U.H., M. Lai, T.Y. Shih, I.M. Verma, E.M. Scolnick, P. Roy-Burman, and N. Davidson. 1979. Heteroduplex analysis of the sequence relationships between the genomes of Kirsten and Harvey sarcoma viruses, their respective parental murine leukemia viruses, and the rat endogenous 30S RNA. *J Virol.* 31:752-60.
- Choudhry, K.S., M. Grover, A.A. Tran, E. O'Brian Smith, K.J. Ellis, and B.H. Lee. 2012. Decreased bone mineralization in children with Noonan syndrome: another consequence of dysregulated RAS MAPKinase pathway? *Mol Genet Metab.* 106:237-40.
- Clark, R., G. Wong, N. Arnheim, D. Nitecki, and F. McCormick. 1985. Antibodies specific for amino acid 12 of the ras oncogene product inhibit GTP binding. *Proc Natl Acad Sci U S A.* 82:5280-4.
- Colvin, J.S., B.A. Bohne, G.W. Harding, D.G. McEwen, and D.M. Ornitz. 1996. Skeletal overgrowth and deafness in mice lacking fibroblast growth factor receptor 3. *Nat Genet.* 12:390-7.
- Corson, L.B., Y. Yamanaka, K.M. Lai, and J. Rossant. 2003. Spatial and temporal patterns of ERK signaling during mouse embryogenesis. *Development.* 130:4527-37.
- Curran, K.L., and R.M. Grainger. 2000. Expression of activated MAP kinase in *Xenopus laevis* embryos: evaluating the roles of FGF and other signaling pathways in early induction and patterning. *Dev Biol.* 228:41-56.
- Dalby, K.N., N. Morrice, F.B. Caudwell, J. Avruch, and P. Cohen. 1998. Identification of regulatory phosphorylation sites in mitogen-activated protein kinase (MAPK)-activated protein kinase-1a/p90rsk that are inducible by MAPK. *J Biol Chem.* 273:1496-505.
- Deng, C., A. Wynshaw-Boris, F. Zhou, A. Kuo, and P. Leder. 1996. Fibroblast growth factor receptor 3 is a negative regulator of bone growth. *Cell.* 84:911-21.
- Der, C.J., T. Finkel, and G.M. Cooper. 1986. Biological and biochemical properties of human rasH genes mutated at codon 61. *Cell.* 44:167-76.
- Ducy, P. 2000. *Cbfa1*: a molecular switch in osteoblast biology. *Dev Dyn.* 219:461-71.
- Ducy, P., R. Zhang, V. Geoffroy, A.L. Ridall, and G. Karsenty. 1997. *Osf2/Cbfa1*: a transcriptional activator of osteoblast differentiation. *Cell.* 89:747-54.

- Elefteriou, F., M.D. Benson, H. Sowa, M. Starbuck, X. Liu, D. Ron, L.F. Parada, and G. Karsenty. 2006. ATF4 mediation of NF1 functions in osteoblast reveals a nutritional basis for congenital skeletal dysplasiae. *Cell Metab.* 4:441-51.
- Ellis, R.W., D. Defeo, T.Y. Shih, M.A. Gonda, H.A. Young, N. Tsuchida, D.R. Lowy, and E.M. Scolnick. 1981. The p21 src genes of Harvey and Kirsten sarcoma viruses originate from divergent members of a family of normal vertebrate genes. *Nature.* 292:506-11.
- Franz-Odendaal, T.A., B.K. Hall, and P.E. Witten. 2006. Buried alive: how osteoblasts become osteocytes. *Dev Dyn.* 235:176-90.
- Fulzele, K., D.S. Krause, C. Panaroni, V. Saini, K.J. Barry, X. Liu, S. Lotinun, R. Baron, L. Bonewald, J.Q. Feng, M. Chen, L.S. Weinstein, J.Y. Wu, H.M. Kronenberg, D.T. Scadden, and P. Divieti Pajevic. 2012. Myelopoiesis is regulated by osteocytes through Gsalpha-dependent signaling. *Blood.* 121:930-9.
- Furthauer, M., J. Van Celst, C. Thisse, and B. Thisse. 2004. Fgf signalling controls the dorsoventral patterning of the zebrafish embryo. *Development.* 131:2853-64.
- Gabay, L., R. Seger, and B.Z. Shilo. 1997. MAP kinase in situ activation atlas during Drosophila embryogenesis. *Development.* 124:3535-41.
- Galabova-Kovacs, G., D. Matzen, D. Piazzolla, K. Meissl, T. Plyushch, A.P. Chen, A. Silva, and M. Baccarini. 2006. Essential role of B-Raf in ERK activation during extraembryonic development. *Proc Natl Acad Sci U S A.* 103:1325-30.
- Ge, C., G. Xiao, D. Jiang, and R.T. Franceschi. 2007. Critical role of the extracellular signal-regulated kinase-MAPK pathway in osteoblast differentiation and skeletal development. *J Cell Biol.* 176:709-18.
- Greenblatt, M.B., J.H. Shim, and L.H. Glimcher. 2013. Mitogen-Activated Protein Kinase Pathways in Osteoblasts. *Annu Rev Cell Dev Biol.*
- Greenblatt, M.B., J.H. Shim, W. Zou, D. Sitara, M. Schweitzer, D. Hu, S. Lotinun, Y. Sano, R. Baron, J.M. Park, S. Arthur, M. Xie, M.D. Schneider, B. Zhai, S. Gygi, R. Davis, and L.H. Glimcher. 2010. The p38 MAPK pathway is essential for skeletogenesis and bone homeostasis in mice. *J Clin Invest.* 120:2457-73.
- Hagemann, C., and J.L. Blank. 2001. The ups and downs of MEK kinase interactions. *Cell Signal.* 13:863-75.
- Hanahan, D., and R.A. Weinberg. 2000. The hallmarks of cancer. *Cell.* 100:57-70.
- Harada, S., and G.A. Rodan. 2003. Control of osteoblast function and regulation of bone mass. *Nature.* 423:349-55.

- Hill, T.P., D. Spater, M.M. Taketo, W. Birchmeier, and C. Hartmann. 2005. Canonical Wnt/beta-catenin signaling prevents osteoblasts from differentiating into chondrocytes. *Dev Cell*. 8:727-38.
- Hitomi, M., and D.W. Stacey. 1999. Cyclin D1 production in cycling cells depends on ras in a cell-cycle-specific manner. *Curr Biol*. 9:1075-84.
- Hurley, J.B., M.I. Simon, D.B. Teplow, J.D. Robishaw, and A.G. Gilman. 1984. Homologies between signal transducing G proteins and ras gene products. *Science*. 226:860-2.
- Janssen, K.P., M. Abal, F. El Marjou, D. Louvard, and S. Robine. 2005. Mouse models of K-ras-initiated carcinogenesis. *Biochim Biophys Acta*. 1756:145-54.
- Johannes, J.M., E.R. Garcia, G.A. De Vaan, and R.S. Weening. 1995. Noonan's syndrome in association with acute leukemia. *Pediatr Hematol Oncol*. 12:571-5.
- Johnson, L., D. Greenbaum, K. Cichowski, K. Mercer, E. Murphy, E. Schmitt, R.T. Bronson, H. Umanoff, W. Edelmann, R. Kucherlapati, and T. Jacks. 1997. K-ras is an essential gene in the mouse with partial functional overlap with N-ras. *Genes Dev*. 11:2468-81.
- Johnson, L., K. Mercer, D. Greenbaum, R.T. Bronson, D. Crowley, D.A. Tuveson, and T. Jacks. 2001. Somatic activation of the K-ras oncogene causes early onset lung cancer in mice. *Nature*. 410:1111-6.
- Kamata, T., and J.R. Feramisco. 1984. Epidermal growth factor stimulates guanine nucleotide binding activity and phosphorylation of ras oncogene proteins. *Nature*. 310:147-50.
- Karnoub, A.E., and R.A. Weinberg. 2008. Ras oncogenes: split personalities. *Nat Rev Mol Cell Biol*. 9:517-31.
- Karsenty, G., H.M. Kronenberg, and C. Settembre. 2009. Genetic control of bone formation. *Annu Rev Cell Dev Biol*. 25:629-48.
- Keilhack, H., F.S. David, M. McGregor, L.C. Cantley, and B.G. Neel. 2005. Diverse biochemical properties of Shp2 mutants. Implications for disease phenotypes. *J Biol Chem*. 280:30984-93.
- Kim, I.S., F. Otto, B. Zabel, and S. Mundlos. 1999. Regulation of chondrocyte differentiation by Cbfa1. *Mech Dev*. 80:159-70.
- Kolanczyk, M., N. Kossler, J. Kuhnisch, L. Lavitas, S. Stricker, U. Wilkening, I. Manjubala, P. Fratzl, R. Sporle, B.G. Herrmann, L.F. Parada, U. Kornak, and S.

- Mundlos. 2007. Multiple roles for neurofibromin in skeletal development and growth. *Hum Mol Genet.* 16:874-86.
- Komori, T., H. Yagi, S. Nomura, A. Yamaguchi, K. Sasaki, K. Deguchi, Y. Shimizu, R.T. Bronson, Y.H. Gao, M. Inada, M. Sato, R. Okamoto, Y. Kitamura, S. Yoshiki, and T. Kishimoto. 1997. Targeted disruption of *Cbfa1* results in a complete lack of bone formation owing to maturational arrest of osteoblasts. *Cell.* 89:755-64.
- Kong, Y.Y., H. Yoshida, I. Sarosi, H.L. Tan, E. Timms, C. Capparelli, S. Morony, A.J. Oliveira-dos-Santos, G. Van, A. Itie, W. Khoo, A. Wakeham, C.R. Dunstan, D.L. Lacey, T.W. Mak, W.J. Boyle, and J.M. Penninger. 1999. OPGL is a key regulator of osteoclastogenesis, lymphocyte development and lymph-node organogenesis. *Nature.* 397:315-23.
- Kronenberg, H.M. 2003. Developmental regulation of the growth plate. *Nature.* 423:332-6.
- Kronenberg, H.M. 2007. The role of the perichondrium in fetal bone development. *Ann N Y Acad Sci.* 1116:59-64.
- Lanske, B., A.C. Karaplis, K. Lee, A. Luz, A. Vortkamp, A. Pirro, M. Karperien, L.H. Defize, C. Ho, R.C. Mulligan, A.B. Abou-Samra, H. Juppner, G.V. Segre, and H.M. Kronenberg. 1996. PTH/PTHrP receptor in early development and Indian hedgehog-regulated bone growth. *Science.* 273:663-6.
- Lee, N.K., H. Sowa, E. Hinoi, M. Ferron, J.D. Ahn, C. Confavreux, R. Dacquin, P.J. Mee, M.D. McKee, D.Y. Jung, Z. Zhang, J.K. Kim, F. Mauvais-Jarvis, P. Ducy, and G. Karsenty. 2007. Endocrine regulation of energy metabolism by the skeleton. *Cell.* 130:456-69.
- Lefebvre, V., P. Li, and B. de Crombrughe. 1998. A new long form of Sox5 (L-Sox5), Sox6 and Sox9 are coexpressed in chondrogenesis and cooperatively activate the type II collagen gene. *EMBO J.* 17:5718-33.
- Li, Y., C. Ge, and R.T. Franceschi. 2009. Differentiation-dependent association of phosphorylated extracellular signal-regulated kinase with the chromatin of osteoblast-related genes. *J Bone Miner Res.* 25:154-63.
- Long, F., U.I. Chung, S. Ohba, J. McMahon, H.M. Kronenberg, and A.P. McMahon. 2004. *Ihh* signaling is directly required for the osteoblast lineage in the endochondral skeleton. *Development.* 131:1309-18.
- Maes, C., T. Kobayashi, M.K. Selig, S. Torrekens, S.I. Roth, S. Mackem, G. Carmeliet, and H.M. Kronenberg. 2010. Osteoblast precursors, but not mature osteoblasts, move into developing and fractured bones along with invading blood vessels. *Dev Cell.* 19:329-44.

- Martin, G.A., D. Viskochil, G. Bollag, P.C. McCabe, W.J. Crosier, H. Haubruck, L. Conroy, R. Clark, P. O'Connell, R.M. Cawthon, and et al. 1990. The GAP-related domain of the neurofibromatosis type 1 gene product interacts with ras p21. *Cell*. 63:843-9.
- Matsushita, T., Y.Y. Chan, A. Kawanami, G. Balmes, G.E. Landreth, and S. Murakami. 2009. Extracellular signal-regulated kinase 1 (ERK1) and ERK2 play essential roles in osteoblast differentiation and in supporting osteoclastogenesis. *Mol Cell Biol*. 29:5843-57.
- McCormick, F. 1993. Signal transduction. How receptors turn Ras on. *Nature*. 363:15-6.
- Mercer, K., S. Giblett, S. Green, D. Lloyd, S. DaRocha Dias, M. Plumb, R. Marais, and C. Pritchard. 2005. Expression of endogenous oncogenic V600EB-raf induces proliferation and developmental defects in mice and transformation of primary fibroblasts. *Cancer Res*. 65:11493-500.
- Mulcahy, L.S., M.R. Smith, and D.W. Stacey. 1985. Requirement for ras proto-oncogene function during serum-stimulated growth of NIH 3T3 cells. *Nature*. 313:241-3.
- Murakami, S., G. Balmes, S. McKinney, Z. Zhang, D. Givol, and B. de Crombrughe. 2004. Constitutive activation of MEK1 in chondrocytes causes Stat1-independent achondroplasia-like dwarfism and rescues the Fgfr3-deficient mouse phenotype. *Genes Dev*. 18:290-305.
- Murakami, S., M. Kan, W.L. McKeehan, and B. de Crombrughe. 2000. Up-regulation of the chondrogenic Sox9 gene by fibroblast growth factors is mediated by the mitogen-activated protein kinase pathway. *Proc Natl Acad Sci U S A*. 97:1113-8.
- Nakamura, T., M. Colbert, M. Krenz, J.D. Molkentin, H.S. Hahn, G.W. Dorn, 2nd, and J. Robbins. 2007. Mediating ERK 1/2 signaling rescues congenital heart defects in a mouse model of Noonan syndrome. *J Clin Invest*. 117:2123-32.
- Nakamura, T., J. Gulick, R. Pratt, and J. Robbins. 2009. Noonan syndrome is associated with enhanced pERK activity, the repression of which can prevent craniofacial malformations. *Proc Natl Acad Sci U S A*. 106:15436-41.
- Nakashima, K., X. Zhou, G. Kunkel, Z. Zhang, J.M. Deng, R.R. Behringer, and B. de Crombrughe. 2002. The novel zinc finger-containing transcription factor osterix is required for osteoblast differentiation and bone formation. *Cell*. 108:17-29.

- Naski, M.C., J.S. Colvin, J.D. Coffin, and D.M. Ornitz. 1998. Repression of hedgehog signaling and BMP4 expression in growth plate cartilage by fibroblast growth factor receptor 3. *Development*. 125:4977-88.
- Ornitz, D.M., and P.J. Marie. 2002. FGF signaling pathways in endochondral and intramembranous bone development and human genetic disease. *Genes Dev*. 16:1446-65.
- Otto, F., A.P. Thornell, T. Crompton, A. Denzel, K.C. Gilmour, I.R. Rosewell, G.W. Stamp, R.S. Beddington, S. Mundlos, B.R. Olsen, P.B. Selby, and M.J. Owen. 1997. Cbfa1, a candidate gene for cleidocranial dysplasia syndrome, is essential for osteoblast differentiation and bone development. *Cell*. 89:765-71.
- Pandit, B., A. Sarkozy, L.A. Pennacchio, C. Carta, K. Oishi, S. Martinelli, E.A. Pogna, W. Schackwitz, A. Ustaszewska, A. Landstrom, J.M. Bos, S.R. Ommen, G. Esposito, F. Lepri, C. Faul, P. Mundel, J.P. Lopez Siguero, R. Tenconi, A. Selicorni, C. Rossi, L. Mazzanti, I. Torrente, B. Marino, M.C. Digilio, G. Zampino, M.J. Ackerman, B. Dallapiccola, M. Tartaglia, and B.D. Gelb. 2007. Gain-of-function RAF1 mutations cause Noonan and LEOPARD syndromes with hypertrophic cardiomyopathy. *Nat Genet*. 39:1007-12.
- Parada, L.F., C.J. Tabin, C. Shih, and R.A. Weinberg. 1982. Human EJ bladder carcinoma oncogene is homologue of Harvey sarcoma virus ras gene. *Nature*. 297:474-8.
- Pulciani, S., E. Santos, A.V. Lauver, L.K. Long, K.C. Robbins, and M. Barbacid. 1982. Oncogenes in human tumor cell lines: molecular cloning of a transforming gene from human bladder carcinoma cells. *Proc Natl Acad Sci U S A*. 79:2845-9.
- Razzaque, M.A., T. Nishizawa, Y. Komoike, H. Yagi, M. Furutani, R. Amo, M. Kamisago, K. Momma, H. Katayama, M. Nakagawa, Y. Fujiwara, M. Matsushima, K. Mizuno, M. Tokuyama, H. Hirota, J. Muneuchi, T. Higashinakagawa, and R. Matsuoka. 2007. Germline gain-of-function mutations in RAF1 cause Noonan syndrome. *Nat Genet*. 39:1013-7.
- Roberts, A.E., T. Araki, K.D. Swanson, K.T. Montgomery, T.A. Schiripo, V.A. Joshi, L. Li, Y. Yassin, A.M. Tamburino, B.G. Neel, and R.S. Kucherlapati. 2007. Germline gain-of-function mutations in SOS1 cause Noonan syndrome. *Nat Genet*. 39:70-4.
- Rodan, G.A., and T.J. Martin. 2000. Therapeutic approaches to bone diseases. *Science*. 289:1508-14.

- Rodda, S.J., and A.P. McMahon. 2006. Distinct roles for Hedgehog and canonical Wnt signaling in specification, differentiation and maintenance of osteoblast progenitors. *Development*. 133:3231-44.
- Sahni, M., D.C. Ambrosetti, A. Mansukhani, R. Gertner, D. Levy, and C. Basilico. 1999. FGF signaling inhibits chondrocyte proliferation and regulates bone development through the STAT-1 pathway. *Genes Dev*. 13:1361-6.
- Schindeler, A., and D.G. Little. 2006. Ras-MAPK signaling in osteogenic differentiation: friend or foe? *J Bone Miner Res*. 21:1331-8.
- Schubbert, S., M. Zenker, S.L. Rowe, S. Boll, C. Klein, G. Bollag, I. van der Burgt, L. Musante, V. Kalscheuer, L.E. Wehner, H. Nguyen, B. West, K.Y. Zhang, E. Sistermans, A. Rauch, C.M. Niemeyer, K. Shannon, and C.P. Kratz. 2006. Germline KRAS mutations cause Noonan syndrome. *Nat Genet*. 38:331-6.
- Shaw, A.C., K. Kalidas, A.H. Crosby, S. Jeffery, and M.A. Patton. 2007. The natural history of Noonan syndrome: a long-term follow-up study. *Arch Dis Child*. 92:128-32.
- Shih, C., L.C. Padhy, M. Murray, and R.A. Weinberg. 1981. Transforming genes of carcinomas and neuroblastomas introduced into mouse fibroblasts. *Nature*. 290:261-4.
- Shih, C., and R.A. Weinberg. 1982. Isolation of a transforming sequence from a human bladder carcinoma cell line. *Cell*. 29:161-9.
- Shih, T.Y., A.G. Papageorge, P.E. Stokes, M.O. Weeks, and E.M. Scolnick. 1980. Guanine nucleotide-binding and autophosphorylating activities associated with the p21src protein of Harvey murine sarcoma virus. *Nature*. 287:686-91.
- Side, L.E., and K.M. Shannon. 1997. Myeloid disorders in infants with Noonan syndrome and a resident's "rule" recalled. *J Pediatr*. 130:857-9.
- Simonet, W.S., D.L. Lacey, C.R. Dunstan, M. Kelley, M.S. Chang, R. Luthy, H.Q. Nguyen, S. Wooden, L. Bennett, T. Boone, G. Shimamoto, M. DeRose, R. Elliott, A. Colombero, H.L. Tan, G. Trail, J. Sullivan, E. Davy, N. Bucay, L. Renshaw-Gegg, T.M. Hughes, D. Hill, W. Pattison, P. Campbell, S. Sander, G. Van, J. Tarpley, P. Derby, R. Lee, and W.J. Boyle. 1997. Osteoprotegerin: a novel secreted protein involved in the regulation of bone density. *Cell*. 89:309-19.
- St-Jacques, B., M. Hammerschmidt, and A.P. McMahon. 1999. Indian hedgehog signaling regulates proliferation and differentiation of chondrocytes and is essential for bone formation. *Genes Dev*. 13:2072-86.

- Tabin, C.J., S.M. Bradley, C.I. Bargmann, R.A. Weinberg, A.G. Papageorge, E.M. Scolnick, R. Dhar, D.R. Lowy, and E.H. Chang. 1982. Mechanism of activation of a human oncogene. *Nature*. 300:143-9.
- Tai, G., J.M. Polak, A.E. Bishop, I. Christodoulou, and L.D. Buttery. 2004. Differentiation of osteoblasts from murine embryonic stem cells by overexpression of the transcriptional factor osterix. *Tissue Eng*. 10:1456-66.
- Taparowsky, E., Y. Suard, O. Fasano, K. Shimizu, M. Goldfarb, and M. Wigler. 1982. Activation of the T24 bladder carcinoma transforming gene is linked to a single amino acid change. *Nature*. 300:762-5.
- Tartaglia, M., E.L. Mehler, R. Goldberg, G. Zampino, H.G. Brunner, H. Kremer, I. van der Burgt, A.H. Crosby, A. Ion, S. Jeffery, K. Kalidas, M.A. Patton, R.S. Kucherlapati, and B.D. Gelb. 2001. Mutations in PTPN11, encoding the protein tyrosine phosphatase SHP-2, cause Noonan syndrome. *Nat Genet*. 29:465-8.
- Tartaglia, M., L.A. Pennacchio, C. Zhao, K.K. Yadav, V. Fodale, A. Sarkozy, B. Pandit, K. Oishi, S. Martinelli, W. Schackwitz, A. Ustaszewska, J. Martin, J. Bristow, C. Carta, F. Lepri, C. Neri, I. Vasta, K. Gibson, C.J. Curry, J.P. Sigüero, M.C. Digilio, G. Zampino, B. Dallapiccola, D. Bar-Sagi, and B.D. Gelb. 2007. Gain-of-function SOS1 mutations cause a distinctive form of Noonan syndrome. *Nat Genet*. 39:75-9.
- Tidyman, W.E., and K.A. Rauen. 2009. The RASopathies: developmental syndromes of Ras/MAPK pathway dysregulation. *Curr Opin Genet Dev*. 19:230-6.
- Trahey, M., and F. McCormick. 1987. A cytoplasmic protein stimulates normal N-ras p21 GTPase, but does not affect oncogenic mutants. *Science*. 238:542-5.
- Tuveson, D.A., A.T. Shaw, N.A. Willis, D.P. Silver, E.L. Jackson, S. Chang, K.L. Mercer, R. Grochow, H. Hock, D. Crowley, S.R. Hingorani, T. Zaks, C. King, M.A. Jacobetz, L. Wang, R.T. Bronson, S.H. Orkin, R.A. DePinho, and T. Jacks. 2004. Endogenous oncogenic K-ras(G12D) stimulates proliferation and widespread neoplastic and developmental defects. *Cancer Cell*. 5:375-87.
- Vojtek, A.B., S.M. Hollenberg, and J.A. Cooper. 1993. Mammalian Ras interacts directly with the serine/threonine kinase Raf. *Cell*. 74:205-14.
- Wang, W., J.S. Nyman, K. Ono, D.A. Stevenson, X. Yang, and F. Elefteriou. 2011. Mice lacking Nf1 in osteochondroprogenitor cells display skeletal dysplasia similar to patients with neurofibromatosis type I. *Hum Mol Genet*. 20:3910-24.
- Winkler, D.G., M.K. Sutherland, J.C. Geoghegan, C. Yu, T. Hayes, J.E. Skonier, D. Shpektor, M. Jonas, B.R. Kovacevich, K. Staehling-Hampton, M. Appleby, M.E.

- Brunkow, and J.A. Latham. 2003. Osteocyte control of bone formation via sclerostin, a novel BMP antagonist. *EMBO J.* 22:6267-76.
- Wu, X., S. Chen, Y. He, S.D. Rhodes, K.S. Mohammad, X. Li, X. Yang, L. Jiang, G. Nalepa, P. Snider, A.G. Robling, D.W. Clapp, S.J. Conway, T.A. Guise, and F.C. Yang. 2011a. The haploinsufficient hematopoietic microenvironment is critical to the pathological fracture repair in murine models of neurofibromatosis type 1. *PLoS One.* 6:e24917.
- Wu, X., J. Simpson, J.H. Hong, K.H. Kim, N.K. Thavarajah, P.H. Backx, B.G. Neel, and T. Araki. 2011b. MEK-ERK pathway modulation ameliorates disease phenotypes in a mouse model of Noonan syndrome associated with the Raf1(L613V) mutation. *J Clin Invest.* 121:1009-25.
- Xiao, G., D. Jiang, P. Thomas, M.D. Benson, K. Guan, G. Karsenty, and R.T. Franceschi. 2000. MAPK pathways activate and phosphorylate the osteoblast-specific transcription factor, Cbfa1. *J Biol Chem.* 275:4453-9.
- Xiong, J., M. Onal, R.L. Jilka, R.S. Weinstein, S.C. Manolagas, and C.A. O'Brien. 2011. Matrix-embedded cells control osteoclast formation. *Nat Med.* 17:1235-41.
- Yagi, K., K. Tsuji, A. Nifuji, K. Shinomiya, K. Nakashima, B. DeCrombrughe, and M. Noda. 2003. Bone morphogenetic protein-2 enhances osterix gene expression in chondrocytes. *J Cell Biochem.* 88:1077-83.
- Yang, X., K. Matsuda, P. Bialek, S. Jacquot, H.C. Masuoka, T. Schinke, L. Li, S. Brancorsini, P. Sassone-Corsi, T.M. Townes, A. Hanauer, and G. Karsenty. 2004. ATF4 is a substrate of RSK2 and an essential regulator of osteoblast biology; implication for Coffin-Lowry Syndrome. *Cell.* 117:387-98.
- Yoon, S., and R. Seger. 2006. The extracellular signal-regulated kinase: multiple substrates regulate diverse cellular functions. *Growth Factors.* 24:21-44.
- Yoshida, H., S. Hayashi, T. Kunisada, M. Ogawa, S. Nishikawa, H. Okamura, T. Sudo, and L.D. Shultz. 1990. The murine mutation osteopetrosis is in the coding region of the macrophage colony stimulating factor gene. *Nature.* 345:442-4.
- Yu, X., S. Chen, O.L. Potter, S.M. Murthy, J. Li, J.M. Pulcini, N. Ohashi, T. Winata, E.T. Everett, D. Ingram, W.D. Clapp, and J.M. Hock. 2005. Neurofibromin and its inactivation of Ras are prerequisites for osteoblast functioning. *Bone.* 36:793-802.
- Zelzer, E., and B.R. Olsen. 2003. The genetic basis for skeletal diseases. *Nature.* 423:343-8.
- Zetser, A., D. Frank, and E. Bengal. 2001. MAP kinase converts MyoD into an instructive muscle differentiation factor in *Xenopus*. *Dev Biol.* 240:168-81.

Zhou, G., V. Lefebvre, Z. Zhang, H. Eberspaecher, and B. de Crombrughe. 1998. Three high mobility group-like sequences within a 48-base pair enhancer of the Col2a1 gene are required for cartilage-specific expression in vivo. *J Biol Chem.* 273:14989-97.

Zou, W., M.B. Greenblatt, J.H. Shim, S. Kant, B. Zhai, S. Lotinun, N. Brady, D.Z. Hu, S.P. Gygi, R. Baron, R.J. Davis, D. Jones, and L.H. Glimcher. 2011. MLK3 regulates bone development downstream of the faciogenital dysplasia protein FGD1 in mice. *J Clin Invest.* 121:4383-92.

## Chapter 2

**Mesenchymal K-ras<sup>G12D</sup> expression leads to Noonan Syndrome-like bone defects that can be rescued by MEK inhibition.**

Simona Nedelcu, Tatsuya Kobayashi and Jacqueline A Lees

SN generated all of the data with contribution from TK for Supplemental Figure 2.  
SN and JAL designed the study, analyzed the data and wrote the paper.

## ABSTRACT

Activating germline K-ras mutations cause Noonan syndrome (NS), which is characterized by several developmental deficits including cardiac defects, cognitive delays and skeletal abnormalities. NS patients have increased signaling through the MAPK pathway. To model NS skeletal defects and understand the effect of hyperactive K-ras signaling on normal limb development, we generated a mouse model in which activated K-ras<sup>G12D</sup> was expressed specifically in mesenchymal progenitors of the limb bud. These mice display short, abnormally mineralized long bones that phenocopy those of NS patients. This defect was first apparent at E14.5, and was characterized by a delay in bone collar formation. Coincident mutation of p53 had no effect on the K-ras<sup>G12D</sup> induced bone defect, arguing that it does not result from senescence or apoptosis. Instead, our data indicate a defect in the appearance and localization of committed osteoblasts. Most importantly, we found that *in utero* delivery of a MEK inhibitor between E10.5 and E14.5 is sufficient to completely suppress the ability of activated K-ras to induce NS-like long bone defects in embryogenesis. Taken together, our data define a critical point in mid-gestation in which elevated MAPK signaling impairs bone collar formation and yield NS-like limb defects. Moreover, they offer insight into possible therapeutic strategies for skeletal defects in patients with Noonan Syndrome.

## INTRODUCTION

Noonan Syndrome (NS) is an autosomal dominant genetic disease that appears with a frequency of 1/1000-1/2500 in newborns (Allanson, 1987; Noonan, 1994); (Nora et al., 1974). It is one of a group of developmental disorders, called RASopathies, which result from germline mutations in components of the RAS/MAPK pathway that increase signaling (Tidyman and Rauen, 2009). Mutations in *PTPN11*, *SOS1*, *RAF1* and *KRAS* have all been identified in NS (Tidyman and Rauen, 2009). 2% of NS patients have activating *KRAS* mutations (Schubbert et al., 2006; Zenker et al., 2007). *KRAS* encodes a small GTPase protein that functions as molecular switch to regulate cell proliferation, differentiation and apoptosis by propagating signals from the tyrosine kinase membrane receptors to various intracellular effector cascades including the MAPK pathway.

NS is characterized by defects in various mesenchymal tissues including cardiovascular abnormalities, short stature, craniofacial dysmorphia and skeletal defects (Nora et al., 1974). Mouse models bearing germline mutations in *PTPN11*, *SOS1* and *RAF1* have been developed, and these display the spectrum of gross anatomical defects characteristic of NS (Araki et al., 2009; Nakamura et al., 2007; Wu et al., 2011). Analysis of these models, as well as an endocardium-specific *PTPN11* mutant mouse strain, has yielded key insight into the underlying basis of the cardiac abnormalities that are the primary cause of death of NS patients (Araki et al., 2004; Araki et al., 2009; Nakamura et al., 2007). Other studies have investigated the nature of the craniofacial defects (Nakamura et al., 2009; Wu et al., 2011). Most importantly, analysis of these NS mouse models showed that

continuous prenatal or postnatal treatment with MEK inhibitors is sufficient to rescue both the cardiac and craniofacial defects (Nakamura et al., 2009; Wu et al., 2011). Given these findings, MEK inhibitors and other Ras pathway modulators are being evaluated for treatment of NS patients (Rauen et al., 2011).

The skeletal deformities represent a major challenge in the life of NS patients, but their etiology is not well understood. Dual-energy X-ray absorptiometry has shown that bone mineralization is decreased in NS children (Choudhry et al., 2012) and urine analysis suggests that this reflects increased bone resorption (Stevenson et al., 2011). However, no biopsies or histological sections of NS patients' bones have been reported. Similarly, the skeletal defects of the *PTPN11*, *SOS1* and *RAF1* mutant NS mouse models have not been probed. At a broader level, the effect of constitutive MAPK pathway activation on osteoblast and chondrocyte differentiation is an area of active investigation (Nakamura et al., 2009; Schindeler and Little, 2006). Indeed, the function of Ras/MAPK signaling in osteogenesis is controversial, as some studies suggest it promotes osteoblast differentiation while others support a suppressive role (Schindeler and Little, 2006).

In this study, we have generated a mouse strain in which activated K-ras<sup>G12D</sup> is expressed in the mesenchyme of the developing embryo to yield hyperactivation of the Ras/MAPK pathway. These animals display severe skeletal abnormalities that resemble those occurring in NS patients. In particular, these animals have profoundly shorter and thicker long bones. Analysis of the timed pregnancies shows that these defects are first apparent around embryonic day E14.5, as evidenced by defective formation of the bone collar. Finally, we show that MEK

inhibitor delivery between E10.5 and E14.5 is sufficient to rescue the bone phenotype. This has important implications for treatment of NS patients.

## RESULTS

### **K-ras<sup>G12D</sup> expression in mesenchymal lineage results in skeletal defects that are reminiscent of those seen in Noonan Syndrome patients.**

Our goal was to generate a mouse model that had hyperactivation of Ras/MAPK signaling within the mesenchymal progenitors of the developing embryo. To achieve this, we used a knock-in mouse strain (Supplemental Fig 1) in which expression of an activating *K-ras* allele, *K-ras<sup>G12D</sup>*, is controlled by the CRE recombinase (Tuveson et al., 2004). Germline *K-ras<sup>G12D</sup>* mutation is not seen in NS patients presumably, extrapolating from mouse studies (Tuveson et al., 2004), because it causes embryonic lethality. However, we chose it for this study because it yields potent Ras/MAPK signaling. We crossed the conditional inducible *K-ras<sup>G12D</sup>* mouse with the *Prx1-Cre* transgenic (Harada and Rodan, 2003; Martin and Olson, 2000), which expresses CRE in mesenchymal progenitors of the limb bud from embryonic day 9.5. Using reporter mice, we have previously confirmed that *Prx1-Cre* yields efficient recombination in bone, cartilage, skeletal muscle and fat lineages (Calo et al., 2010).

We found that *Prx1-Cre;K-ras<sup>G12D</sup>* mutants were present at the expected Mendelian ratio at E18.5 (data not shown). However, these mutants failed to thrive. The majority died soon after birth, but rare mutants lived up to, but never beyond, three weeks of age. Notably, the *Prx1-Cre;K-ras<sup>G12D</sup>* mutants were all significantly

smaller than their wild type littermates, as illustrated with representative P18 littermates (Figure 1A). Most importantly, these animals had profound skeletal abnormalities. In particular, the front and hind limbs were greatly shortened, and the fingers and toes were clubbed (Figure 1B). These anatomical defects are reminiscent of those occurring in human NS patients. Additionally, we found that the hind limbs of *Prx1-Cre;K-ras<sup>G12D</sup>* mutants were paralyzed, impeding their ability to feed from their mothers and likely explaining their failure to thrive.

We conducted H&E staining of limb sections taken from neonatal animals, and found that the limbs of *Prx1-Cre;K-ras<sup>G12D</sup>* mutants were consistently shorter and thicker than those of wildtype controls (see Figure 1C, D). The mutant limbs had abnormal mineralization in both the primary and the secondary ossification centers, and there was a dramatic increase in the density of the trabecular bone. Indeed, the bone marrow space was almost completely absent in *Prx1-Cre;K-ras<sup>G12D</sup>* mutants. Additionally, cartilage defects were clearly apparent. The growth plates of the long bones were highly disorganized (Figure 1C) and higher magnification showed that the layer of hypertrophic chondrocytes was much thinner in the mutants than in littermate controls (Figure 1D). Notably, these cartilage defects resembled those arising in mice with activating MEK1 mutations (Ge et al., 2007), suggesting that the bone defects reflect hyperactivation of the MAPK pathway; a conclusion we validate below.

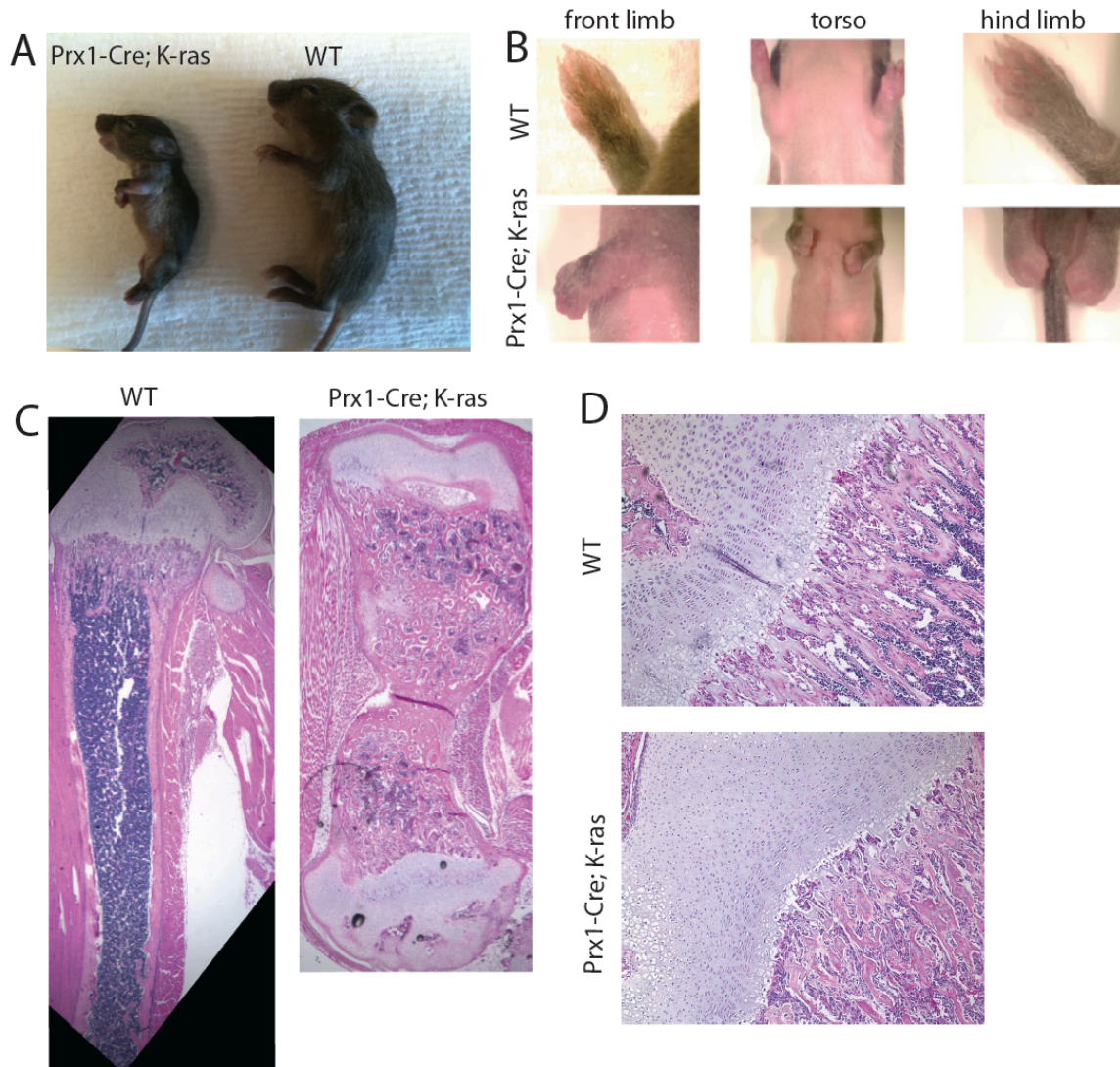


**Figure 1. Expression of K-ras<sup>G12D</sup> in mesenchymal progenitors causes Noonan-like skeletal defects.** (A) Representative 18-days old *Prx1-Cre;K-ras<sup>G12D</sup>* neonates are smaller than their wildtype littermates and (A,B) their front and hind limbs are greatly shortened and have clubbed feet. (C). H&E staining of femurs sections from P18 neonates shows that the mutant femur is shorter and thicker and it has increased mineralization of the trabecular region. This, and (D) higher magnification shows that the mutant growth plate is disorganized and layer of hypertrophic chondrocytes is reduced.

We also conducted a careful analysis of other tissues within *Prx1-Cre;K-ras<sup>G12D</sup>* mutants. We observed no detectable craniofacial abnormalities (even though the heads appeared slightly smaller) and no cardiac defects (data not shown). This is entirely consistent with the fact that *Prx-cre* is poorly expressed in the bones of the head and in cardiac tissue (Martin and Olson, 2000). We confirmed that the conditional *K-ras<sup>G12D</sup>* allele was efficiently recombined in all of the known *Prx-Cre* expressing tissues including the long bones, skeletal muscle and adipose tissue but found that the resulting K-ras<sup>G12D</sup> expression yielded developmental abnormalities only in the bone (Figure 1 and data not shown). This striking specificity for bone, but not muscle or fat, defects recapitulates that seen in human NS patients with germline RAS/MAPK pathway mutations.

To confirm the skeletal defect results solely from the expression of K-ras<sup>G12D</sup> expression in bone and cartilage, we also crossed the conditional *K-ras<sup>G12D</sup>* allele with the *Col2-Cre* transgenic mice. This induces Cre expression to the Col2-positive osteochondral progenitors, which give rise to both chondrocytes and osteoblasts in the developing bone. As anticipated, these animals displayed skeletal defects similar to those of the *Prx1-Cre;K-ras<sup>G12D</sup>* mutants including shorter and thicker long bones with increased trabecular and cortical bone mineralization and aberrant growth plates (Supplemental Figure 2).

**The skeletal defects in *Prx1-Cre, K-ras<sup>G12D</sup>* mice reflect a defect in bone collar development at E14.5.**

To establish the etiology of the skeletal defects resulting from *K-ras<sup>G12D</sup>* expression, we used timed pregnancies to compare skeletal development in *Prx1-Cre;K-ras<sup>G12D</sup>* mutants with those of wildtype controls at various stages of embryonic development. Initially, we examined skeletons of E18.5 embryos using whole mount staining with Alizarin Red, which detects calcium deposits within mineralized bone, and Alcian Blue, which detects the cartilage matrix (Figure 2A). As with the neonatal mutant phenotypes, the *Prx1-Cre;K-ras<sup>G12D</sup>* E18.5 embryos clearly displayed major skeletal abnormalities of which the most striking was the shortening and thickening of both front and hind limbs (Figure 2A and B). We also conducted Alizarin Red staining of histological sections from E18.5 limbs (Figure 2C). Again, we found that the site of mineralization was abnormal and the level of trabecular and cortical bone was greatly increased (Figure 2C). The defective nature of long bone differentiation was further illuminated by H&E staining of sections, which revealed both the abnormal pattern of mineralization and the presence of atypical growth plates within the greatly shortened and thickened bones (Figure 2D).

We examined successively earlier development stages to determine when these defects arose. At E16.5, we observed a similar aberrant bone morphology that included both shortened and thickened long bones (data not shown). Our analysis traced the earliest morphological indication of bone abnormalities to E14.5 (Figure

2D). At this stage, the cartilage template of the developing long bones was the appropriate

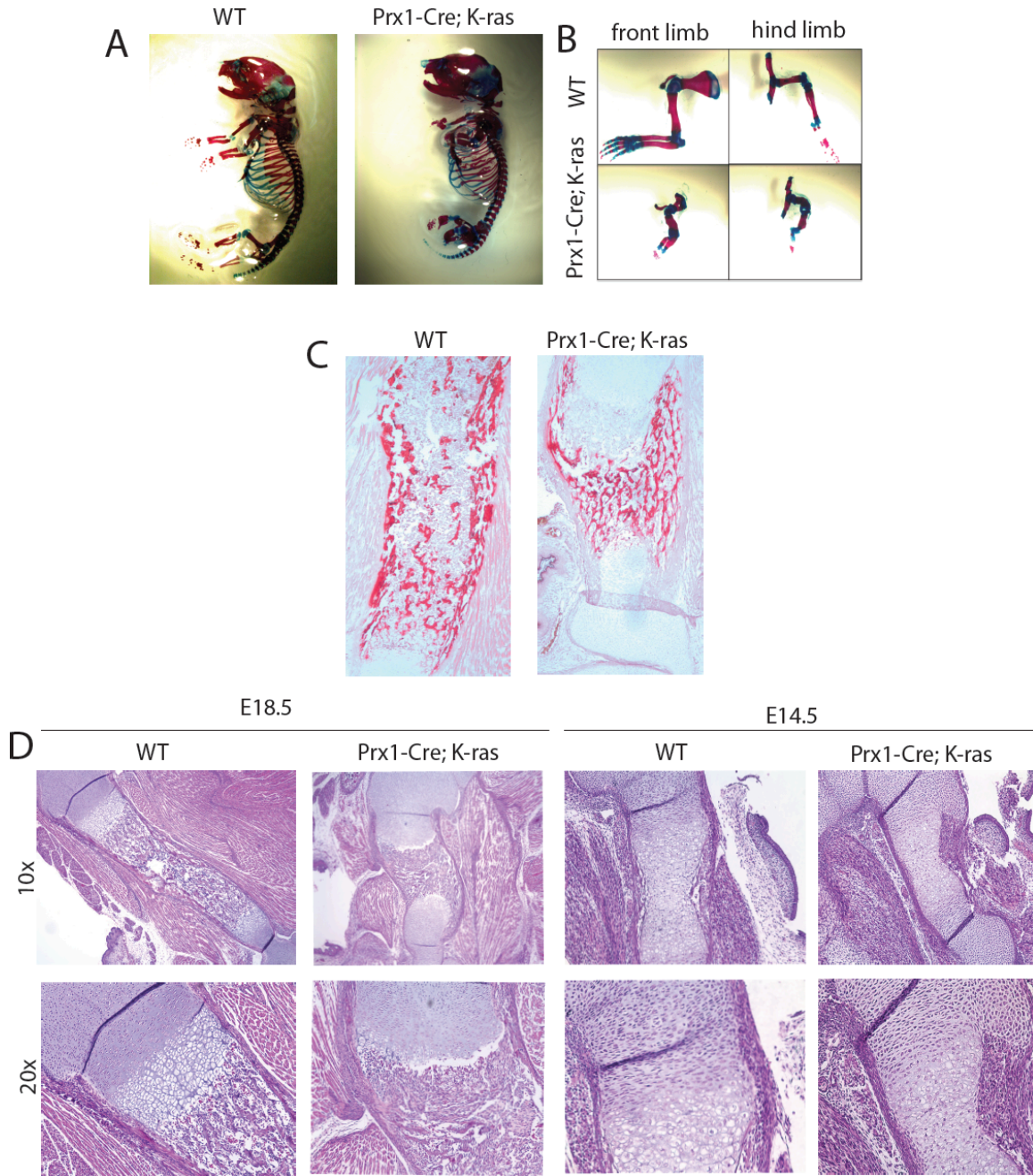


**Figure 2. Defects in *Prx1-Cre; K-ras<sup>G12D</sup>* mutants appear early during embryonic development.** (A, B) Whole mount skeletal staining with Alizarin Red (staining bone) and Alcian Blue (staining cartilage) of E18.5 embryos show that mutants have aberrant skeletal development and that the mutant limbs are much smaller than wildtype controls. (C) Alizarin Red staining of E18.5 humerus sections shows an increased level of trabecular bone in the mutants. (D) H&E staining of sections from representative E18.5 and E14.5 embryo limbs shows defects at all stages.

size in *Prx1-Cre;K-ras<sup>G12D</sup>* mutants and the perichondrium also appeared grossly normal. However, while we consistently detected both bone collar formation and the invasion of osteoblasts into the center of the bone in wildtype E14.5 embryos (n = 5/5) both processes were completely absent in the *Prx1-Cre;K-ras<sup>G12D</sup>* E14.5 (n = 5/5) littermates (Figure 2D). Since these are observed in E16.5 *Prx1-Cre;K-ras<sup>G12D</sup>* embryos, we conclude that hyperactivation of K-ras signaling acts to delay bone differentiation at this critical developmental stage.

It is well established that the activated K-ras can induce senescence and/or apoptosis *in vitro* or *in vivo* in a p53 dependent manner. We hypothesized that these events could be responsible for the disrupted bone development in our *Prx1-Cre;K-ras<sup>G12D</sup>* mutants. To test this possibility, we crossed a conditional *p53* mutant allele into our *Prx1-Cre;K-ras<sup>G12D</sup>* model. Remarkably, we found that p53 loss did not alter the bone phenotype of *Prx1-Cre;K-ras<sup>G12D</sup>* embryos (data not shown), arguing that the defect is unlikely to result from either programmed cell death or senescence.

These findings suggest that activated K-ras has a more direct effect on the differentiation process. To address this possibility, we examined humerus sections from E16.5 and E14.5 embryos by *in situ* hybridization (ISH) for classic bone and cartilage markers. Specifically, we stained for Col2, a marker of osteochondral progenitors and also some adult chondrocytes, and Col1, a marker of committed osteoblasts. Col2 staining was observed in the epiphyses of *Prx1-Cre;K-ras<sup>G12D</sup>* mutant bones at both E16.5 and E14.5 and, despite the aberrant bone morphology, the pattern closely resembled that of wildtype controls (Figure 3A and B). In

contrast, Col1 staining differed greatly between mutants and controls. At E16.5, Col1 was detected at significant levels in both genotypes, confirming the presence of committed osteoblasts, but the locations were completely different (Figure 3A). Specifically, Col1 staining was detected along the length of the bone shaft and the internal region where trabecular bone is formed in wildtype limbs, but it was largely concentrated outside of the developing bone structure in the mutants. Furthermore, at E14.5, we found that Col1 staining was restricted to the bone collar in wildtypes but was completely absent in *Prx1-Cre;K-ras<sup>G12D</sup>* mutant long bones.

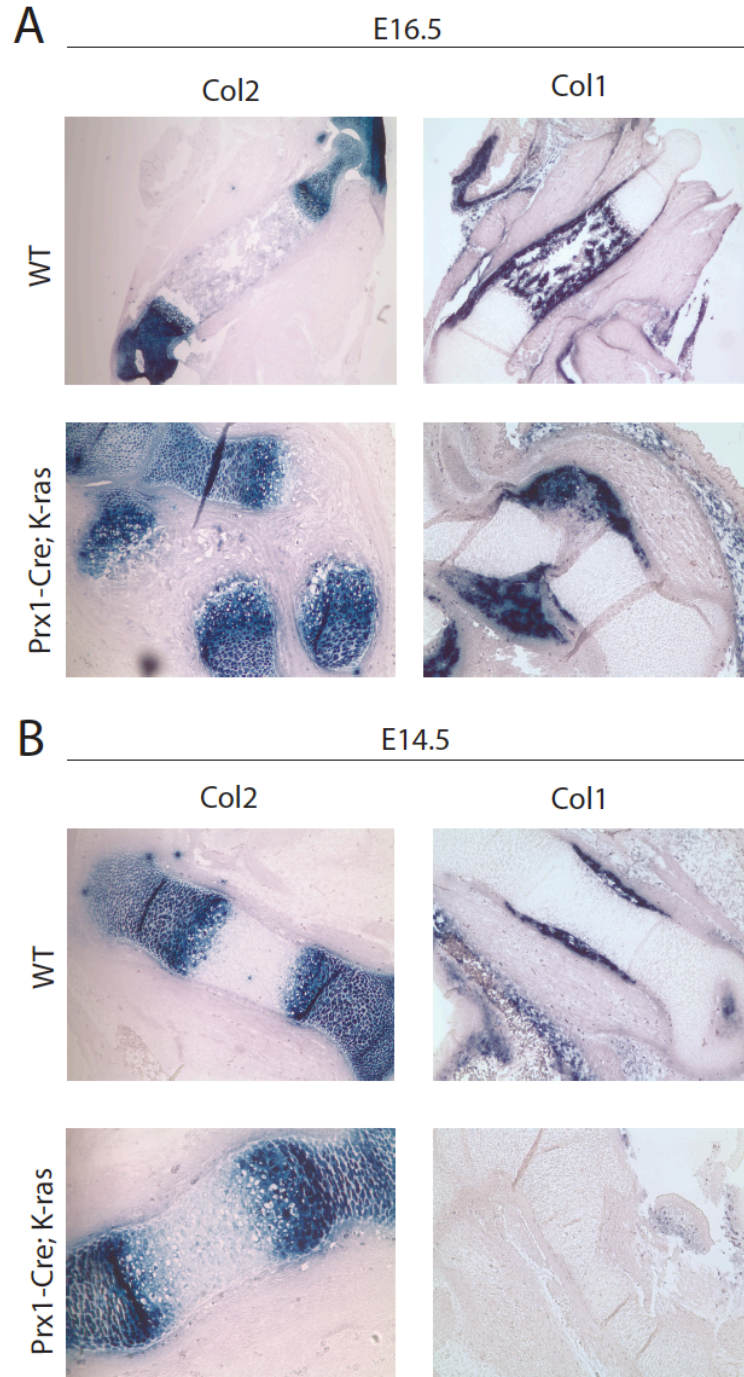


**Figure 3. In situ hybridization for bone and cartilage markers on E16.5 and E14.5 limb sections. (A) ISH for Col1 and Col2 in E16.5 embryos. (B). ISH for Col2 and Col1 in E14.5 embryos (staining is described in more detail in the text).**

Taken together, these findings argue that hyperactivation of K-ras<sup>G12D</sup> in the limb mesenchymal progenitors does not prevent the formation, or appropriate localization, of the Col2-positive osteochondral progenitors or committed chondrocytes. Instead, K-ras<sup>G12D</sup> significantly delays the timing of appearance of the Col1-positive, osteoblastic lineages and thus formation of the bone collar. These Col1-positive cells eventually arise but they accumulate in an aberrant location surrounding, rather than inside, the bone. This has the potential to explain the observed deposition of bone in the lateral rather than the longitudinal axis, which results in thicker but shorter bones.

**Administration of MEK inhibitor during E10.5 to E14.5 is sufficient to rescue the Noonan Syndrome-like bone defect in *Prx1-Cre; K-ras<sup>G12D</sup>* mutants.**

There is considerable evidence to indicate that the defects in RASopathies, including NS, result from deregulation of MAPK signaling. Thus, we screened our K-ras<sup>G12D</sup> mutant long bones for evidence of MAPK activation by conducting IHC for phospho-MEK (pMEK), the active form of MEK. At E14.5, we detected elevated expression of pMEK in the nuclei of the chondrocytes in *Prx1-Cre;K-ras<sup>G12D</sup>* mutants versus wildtype littermates (Figure 4A). Thus, the MAPK pathway is hyperactivated at the timepoint we identified as being critical in the development of the NS-like mutant bone phenotype.

Given this finding, we wanted to determine whether inhibition of MAPK signaling could suppress this bone development defect. For this, we used the ATP-noncompetitive MEK inhibitor PD0325901 (Barrett et al., 2008). This drug (at

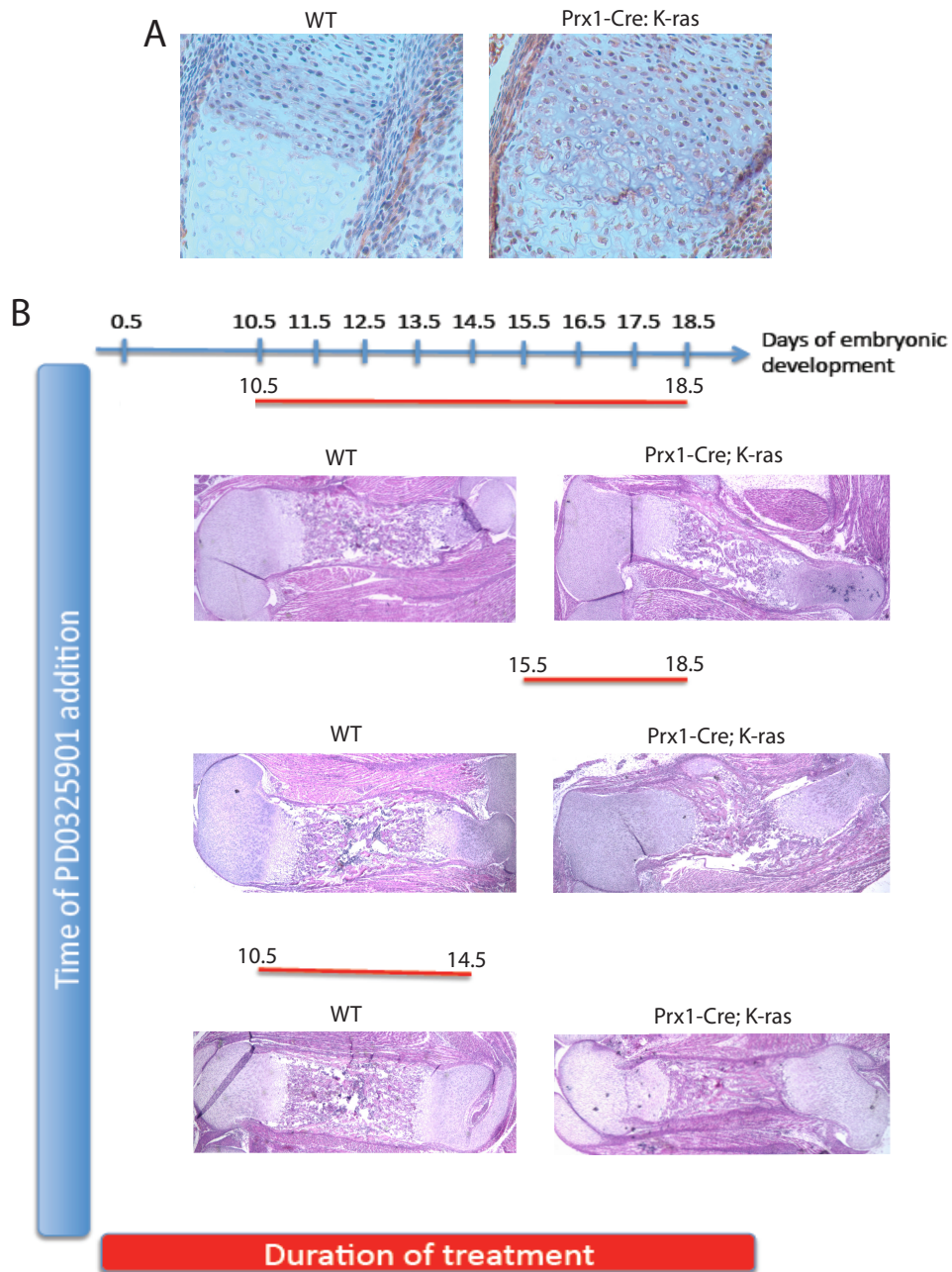


**Figure 4. MEK inhibitor treatment during embryonic development rescues the bone phenotypes in *Prx1-Cre;K-ras<sup>G12D</sup>* mutants.** (A) IHC for pMEK at E14.5 shows that there is increased pMEK expression in the mutant. (B) MEK inhibitor treatment strategy described in more detail in text.

5mg/kg body weight), or vehicle control, was injected into the peritoneal cavity of pregnant mothers for various time periods. Initially, we began treatment at E10.5 and continued daily until E17.5 to essentially encompass the full time period of *K-ras<sup>G12D</sup>* activation. The females (n=6 for drug and 4 for vehicle control) were sacrificed at E18.5 and the limbs of the resulting *Prx1-Cre; K-ras<sup>G12D</sup>* mutant embryos (n=4 for drug and 3 for vehicle control) were compared to those of littermate controls (n=4 for drug and 3 for vehicle control) by sectioning and H&E analysis. Importantly, we saw no detectable difference in the long bones of wildtype pups treated with drug versus vehicle control (Figure 4B and data not shown), indicating that MEK inhibition does not modulate normal bone development. In stark contrast, we found that treatment with MEK inhibitor, but never the vehicle control, was sufficient to completely rescue the bone defect of the *Prx1-Cre; K-ras<sup>G12D</sup>* mutants (Figure 4B). Specifically, the PD0325901-treated, mutant limbs were of normal length and thickness, and their levels of mineralization and of trabecular bone were now comparable to wildtype controls. Thus, we conclude that MAPK signaling is the primary cause of the bone growth defect in the *Prx1-Cre; K-ras<sup>G12D</sup>* mice, and that MEK inhibition is an effective treatment.

We wanted to determine whether shorter periods of drug treatment could also suppress the bone defects. Thus, we conducted additional experiments using treatment only between E15.5 and E18.5 or E10.5 and E14.5. Again, embryos were collected at E18.5 and their limbs analyzed. As with the longer treatment, bone development was unaltered in wildtype pups exposed to drug in either time

window (Figure 4B and data not shown). For the E15.5 to E18.5 treatment window, the *Prx1-Cre, K-ras<sup>G12D</sup>* limbs displayed the full spectrum of NS-like defects in the case of both vehicle (n=5) and drug (n=3) treated animals. In contrast, the mutant bone defect was completely rescued in animals treated from E10.5 to E14.5 with MEK inhibitor (n=5) but not vehicle (n=3) (Figure 4B). Taken together, these experiments define a critical time in bone development, between E10.5 and approximately E14.5, in which upregulation of MAPK pathway signaling is sufficient to derail the process of bone development and yield long bone defects that phenocopy those of NS patients.

## DISCUSSION

In this study, we have generated mouse models in which activation of K-ras<sup>G12D</sup> in either the mesenchymal progenitors of the limb bud, or the Col2-positive osteochondroprogenitors, recapitulates the stunted long bones encountered in patients with Noonan Syndrome. We show that the bones are greatly shortened and thickened, and they display abnormal mineralization in both primary and secondary ossification centers and a stark increase in the density of the trabecular bone. We also see disorganization of the growth plate, and a thinning of hypertrophic chondrocyte layer. The presence of both bone and cartilage abnormalities suggests defects in both osteoblast and chondrocyte differentiation and/or disruption of interplay between the two.

Our phenotypic analysis tracked the origin of the K-ras<sup>G12D</sup> mutant bone defects to around E14.5. At this time, the mutant bones show no sign of either bone collar formation or invasion of osteoblasts into the center of the bone. The osteoblasts that form the bone collar are known to originate from Col2-positive osteochondroprogenitors, which migrate to the site of the future bone collar and differentiate into Col1-positive cells (Maes et al., 2010). We showed that the K-ras<sup>G12D</sup> mutant bones display a normal pattern of Col2 staining at both E14.5 and E16.5. In contrast, Col1 staining is completely absent at E14.5 and it accumulates in an aberrant location surrounding, rather than inside, the bone at E16.5. Based on these observations, we hypothesize that activated K-ras<sup>G12D</sup> somehow impairs the migration of Col2-positive osteochondroprogenitors, such that they eventually differentiate into Col1-positive osteoblasts in the wrong location. Notably, this

migration defect hypothesis is supported by prior analyses of zebrafish models for Noonan and Cardio-Facio-Cutaneous syndromes, which showed that expression of mutant RAS, BRAF or MEK disrupts cell movement defects during gastrulation (Anastasaki et al., 2009; Runtuwene et al., 2011). In the future, it would be interesting to stain for Indian Hedgehog (Ihh) because this signals to the Col2-positive osteochondroprogenitors at the perichondrium and directs them to commit to the osteoblast lineages. Additionally, we could conduct lineage tracing of the Col2-positive osteochondroprogenitors through the generation and analysis of *Col2-CreERT;K-ras<sup>G12D</sup>;GFP* embryos. Ultimately, regardless of the underlying mechanism, we believe that the inappropriate positioning of the Col1-positive osteoblasts is responsible for the aberrant deposition of bone in the lateral, rather than the longitudinal, axis.

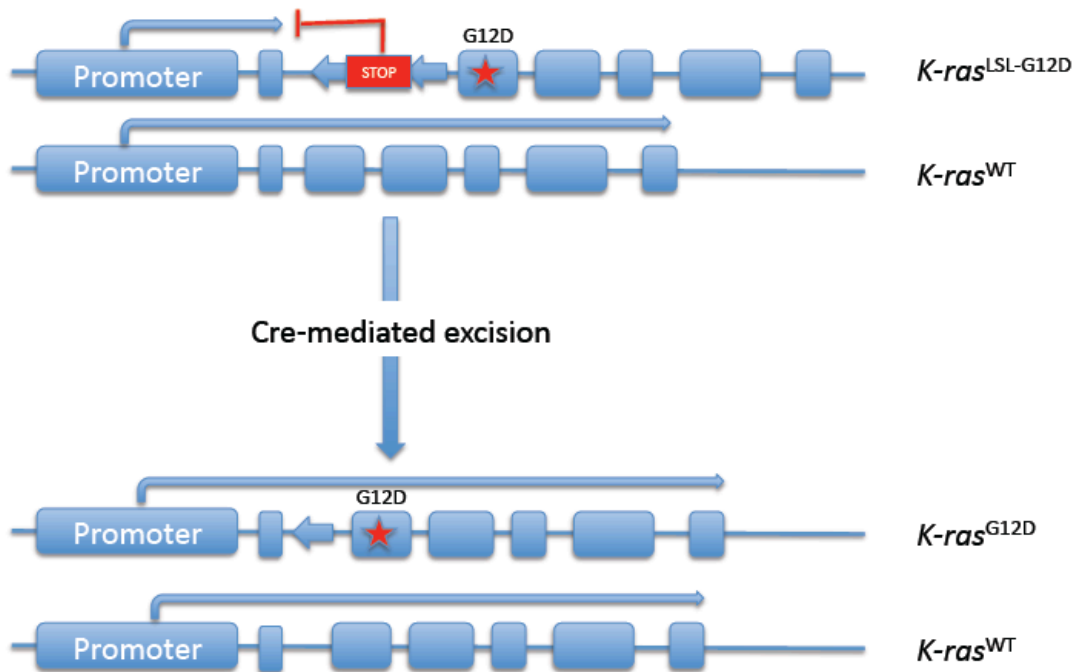
In addition to elucidating the etiology of NS bone defects, our study provided insight into their potential treatment. Specifically, we found that delivery of the MEK inhibitor PD0325901 *in utero* was sufficient to completely prevent the NS-like long bone defects up to E18.5. Indeed, this treatment was effective when limited to a relatively small time window between E10.5 and around E14.5. This yields two key conclusions. First, it argues that MAPK pathway activation is important for the development of the NS-like mutant bone phenotype. Second, it proves that the bone developmental defects result from errors that occur during the establishment of bone commitment, presumably the defect in bone collar formation discussed above.

It is important to note that our data do not establish whether the bone defects are a direct consequence of elevated MAPK signaling, or whether it reflects a

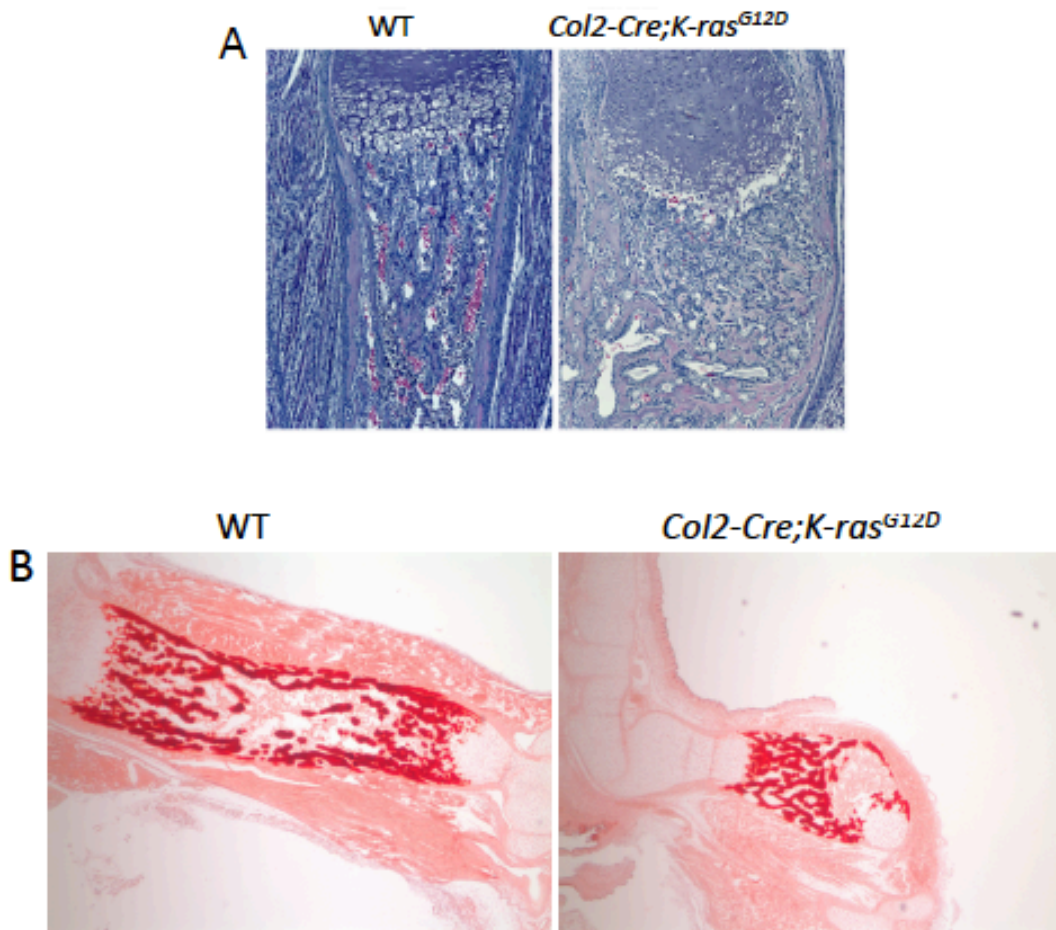
downstream event. Specifically, prior studies have established that MAPK signaling can induce negative feedback loops (REF) and that treatment with MEK inhibitors modulates the expression of such upstream MAPK regulators in K-ras mutant tumors (Nissan et al., 2013). Additionally, since we examined the PD0325901 treated embryos at E18.5, we cannot preclude the possibility that the presence of activated K-ras<sup>G12D</sup> signaling post birth might lead to the formation of other bone defects in neonates/adult animals. We tried to address this issue by allowing treated mothers to give birth. Unfortunately, we found that almost all of the pups died irrespective of their genotype, and irrespective of whether the mother was injected with MEK inhibitor or vehicle control. Thus, we believe that injection scheme itself causes the mothers to reject their pups, and additional experiments will be required to address this question.

Over the past decade, the development and performance of clinical trials in patients with Noonan Syndrome has rapidly increased (Rauen et al., 2011). Many of these trials aim to modify signaling through the aberrantly activated Ras/MAPK pathway. MEK inhibitors have been tested in preclinical mouse models, including PTPN11 and RAF mutant models of Noonan Syndrome and an FGFR model of Apert Syndrome, and shown to suppress both the cardiac and craniofacial defects (Chen et al., 2010; Nakamura et al., 2009; Wu et al., 2011) Our study now shows that such treatments would also successfully rescue the skeletal defects of NS patients.

## SUPPLEMENTAL FIGURES



**Supplemental Figure 1.** (Tuveson et al., 2004) Schematic representation of the *K-ras<sup>G12D</sup>* gene showing the loxP sites and location of the STOP cassette. Expression of Cre removes the STOP cassette located in front of the second exon containing the G12D point mutation, and allows expression of a constitutive form of K-ras.



**Supplemental Figure 2.** *Col2;K-ras<sup>G12D</sup>* mice (at day 1 after birth) have a similar phenotype as the *Prx1-Cre;K-ras<sup>G12D</sup>* mutant mice as shown by (A) H&E sections and (B) Alizarin Red staining of limb sections. The limbs are shorter and thicker, and display increased trabecular and cortical mineralization.

## **MATERIALS AND METHODS**

### *Mouse husbandry and tissue collection*

Animal procedures followed protocols approved by MIT's Committee on Animal Care. The *Osxl-Cre*, *Prx1-Cre* and *K-ras<sup>G12D/+</sup>* animals were maintained on a mixed genetic background. Tissues were fixed in PBS with 3.7% formaldehyde. Prior to paraffin sectioning, soft tissues were dehydrated via an ethanol series, while bone-containing tissue was decalcified in 0.46M EDTA, 2.5% Ammonium Hydroxide pH 7.2. All paraffin embedded sections were cut at 5µm, dewaxed and stained with H&E.

### *Skeletal stainings*

Embryos were sacrificed, skinned and eviscerated. The remaining tissue was fixed in 95% ethanol for 4 days, transferred to acetone for 3 days, and subsequently transferred to staining solution of 0.015% Alcian Blue 8GX (Sigma), 0.005% Alizarin Red S(Sigma), and 5% glacial acetic acid in ethanol at 37°C for 2 days and at room temperature for a one more day. Tissue was cleared in 1% potassium hydroxide for several days and then stored in glycerol.

### *Alizarin Red staining*

For Alizarin red staining, sections were rinsed in water, placed in 2% Alizarin Red S (pH 4.2) for 5 min, dipped 20 times in acetone followed by acetone:xylene (1:1), and then mounted.

### *In situ hybridization*

Tissues were fixed in 4% paraformaldehyde/PBS overnight at 4°C, processed, embedded in paraffin, and cut. Non-radioactive ISH, with digoxigenin (DIG)-labeled probes (Chung et al., 1998; Murtaugh et al., 2001) was performed as described previously (Chung et al., 1998). In brief, sections were postfixated with 4% PFA-PBS for 15 min. After washing with PBS, sections were digested with 1 pg/ml proteinase-K (37 C; 15 min) in PBS and again treated with 4% PFA-PBS (10 min). Sections then were sequentially washed with PBS, acetylated with 0.25% acetic anhydride in the presence of triethanolamine (1 M; 10 min), dehydrated with increasing concentrations of ethanol, and air dried. Hybridizations with complementary RNAs were performed in a humidified chamber in a solution containing 50% formamide, 10% dextran sulfate, 1 X Denhardt's solution, 600 mM NaCl, 10 mM Tris-HCl, 1 mM EDTA, 50 mM dithiothreitol, 0.25% sodium dodecyl sulfate, and 200 pg/ml transfer RNA (18 h; 55 C). After hybridization, sections were washed briefly with 5 X SSC at 50°C, 50% formamide- X SSC (50 C; 30 min), and 10 mM Tris-HCl (pH 7.6)-500 mM NaCl-1 mM EDTA (TNE; 37 C; 10 min). Sections were then treated with 10 pg/ml ribonuclease-A in TNE (37 C; 30 min). After being washed with TNE, sections were incubated once with 2 X SSC (50 C; 20 min) and twice with 0.2 X SSC (50 C; 20 min), dehydrated with increasing concentrations of ethanol, and air-dried.

### *Immunohistochemistry*

pMEK immunohistochemistry was performed with a modified citric acid unmasking protocol. Briefly, paraffin was removed from slides, followed by incubation in 0.5%

H2O2/methanol for 15 min and antigen retrieval using citrate buffer (pH 6.0) in a microwave for 15 min. Slides were blocked for 1 h at room temperature in 10% goat serum in PBS. pMEK (1:100; Cell Signaling, 9661) antibodies were used in 0.15% Triton/PBS overnight at 4°C. Secondary antibodies (Vector Laboratories) were used at 1:200 in PBS with 2% goat serum, detected using a DAB substrate kit (Vector Laboratories), and counterstained with haematoxylin.

#### *Drug treatment*

N-([R]-2,3-dihydroxy-propoxy)-3,4-difluoro-2-(2-fluoro-4-iodo-phenylamino)-benzamide (PD0325901) was synthesized according to the disclosure in document WO2007042885(A2). All chemicals necessary for the synthesis were purchased from Sigma-Aldrich. PD0325901 was dissolved in DMSO at a concentration of 50 mg/ml, then resuspended in vehicle (0.5% hydroxypropyl methylcellulose with 0.2% Tween 80) at a concentration of 0.5 mg/ml, and injected i.p. (5 mg/kg BW) daily for the indicated times. Control mice were injected with vehicle.

## REFERENCES

- Allanson, J.E. 1987. Noonan syndrome. *J Med Genet.* 24:9-13.
- Anastasaki, C., A.L. Estep, R. Marais, K.A. Rauen, and E.E. Patton. 2009. Kinase-activating and kinase-impaired cardio-facio-cutaneous syndrome alleles have activity during zebrafish development and are sensitive to small molecule inhibitors. *Hum Mol Genet.* 18:2543-54.
- Araki, T., G. Chan, S. Newbigging, L. Morikawa, R.T. Bronson, and B.G. Neel. 2009. Noonan syndrome cardiac defects are caused by PTPN11 acting in endocardium to enhance endocardial-mesenchymal transformation. *Proc Natl Acad Sci U S A.* 106:4736-41.
- Barrett, S.D., A.J. Bridges, D.T. Dudley, A.R. Saltiel, J.H. Fergus, C.M. Flamme, A.M. Delaney, M. Kaufman, S. LePage, W.R. Leopold, S.A. Przybranowski, J. Sebolt-Leopold, K. Van Becelaere, A.M. Doherty, R.M. Kennedy, D. Marston, W.A. Howard, Jr., Y. Smith, J.S. Warmus, and H. Tecle. 2008. The discovery of the benzhydroxamate MEK inhibitors CI-1040 and PD 0325901. *Bioorg Med Chem Lett.* 18:6501-4.
- Calo, E., J.A. Quintero-Estades, P.S. Danielian, S. Nedelcu, S.D. Berman, and J.A. Lees. 2010. Rb regulates fate choice and lineage commitment in vivo. *Nature.* 466:1110-4.
- Chen, P.C., H. Wakimoto, D. Conner, T. Araki, T. Yuan, A. Roberts, C. Seidman, R. Bronson, B. Neel, J.G. Seidman, and R. Kucherlapati. 2010. Activation of multiple signaling pathways causes developmental defects in mice with a Noonan syndrome-associated *Sos1* mutation. *J Clin Invest.* 120:4353-65.
- Choudhry, K.S., M. Grover, A.A. Tran, E. O'Brian Smith, K.J. Ellis, and B.H. Lee. 2012. Decreased bone mineralization in children with Noonan syndrome: another consequence of dysregulated RAS MAPKinase pathway? *Mol Genet Metab.* 106:237-40.
- Chung, U.I., B. Lanske, K. Lee, E. Li, and H. Kronenberg. 1998. The parathyroid hormone/parathyroid hormone-related peptide receptor coordinates endochondral bone development by directly controlling chondrocyte differentiation. *Proc Natl Acad Sci U S A.* 95:13030-5.
- Ge, C., G. Xiao, D. Jiang, and R.T. Franceschi. 2007. Critical role of the extracellular signal-regulated kinase-MAPK pathway in osteoblast differentiation and skeletal development. *J Cell Biol.* 176:709-18.
- Harada, S., and G.A. Rodan. 2003. Control of osteoblast function and regulation of bone mass. *Nature.* 423:349-55.

- Maes, C., T. Kobayashi, M.K. Selig, S. Torrekens, S.I. Roth, S. Mackem, G. Carmeliet, and H.M. Kronenberg. 2010. Osteoblast precursors, but not mature osteoblasts, move into developing and fractured bones along with invading blood vessels. *Dev Cell*. 19:329-44.
- Martin, J.F., and E.N. Olson. 2000. Identification of a prx1 limb enhancer. *Genesis*. 26:225-9.
- Murtaugh, L.C., L. Zeng, J.H. Chyung, and A.B. Lassar. 2001. The chick transcriptional repressor Nkx3.2 acts downstream of Shh to promote BMP-dependent axial chondrogenesis. *Dev Cell*. 1:411-22.
- Nakamura, T., M. Colbert, M. Krenz, J.D. Molkenin, H.S. Hahn, G.W. Dorn, 2nd, and J. Robbins. 2007. Mediating ERK 1/2 signaling rescues congenital heart defects in a mouse model of Noonan syndrome. *J Clin Invest*. 117:2123-32.
- Nakamura, T., J. Gulick, R. Pratt, and J. Robbins. 2009. Noonan syndrome is associated with enhanced pERK activity, the repression of which can prevent craniofacial malformations. *Proc Natl Acad Sci U S A*. 106:15436-41.
- Nissan, M.H., N. Rosen, and D.B. Solit. 2013. ERK Pathway Inhibitors: How Low Should We Go? *Cancer Discov*. 3:719-21.
- Noonan, J.A. 1994. Noonan syndrome. An update and review for the primary pediatrician. *Clin Pediatr (Phila)*. 33:548-55.
- Nora, J.J., A.H. Nora, A.K. Sinha, R.D. Spangler, and H.A. Lubs. 1974. The Ullrich-Noonan syndrome (Turner phenotype). *Am J Dis Child*. 127:48-55.
- Rauen, K.A., A. Banerjee, W.R. Bishop, J.O. Lauchle, F. McCormick, M. McMahon, T. Melese, P.N. Munster, S. Nadaf, R.J. Packer, J. Sebolt-Leopold, and D.H. Viskochil. 2011. Costello and cardio-facio-cutaneous syndromes: Moving toward clinical trials in RASopathies. *Am J Med Genet C Semin Med Genet*. 157:136-46.
- Runtuwene, V., M. van Eekelen, J. Overvoorde, H. Rehmann, H.G. Yntema, W.M. Nillesen, A. van Haeringen, I. van der Burgt, B. Burgering, and J. den Hertog. 2011. Noonan syndrome gain-of-function mutations in NRAS cause zebrafish gastrulation defects. *Dis Model Mech*. 4:393-9.
- Schindeler, A., and D.G. Little. 2006. Ras-MAPK signaling in osteogenic differentiation: friend or foe? *J Bone Miner Res*. 21:1331-8.
- Schubbert, S., M. Zenker, S.L. Rowe, S. Boll, C. Klein, G. Bollag, I. van der Burgt, L. Musante, V. Kalscheuer, L.E. Wehner, H. Nguyen, B. West, K.Y. Zhang, E. Siermans, A. Rauch, C.M. Niemeyer, K. Shannon, and C.P. Kratz. 2006. Germline KRAS mutations cause Noonan syndrome. *Nat Genet*. 38:331-6.

- Stevenson, D.A., E.L. Schwarz, J.C. Carey, D.H. Viskochil, H. Hanson, S. Bauer, H.Y. Weng, T. Greene, K. Reinker, J. Swensen, R.J. Chan, F.C. Yang, L. Senbanjo, Z. Yang, R. Mao, and M. Pasquali. 2011. Bone resorption in syndromes of the Ras/MAPK pathway. *Clin Genet.* 80:566-73.
- Tidyman, W.E., and K.A. Rauen. 2009. The RASopathies: developmental syndromes of Ras/MAPK pathway dysregulation. *Curr Opin Genet Dev.* 19:230-6.
- Tuveson, D.A., A.T. Shaw, N.A. Willis, D.P. Silver, E.L. Jackson, S. Chang, K.L. Mercer, R. Grochow, H. Hock, D. Crowley, S.R. Hingorani, T. Zaks, C. King, M.A. Jacobetz, L. Wang, R.T. Bronson, S.H. Orkin, R.A. DePinho, and T. Jacks. 2004. Endogenous oncogenic K-ras(G12D) stimulates proliferation and widespread neoplastic and developmental defects. *Cancer Cell.* 5:375-87.
- Wu, X., J. Simpson, J.H. Hong, K.H. Kim, N.K. Thavarajah, P.H. Backx, B.G. Neel, and T. Araki. 2011. MEK-ERK pathway modulation ameliorates disease phenotypes in a mouse model of Noonan syndrome associated with the Raf1(L613V) mutation. *J Clin Invest.* 121:1009-25.
- Zenker, M., K. Lehmann, A.L. Schulz, H. Barth, D. Hansmann, R. Koenig, R. Korinthenberg, M. Kreiss-Nachtsheim, P. Meinecke, S. Morlot, S. Mundlos, A.S. Quante, S. Raskin, D. Schnabel, L.E. Wehner, C.P. Kratz, D. Horn, and K. Kutsche. 2007. Expansion of the genotypic and phenotypic spectrum in patients with KRAS germline mutations. *J Med Genet.* 44:131-5.

## **ACKNOWLEDGEMENTS**

We thank Shigeki Nishimori and Tatsuya Kobayashi (MGH) for providing the *in situ* hybridization RNA probes for Col2, Col1 and OPN markers. We thank Tatsuya Kobayashi for generating the *Col2;K-ras<sup>G12D</sup>* mutant mice. We thank Tatsuya Kobayashi and Henry Kronenberg (MGH) for useful discussions regarding the experimental design of studies presented in this chapter. We thank the members of the Lees and Kronenberg laboratory for valuable input during this study. This work was supported by an NCI/NIH grant to J.A.L. who is a Ludwig Scholar at MIT. S.N. was supported by a D.H. Koch Graduate Fellowship.

## Chapter 3

### **Expression of K-ras<sup>G12D</sup> in the osteoblast lineage differentially affects osteoblast differentiation in a time-dependent manner**

Simona Nedelcu and Jacqueline A Lees

SN conducted all of the experiments in this study. SN and JAL designed the study, analyzed the data and wrote the paper.

## ABSTRACT

The Ras/mitogen-activated protein kinase (MAPK) pathway provides a major link between the cell surface and the nucleus to control cell proliferation and differentiation upon stimulation with various extracellular signals. However, its *in vivo* role in skeletal development is still controversial, with some studies supporting a positive role for Ras/MAPK, and others arguing for a suppressive role. In this study, we have elucidated the effects of ectopic K-ras/MAPK signaling on skeletal development by using transgenic mice in which expression of K-ras<sup>G12D</sup> was induced specifically in osteoblast precursors at different times during the development. This analysis defined two distinct time windows when during which expression of active K-ras resulted in opposing phenotypes. In the first time window, between approximately E11.5 and E14.5, K-ras<sup>G12D</sup> expression greatly impaired osteoblast terminal differentiation and thus caused dramatic bone loss. In stark contrast, activation of K-ras<sup>G12D</sup> at birth greatly enhanced osteoblast differentiation and consequently mineralization of the long bones. Thus, our data show that appropriate Ras/MAPK pathway signaling plays a critical role in osteoblast differentiation and that K-ras<sup>G12D</sup> has distinct, temporal dependent roles on osteoblastic fate.

## INTRODUCTION

Bone development is a carefully regulated process, in which expression of specific factors characterizes each stage of development. The first step in endochondral bone formation, is the migration of Prx expressing mesenchymal progenitors to the matrices of the future bones (Supp Fig 1-A). The cells located at the center of these mesenchymal condensations will differentiate into Col2 expressing chondrocytes and start proliferating (Supp Fig 1-B). Chondrocytes at the center of the template stop proliferating and mature into ColX hypertrophic chondrocytes that will undergo apoptosis (Supp Fig 1-C). The death of hypertrophic chondrocytes is followed by recruitment of Osx expressing osteoblasts (Supp Fig 1-D). At the primary spongiosa (PS), Osx expressing osteoblasts differentiate into Col1-expressing committed osteoblasts. The Col1 osteoblasts further differentiate into Osetocalcin (OC) expressing osteoblasts. Some other markers that characterize final stages of osteoblast differentiation are ALP (Alkaline phosphatase), BSP (Bone sialo-protein) and OPN (Osteopontin). Concurrently, the cells at the periphery of the chondrocyte template will become the perichondrium which signals back and forth with the underlying cartilage and causes Col2 expressing chondrocytes to differentiate into Col1-osteoblasts, that form the bone collar (Supp Fig 1-D). In the long bones, chondrocytes continue to proliferate and cartilage matrix is deposited, causing the bone to grow in length. This is a process that starts in embryogenesis and is completed around puberty.

In bone biology, the MAPK signaling pathway has been implicated in the response of bone to a variety of signals, including growth factors (Chen et al., 2004;

Hurley et al., 1996; Xiao et al., 2002), extracellular matrix–integrin binding (Takeuchi et al., 1997), and mechanical loading (You et al., 2001). Direct evidence for the importance of MAPK itself in bone development comes from analysis of Erk 1 mutant mice. Specifically, deletion of Erk1, in either the germline or only in the developing limb mesenchyme, yields reduced bone mineralization thereby establishing the necessity of ERK activity for proper osteoblast function (Matsushita et al., 2009).

Many other mouse models have probed the role of upstream regulators of MAPK in bone development (Ge et al., 2007; Greenblatt et al., 2010; Zou et al., 2011). These have led to some confusion as some studies support a stimulatory role for this signaling pathway while others propose an inhibitory role. Indeed, even the same player has been reported to have opposing roles in different settings. For example, *in vivo* deletion of *NF1* (a Ras inhibitor) in committed osteoblasts using the *Col1* promoter yielded increased bone mass (Elefteriou et al., 2006) whereas *NF1* deletion in osteochondral progenitors using the *Col2* promoter impaired osteoblast differentiation and reduced bone mass (Wang et al., 2011; Wu et al., 2011b). These contradictory results strongly suggest that loss of NF1, and consequent deregulation of MAPK, can either activate or repress osteoblast development when triggered in uncommitted multipotent progenitors versus mature osteoblasts.

In Chapter 2, we showed that constitutive expression of K-ras in limb mesenchymal progenitors and subsequent lineages, including osteoblasts, yielded abnormal mineralization of the long bones. Here, we wanted to directly assess the consequences of inducing constitutive K-ras expression only in osteoblast

precursors. To this end, we developed a transgenic mouse strategy involving selective expression of an active form of K-ras specifically in osteoblast progenitors using the osterix (*Osx1*) promoter. Importantly, the *Osx1-Cre* mice were designed such that the expression of Cre recombinase is under the transcriptional regulation of the *Osx1* promoter and also a Tet-Off cassette. This Tet-Off cassette provides an additional level of temporal control specifically within the osteoblast lineage (Rodda and McMahon, 2006). Thus, we can not only restrict the expression of activated K-ras to osteoblasts progenitors, but further limit its activation to specific time points during embryonic development or after birth. Using this system, we show that expression of K-ras<sup>G12D</sup> during embryonic development leads to a decrease in bone mass, while expression of K-ras<sup>G12D</sup> after birth leads to an increase in bone mass. This explains previously contradictory results in the field about the effects of aberrant MAPK during bone development by suggesting that activated K-ras can both stimulate and inhibit osteoblast differentiation, depending on the time it is expressed in osteoblasts. Additionally, our data reinforce our prior conclusion (Chapter 2) that E14.5 is a critical period in bone development, and it directly proves that hyperactive K-ras<sup>G12D</sup> acts to disrupt osteoblast fate commitment *in vivo* and *in vitro*.

## RESULTS

### **Embryonic expression of K-ras<sup>G12D</sup> in osteoblast progenitors leads to strong skeletal defects in both long bones and the calvaria.**

To test the consequences of osteoblast-restricted expression of K-ras<sup>G12D</sup>, we utilized Osterix-Cre transgenic mice (*Osx1-Cre*) to restrict Cre expression to osteoblasts progenitors. Endogenous *Osx* is first expressed around E12.5 (Nakashima et al., 2002). However, the *Osx1-Cre* mice were designed such that the *Osx1* promoter controls the expression of a Tet-Off Cre recombinase protein (Rodda and McMahon, 2006). In a Tet-Off system a tetracycline-controlled transactivator protein (*tTA*) regulates expression of a target gene that is under transcriptional control of a tetracycline-responsive promoter element (TRE). In the absence of doxycycline (Dox), *tTA* binds to the TRE and activates transcription of the target gene. In contrast, the presence of Dox prevents *tTA* binding to the TRE and thus the target gene remains inactive (Gossen and Bujard, 1992; Kistner et al., 1996). Thus, in *Osx1-Cre* mice Cre should be expressed in the osteoblast lineage specifically in the absence, but not the presence, of doxycycline.

First, we wanted to validate the tissue-specific localization of the *Osx1-Cre* transgene expression. For this, we crossed *Osx1-Cre* mice with the LSL-*LacZ* reporter mice. We performed  $\beta$ -galactosidase staining of whole *Osx1-Cre;LacZ* embryos at day 1 of life and showed that the *Osx* transgene expression is restricted to the bones of the skeleton and the calvaria, and is not present in muscle or fat (Figure 1A). Having established this specificity, we generated *Osx1-Cre;K-ras<sup>G12D</sup>* mice. Initially, we

allowed these to develop in the absence of doxycycline administration, such that activated K-ras<sup>G12D</sup> is induced at the normal time of *Osx* expression. *Osx1-Cre;K-ras<sup>G12D</sup>* mice were expected to arise from our cross at a frequency of 1 in 4 but we found no surviving mutants from more than 10 litters. Our analysis showed that the *Osx1-Cre;K-ras<sup>G12D</sup>* mutants all died at birth. The mutant mice were all smaller than the wild type littermates and they displayed strong bone abnormalities (Figure 1B). Whole mount skeletal staining with Alizarin Red and Alcian Blue showed that the skeleton of P1 mutants was severely abnormal; their spines were severely deformed and there were also clear defects in the development of the long bones and the calvaria (Figure 1B). Specifically, the mutant long bones were shorter and much thinner than those of wild type littermate controls. Furthermore, mutant limbs were thin, brittle and fractured at the middle (Figure 1C). Additionally, the calvaria of the *Osx1-Cre;K-ras<sup>G12D</sup>* mutants was under-mineralized, reminiscent of the long bones phenotype (Figure 1D). Since the calvaria forms through direct differentiation of mesenchymal progenitors to osteoblasts, with no cartilage intermediate, we can conclude that hyperactive K-ras expression causes a cell intrinsic defect in osteoblast differentiation.

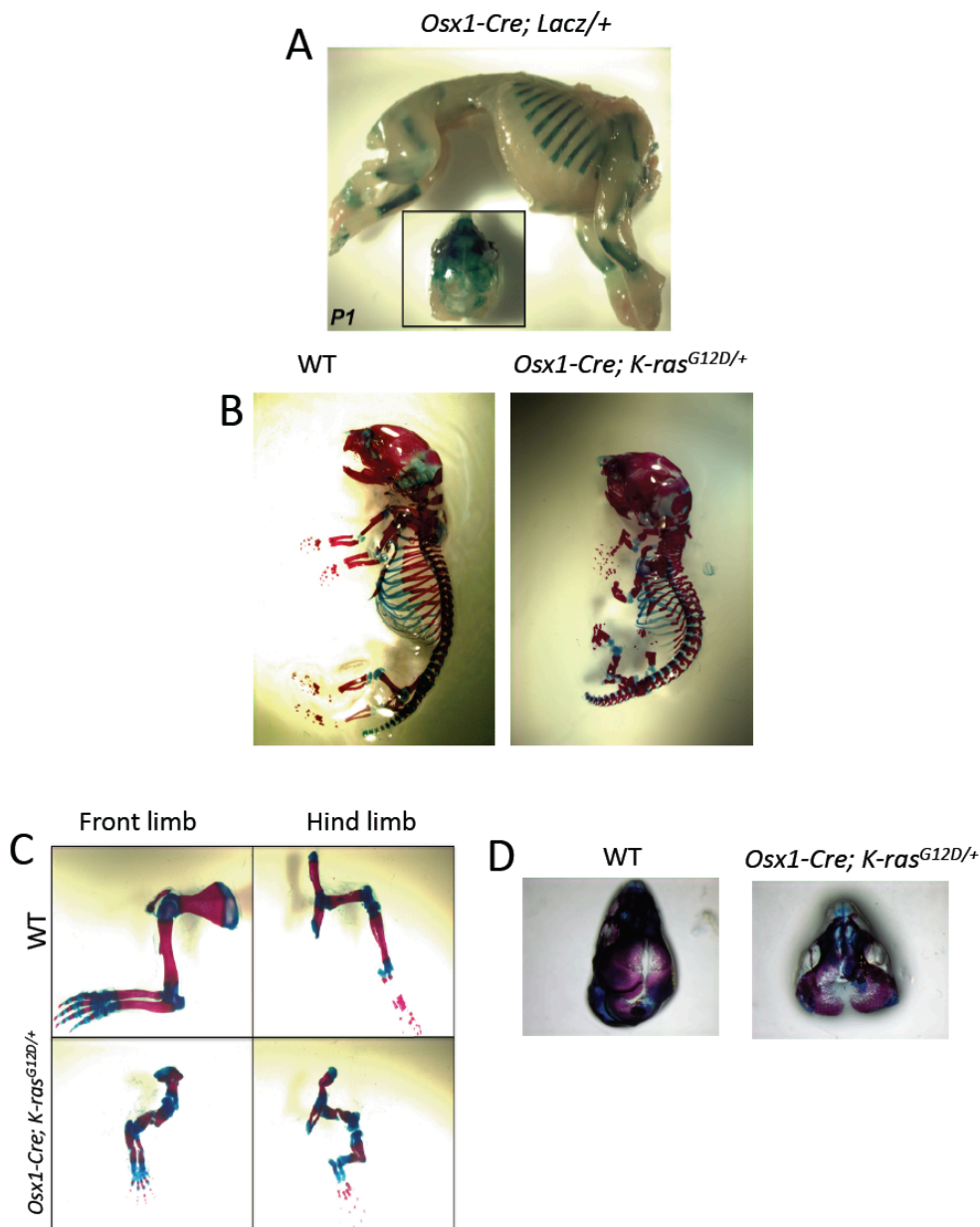


**Figure 1. Embryonic expression of K-ras<sup>G12D</sup> in osteoblast precursors under the control of the Osx1 promoter leads to strong skeletal defects.** (A) β-galactosidase staining of *Osx1-Cre;LacZ* mice shows that the Osx transgene is exclusively expressed in the bones of the skeleton and in the skull. (B) Whole mount staining with Alizarin Red and Alcian Blue of P1 pups shows that *Osx1-Cre;K-ras<sup>G12D</sup>* mice have strong skeletal defects. (C) Limbs of the mutant mice are shorter than those of wildtype controls and they are fractured at the middle. (D) The calvaria of mutant mice is undermineralized compared to controls, as visualized by staining with Alizarin Red and Alcian Blue.

## **Bone fractures appear early during embryonic development in *Osx1-Cre;K-ras<sup>G12D</sup>* mutants**

We analyzed limbs at consecutive days of embryonic development to identify when the defect appears in *Osx1-Cre;K-ras<sup>G12D</sup>* mutants. Additionally, we wanted to determine whether the fractures we see at birth result from the mechanical stress of birth or whether they exist *in utero* and thus reflect a developmental defect. At E18.5, H&E analysis showed that the mutant long bones were under-mineralized compared to wildtype control and they appeared to be fractured (Figure 2A). Moreover, connective tissue seemed to have replaced bone in the shaft of the long bones. The same phenotype was seen in the long bones at E16.5 (Figure 2B). At E14.5 the defects were more subtle but still clearly apparent (Figure 2C). At this stage, in the wild type limbs osteoblasts had invaded the middle of the bone and they were clearly secreting mineralized matrix to replace the cartilage. In the mutants, there was no sign of mineralization on the sides of the bone and no detectable osteoblast invasion. Instead, at this early stage, the limbs already appeared fractured. Alizarin Red staining of E18.5 limb sections augmented what we saw in the H&E sections; there was little staining in the mutant bones indicating that there are very few calcium deposits and thus reduced bone mineralization (Figure 2D).

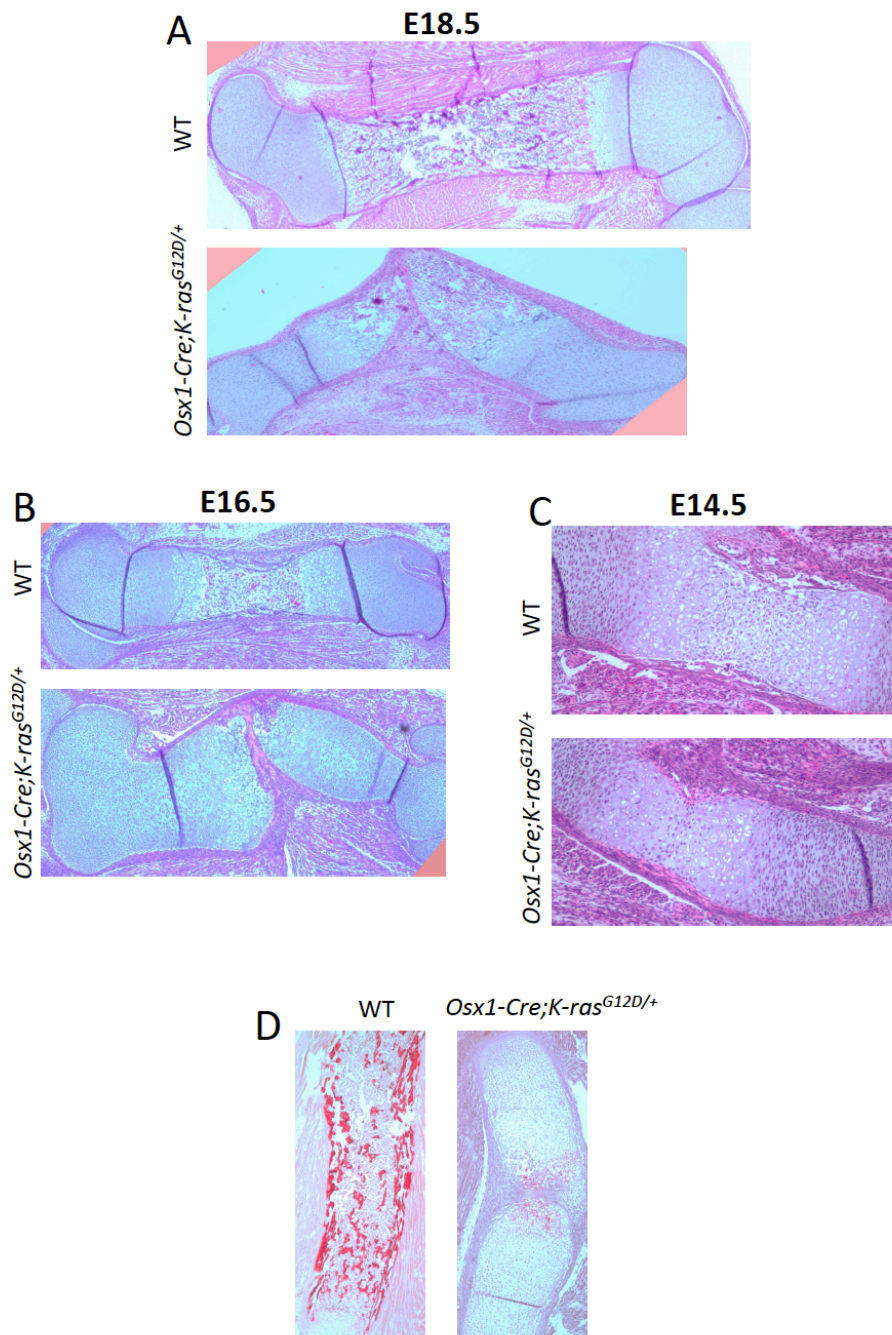


**Figure 2. Consecutive analysis of embryonic stages reveals that the fracture defect appears early during embryonic development.** (A-B) H&E sections of (A) E18.5 and (B) E16.5 embryo limbs show the fracture and under mineralization defects resulting from *K-ras<sup>G12D</sup>* expression in osteoblast precursors. (C) H&E sections of E14.5 embryos show a subtle difference between mutant and control limbs. (D) Alizarin Red staining of E18.5 limb sections shows that there is very little mineralization present in the *Osx1-Cre;K-ras<sup>G12D/+</sup>* long bones.

In parallel with our analysis of H&E sections, we also screened for molecular markers of osteoblast differentiation using *in situ* hybridization (ISH). Col2 is a marker of osteochondral progenitors, which give rise to both chondrocytes and osteoblasts. (Maes et al., 2010) have established that these Col2-positive osteochondral progenitors commit to the osteoblast lineage through two distinct differentiation schemes, depending on their location. Specifically, some give rise to Col1 expressing cells that first appear in the region of the bone collar around E14.5, while others become *Osx*-positive cells and migrate to the middle of the bone. Subsequently, these *Osx*-positive cells further differentiate into Col1 expressing, committed osteoblasts. Given these established differentiation mechanisms, we screened our mice for both Col2 and Col1 expression. *ISH* for Col2 at E14.5 showed that osteochondral progenitors were located appropriately and present at comparable levels in the *Osx1-Cre;K-ras<sup>G12D</sup>* mutants and wild type controls (Figure 3A). *ISH* for Col1 at E14.5 showed that the bone collar was present at this stage in the mutants. However, at E18.5, Col1 cells were present at high levels in wildtype controls but were largely absent in the mutants (Figure 3B).

We also conducted *ISH* for Osteopontin (OPN), a late stage differentiation marker that is expressed in both chondrocytes and osteoblasts. We found that OPN expression was present in the mutants at E18.5 and it was essentially normal in the chondrocytes compartment (Figure 3B). In contrast, we found no detectable staining in the region of the bone where osteoblasts normally reside, which is

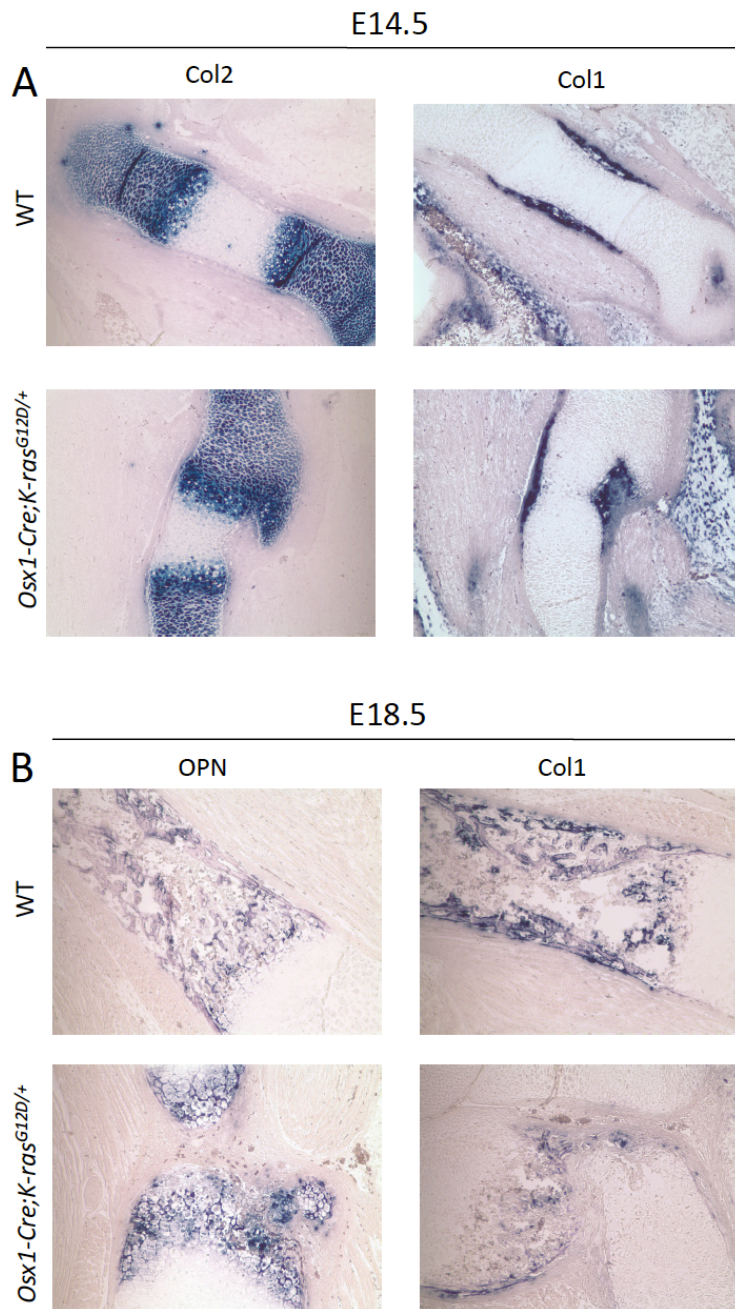


**Figure 3. *In situ* hybridization analysis for osteoblast markers at different stages of embryonic development.** (A) ISH at E14.5 shows similar expression of both Col2 and Col1 markers in mutant versus control limbs. (B) At E18.5, there are very few Col1 cells present in the mutant limbs. OPN staining is present in both mutants and controls in the chondrocyte compartment but is absent in the region of the mutant bone where osteoblasts should reside.

essentially the region of the fracture. Notably, in addition to be OPN negative, the tissue in this fracture site was also Col1 negative suggesting that these cells do not originate from osteoblast precursors. We hypothesize that this is fibrotic tissue. Taken together, our analyses show that induction of hyperactive K-ras expression within osteoblast precursors is sufficient to completely block terminal osteoblast differentiation.

**Expression of K-ras<sup>G12D</sup> has different effects on osteoblast terminal differentiation when induced during embryonic development versus after birth.**

Experiments to date were conducted in the absence of Dox, and thus expression of K-ras<sup>G12D</sup> was triggered by the expression of *Osx* in osteoblast progenitors around E12.5. We wanted to extend this analysis to determine the consequences of activating K-ras<sup>G12D</sup> in the same progenitor population (ie under the control of *Osx*) at other stages of skeletal development. For this, *Osx1-Cre* males were crossed with *K-ras<sup>G12D</sup>* females and, when plugs were detected, the pregnant females were transferred to doxycycline-containing food. This acts to prevent the expression of the Cre recombinase, and thus K-ras<sup>G12D</sup> expression in the developing embryos. At various stages of pregnancy, E9.5, E11.5, E14.5, E16.5 and E18.5, the pregnant females were switched to normal food to relieve inhibition of Cre and allow K-ras<sup>G12D</sup> expression specifically in *Osx* positive cells in the embryos. Skeletal development was then assessed at E18.5. When we released Cre at either E9.5 or E11.5, the mice displayed short, under-mineralized and fractured bones that

phenocopied those of the non-Dox treated mutants (Figure 4A). In stark contrast, we found that delaying the expression of Cre until E14.5, E16.5 and E18.5 completely rescued both the bone defects and the embryonic lethality (Figure 4A). This identifies a period of embryonic development somewhere around E14.5 in which the *Osx*-positive osteoblast precursors are especially vulnerable to the hyperactive K-ras expression.

We next wanted to investigate the effects of activating K-ras<sup>G12D</sup> in the osteoblast lineage after birth. To do this, we followed the development of mice in which the *Osx*-Cre expression was inhibited throughout gestation via Dox treatment and induced right after birth via Dox withdrawal. We analyzed the resulting *Osx1-Cre;K-ras<sup>G12D</sup>* animals at 2 weeks and 6 weeks of age. The bone phenotype of these mice was remarkably different from that of animals in which K-ras<sup>G12D</sup> was expressed in osteoblasts through embryogenesis. Specifically, instead of fractured and under-mineralized bones, the long bones had increased mineralization in their trabecular area. Indeed, the bone matrix was abnormally thick and it had almost completely filled the bone marrow space (Figure 4B). Thus, our data shows that hyperactivation of K-ras<sup>G12D</sup> yields different outcomes at different stages of skeletal development; it blocks bone formation when induced in mid-embryogenesis but greatly enhances this process when triggered in neonates.

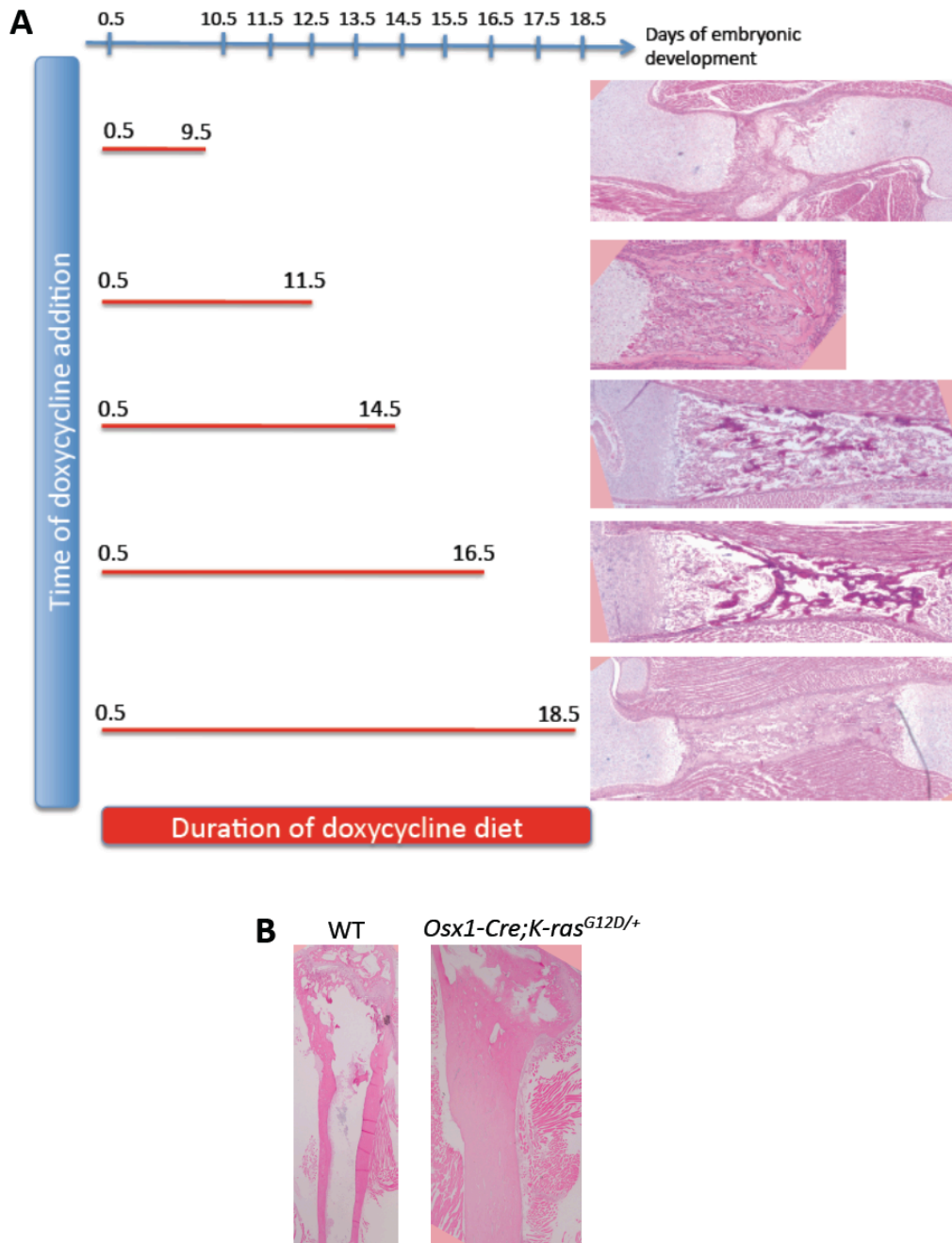


**Figure 4. Distinct temporal effects of K-ras<sup>G12D</sup> expression in osteoblasts.** (A) Inhibition of Cre in *Osx1-Cre; K-ras<sup>G12D</sup>* mice until E14.5, E16.5 and E18.5 completely rescues the bone phenotype in embryos analyzed at E18.5. When Cre is inhibited until E9.5 and E11.5 the phenotype is not rescued, and the bones are short and thin, fractured at the middle. (B) *Osx1-Cre;K-ras<sup>G12D/+</sup>* mice treated with Dox from conception until birth, were analyzed at 6 weeks old and show an increase in mineralization and a lack of bone marrow in the long bones.

## **K-ras<sup>G12D</sup> changes fate commitment of osteoblasts from bone to fat in an *in vitro* setting**

Having seen differential effects of K-ras on osteoblast differentiation in different *in vivo* settings, we wanted to establish whether/how K-ras affected osteoblast differentiation *in vitro*. By staining for  $\beta$ -galactosidase in *Osx1-Cre;LacZ* mice, we showed above that *Osx1* is highly expressed in the calvaria of mice at E18.5 (Figure 1A). Thus, we isolated osteoblast precursors from the calvaria of E18.5 *Osx1-Cre;K-ras<sup>G12D</sup>* and wildtype littermates that had not been exposed to Dox, and thus expressed K-ras<sup>G12D</sup> from mid-gestation. These cells were placed in culture and tested for their ability to differentiate into either bone or fat in response to appropriate induction media (Figure 5A). The extent of bone and fat differentiation was assessed by staining with Alizarin Red (for bone matrix) or Oil-red-O (for lipid droplets). As expected, the wildtype osteoblast precursors were able to differentiate into bone but not fat *in vitro* (Figure 5B). In stark contrast, cells from *Osx1-Cre;K-ras<sup>G12D</sup>* mutants displayed a reduced ability to make bone matrix and they had also acquired the capacity to differentiate into fat (n=5).

These observations have important relevance for skeletal diseases that display a defect in the normal bone to fat ratio within limbs. Studies on animal models for osteoporosis indicate that this disease is caused by an unbalance between the amounts of mineralized bone and fat found in the long bones. When there is too much fat, osteoporosis occurs, making the bones fragile and brittle. Studies have suggested that osteoblasts can switch fate and differentiate to adipocytes, leading to the osteoporotic phenotypes (Wu et al., 2011a).

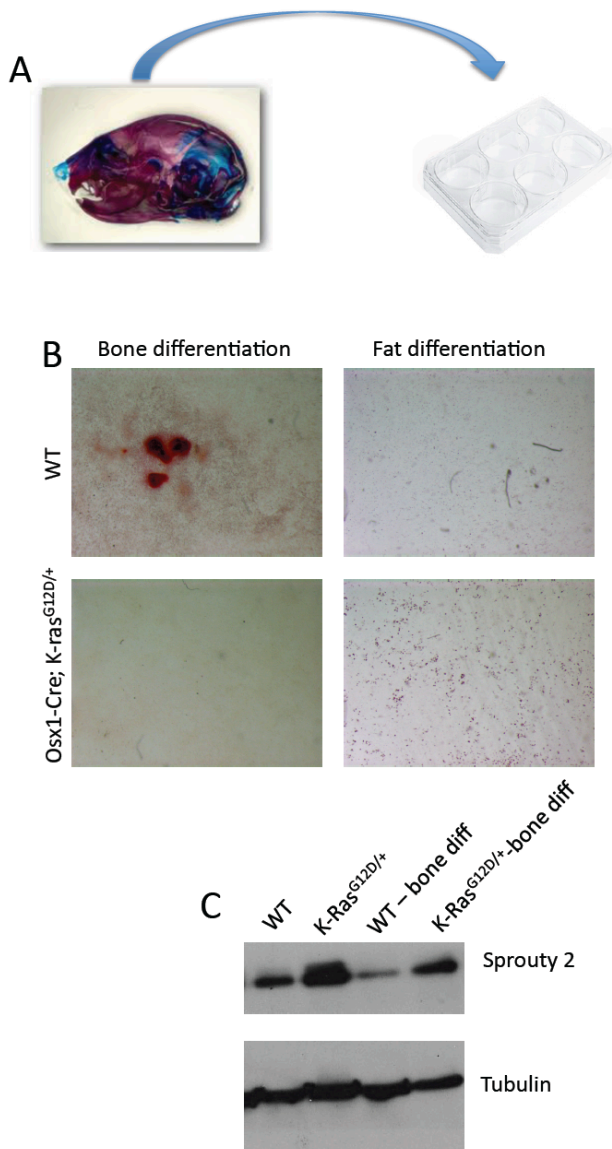


**Figure 5. Expression of K-ras<sup>G12D</sup> inhibits *in vitro* the differentiation of osteoblasts to bone and promotes fat differentiation.** (A) Osteoblasts are isolated from the calvaria of *Osx1-Cre; K-ras<sup>G12D</sup>* mutants and cultured on 6-well plates in special bone or fat differentiation media. (B) After 14 days of *in vitro* differentiation K-ras<sup>G12D</sup> osteoblasts do not form bone compared to wild type osteoblasts, however they acquire the new ability to differentiate into adipocytes. (C). Western Blot analysis shows that osteoblasts expressing K-ras<sup>G12D</sup> express increased levels of Sprouty2 when they are freshly collected from the calvaria. The expression of Spy2 goes down after 14 days in bone differentiation medium.

To better understand the molecular basis of the altered fate commitment of the *Osx1-Cre;K-ras<sup>G12D</sup>* mutant osteoblasts, we investigated the expression of other members of the MAPK pathway within these cells. Sprouty2 is an inhibitor of Ras and the MAPK signaling pathway. By suppressing the Ras/MAPK pathway and generating a negative feedback loop during development, Sprouty is known to regulate several signaling pathways and affects common signal mediators. In particular, Sprouty has been shown to act as a switch of mesenchymal stem cell lineage allocation (Urs et al., 2010). Thus we examined the levels of Sprouty2 in the calvarial osteoblast precursors from *Osx1-Cre;K-ras<sup>G12D</sup>* and wildtype mice by western blotting (Figure 5C). This analysis showed that Sprouty2 was expressed at higher levels in the K-ras<sup>G12D</sup>-expressing versus the wildtype osteoblasts. Notably, induction of bone differentiation caused the Sprouty2 to be downregulated in both genotypes, but the levels were still higher in mutant versus wildtype cells. Thus, deregulation of members of the Sprouty family might contribute to the altered *in vitro* differentiation capacity of the K-ras mutant osteoblasts.

## DISCUSSION

In this study, by specifically expressing hyperactive K-ras in osteoblast precursors under the control of the *Osx* promoter, we have identified two important time windows in which K-ras<sup>G12D</sup> expression yields divergent effects on osteoblast differentiation. First, our data show that K-ras<sup>G12D</sup> expression negatively regulates osteoblast differentiation when it is expressed in osteoblast precursors during embryonic development. In this context, hyperactive K-ras yields fragile, fractured bones and an under mineralized calvaria in the mutant mice. In contrast, when K-ras<sup>G12D</sup> is expressed in osteoblast precursors after birth, we show that it positively regulates bone development and osteoblast differentiation, leading to increased mineralization in the long bones.

One possible explanation for the opposing phenotypes described above, is that activation of K-ras<sup>G12D</sup> causes a differentiation block in *Osx*-expressing osteoblasts only in early, and not later, stages of development. This inability to produce mineralizing osteoblasts could be caused by the apoptosis of *Osx*-expressing cells, a block in their differentiation potential and/or reflect an alteration in the fate commitment of the osteoblastic precursors. K-ras<sup>G12D</sup> is known to induce apoptosis in a *p53* dependent manner. Thus, to assess whether K-ras<sup>G12D</sup> expression induces osteoblast apoptosis, we generated *Orx1-Cre;p53<sup>c/c</sup>;K-ras<sup>G12D</sup>* mice and showed that E18.5 animals display the same bone defects as *Osx1-Cre;K-ras<sup>G12D</sup>* mutants, including thin, under-mineralized and broken long bones. Based on these findings, we believe that the bone phenotype of *Osx1-Cre;K-ras<sup>G12D</sup>* is unlikely to be due to programmed cell death or senescence.

We note that expression of K-ras<sup>G12D</sup> in *Osx*-expressing cells after birth does not affect their survival, or their ability to differentiate normally and populate the center of the bone. We speculate that, at this stage, K-ras<sup>G12D</sup> acts more as an oncogene, presumably by stimulating an abnormally high rate of proliferation in the *Osx*-expressing cells and causing them to completely fill the bone marrow space within the long bones. Obviously, it will be interesting to understand why *Osx*-expressing osteoblasts in mid-gestation versus in neonates respond so differently to K-ras<sup>G12D</sup>. It is possible that these cells have differences in their intrinsic gene expression pattern that accounts for their opposing responses to K-ras<sup>G12D</sup> activation. Alternatively, the opposing response may result from distinct external/environmental cues that exist at each of these stages. Obviously, these two hypotheses are not mutually exclusive.

We have identified a developmental time window, around embryonic day E14.5, when activated K-ras is necessary to cause the mutant phenotype in *Osx1-Cre;K-ras<sup>G12D</sup>* embryos. If we protect this period from constitutive K-ras expression, by doxycycline treatment, we completely suppress the embryonic bone defect. We note that this critical developmental time window is not completely defined since the doxycycline regulatable Tet-Off system has some caveats. First, since we did observe some positive LacZ staining in *Osx1-Cre;LacZ* embryos that were treated with doxycycline from conception until the time of sacrifice at E18.5, we note that Dox does not completely prevent Cre expression. Second, the precise time of doxycycline clearance from the body once the diet has stopped is unclear, and may

even vary at different locations in the body or at different stages of development. Despite these limitations, the embryonic time window identified in this current study converges on the same time window identified in chapter 2 in which MEK inhibitor treatment of the *Prx1-Cre; K-ras<sup>G12D</sup>* mutants until E14.5 was sufficient to rescue their embryonic mutant limb phenotype. Future studies will be needed to determine which events in normal bone development at E14.5 are derailed by *K-ras<sup>G12D</sup>* expression in each of these models.

We would also like to learn more about the bone overgrowth that arises in the *Osx1-Cre;K-ras<sup>G12D</sup>* mutants in which *K-ras<sup>G12D</sup>* is activated starting at birth. Unfortunately, we found that these animals sometimes get lung tumors and skin papillomas around 6 weeks of age (data not shown). This is most probably due to leaky *K-ras<sup>G12D</sup>* expression in other tissues, since *K-ras* is a powerful oncogene known to cause lung and skin tumors in mice. We note that there are reports of human osteosarcomas caused by mutations in members of the *K-ras*/MAPK pathway (Ikeda et al., 1989) and it is possible that the *Osx1-Cre;K-ras<sup>G12D/+</sup>* mouse model would eventually develop bone tumors. However, since the lung tumors appear faster, the mice die before we are able to assess whether osteosarcoma might develop.

The MAPK pathway is known to control stem cell/ progenitor lineage decision in differentiating systems, such as muscle and fat. For example, in fat ERK1 phosphorylates PPAR $\gamma$  and inhibits its activity, blocking adipogenesis as a result (Adams et al., 1997). In *X. laevis* muscle differentiation, MAPK increases the levels of XMyoD, a master regulator of muscle differentiation (Zetser et al., 2001). Thus, it is

possible that in the context of osteogenesis, MAPK pathway also plays a role in controlling the decision of osteoblasts to differentiate into bone-forming cells versus adipocytes. The ability of K-ras<sup>G12D</sup> expression to induce a fate change in osteoblasts from bone to fat may offer an explanation of the exhaustion of osteoblasts capable of forming mineralized bone we observe in the *Osx1-Cre;K-ras<sup>G12D</sup>* mutant limbs during embryonic development. Since we cannot test this hypothesis *in vivo*, due to embryonic bones being too young to accumulate fat, we have used an *in vitro* approach. Specifically, we isolated osteoblasts from the calvaria of *Osx1-Cre;K-ras<sup>G12D</sup>* mutant mice and showed *in vitro* that they have acquired a novel ability to differentiate to adipocytes, while their osteogenic ability is impaired. These experiments suggest a role for the MAPK pathway in controlling the decision of osteoblasts to differentiate into mature osteoblasts capable of secreting mineralized matrix or into fat forming cells. We further show that Sprouty2 is over-expressed in osteoblasts that express K-ras<sup>G12D</sup>, and its expression goes down as they differentiate into bone. Future studies could analyze in depth the molecular mechanisms through which aberrant MAPK signaling regulates osteoblast differentiation. For example, one can investigate if K-ras<sup>G12D</sup> acts directly through Sprouty, and whether Sprouty is essential in determining the expanded fate specification conferred by K-ras activation in osteoblasts.

Interestingly, it may be possible to use our model to investigate if K-ras<sup>G12D</sup> has a similar effect on osteoblast fate specification in an *in vivo* setting. Specifically, we can analyze *Osx1-Cre;K-ras<sup>G12D</sup>* adults, in which K-ras<sup>G12D</sup> was activated after birth. An increase in the amount of fat in the long bones of these mice would show

that *in vivo* activated K-ras is sufficient to induce osteoblasts to change fate and become adipocytes. This type of study would be very relevant to the field of osteoporosis research. Osteoporosis is a disease in which the bones become fragile and brittle because the bone mass is drastically reduced and replaced by fat. Thus, we have developed a mouse model that may be useful for addressing this important, disease relevant question.

## SUPPLEMENTARY FIGURES

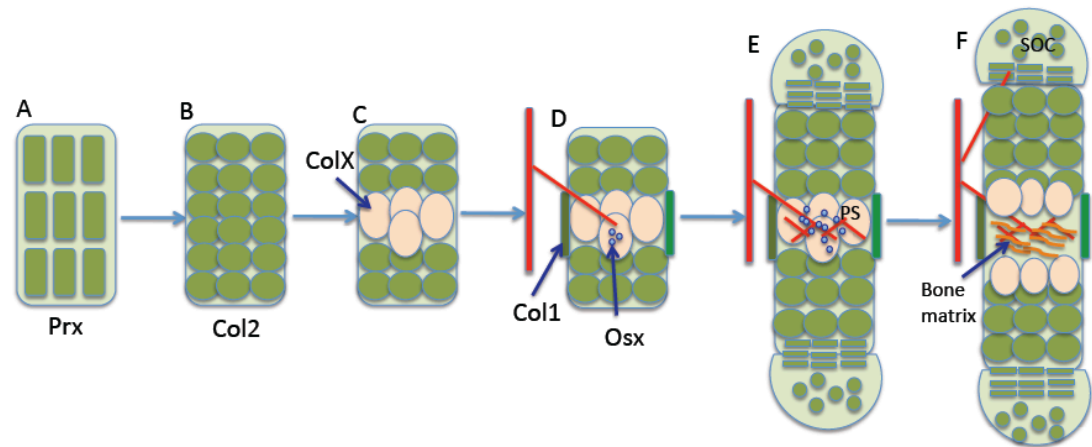


**Figure S1. Schematic representation of endochondral bone formation.** Adapted from (Karsenty et al., 2009) and described in more detail in the text.

## **METHODS**

### *Mouse husbandry and tissue collection*

Animal procedures followed protocols approved by MIT's Committee on Animal Care. The *Oxsl-Cre*, *Prx1-Cre* and *K-ras<sup>G12D/+</sup>* animals were maintained on a mixed genetic background. Tissues were fixed in PBS with 3.7% formaldehyde. Prior to paraffin sectioning, soft tissues were dehydrated via an ethanol series, while bone-containing tissue was decalcified in 0.46M EDTA, 2.5% Ammonium Hydroxide pH 7.2. All paraffin embedded sections were cut at 5µm, dewaxed and stained with H&E.

### *Skeletal stainings*

Embryos were sacrificed, skinned and eviscerated. The remaining tissue was fixed in 95% ethanol for 4 days, transferred to acetone for 3 days, and subsequently transferred to staining solution of 0.015% Alcian Blue 8GX (Sigma), 0.005% Alizarin Red S (Sigma), and 5% glacial acetic acid in ethanol at 37°C for 2 days and at room temperature for a one more day. Tissue was cleared in 1% potassium hydroxide for several days and then stored in glycerol.

### *Alizarin Red staining*

For Alizarin Red staining, sections were rinsed in water, placed in 2% Alizarin Red S (pH 4.2) for 5 min, dipped 20 times in acetone followed by acetone:xylene (1:1) washing, and then mounted.

### *Calvarial Osteoblasts Preparation and Culture*

Calvaria from embryonic day 18.5 embryos were removed and carefully cleaned in sterile PBS. Then calvaria was treated with several rounds of collagenase/trypsin digestion at 37°C, and plated onto six-well plates for 2 days in  $\alpha$ MEM with 10% fetal bovine serum and penicillin/streptomycin. For differentiation,  $3.5 \times 10^5$  cells were plated onto a well of a 6-well tissue culture plates. Upon reaching confluence, calvarial osteoblasts were treated with medium supplemented with 50  $\mu$ g/mL of ascorbic acid and 10 mmol/L of p- glycerol-phosphate. Adenovirus (University of Iowa Gene Transfer Vector Core) was added to the medium at 100 plaque-forming units per cell and washed away 24 h later. To assay for calcium deposits, plates were stained with 1% Alizarin Red S solution (pH 5.0)

### *X-Gal Staining*

Adult and embryonic tissues were stained for  $\beta$ -galactosidase activity as described in (Parisi et al., 2007). Briefly, dissected tissues were fixed, rinsed, and then stained overnight at 37°C in X-Gal staining solution. Samples were then rinsed and fixed again before being processed for paraffin embedding. Sections were cut at 5  $\mu$ m and counterstained with Nuclear Fast Red.

### *In situ hybridization*

Tissues were fixed in 4% paraformaldehyde/PBS overnight at 4°C, processed, embedded in paraffin, and cut. Non-radioactive ISH, with digoxigenin (DIG)-labeled probes (Chung et al., 1998; Murtaugh et al., 2001) was performed as described

previously (Chung et al., 1998). In brief, sections were postfixed with 4% PFA-PBS for 15 min. After washing with PBS, sections were digested with 1 pg/ml proteinase-K (37 C; 15 min) in PBS and again treated with 4% PFA-PBS (10 min). Sections then were sequentially washed with PBS, acetylated with 0.25% acetic anhydride in the presence of triethanolamine (1 M; 10 min), dehydrated with increasing concentrations of ethanol, and air dried. Hybridizations with complementary RNAs were performed in a humidified chamber in a solution containing 50% formamide, 10% dextran sulfate, 1 X Denhardt's solution, 600 mM NaCl, 10 mM Tris-HCl, 1 mM EDTA, 50 mM dithiothreitol, 0.25% sodium dodecyl sulfate, and 200 pg/ml transfer RNA. After hybridization, sections were washed briefly with 5 X SSC at 50°C, 50% formamide- 10X SSC (50 C; 30 min), and 10 mM Tris-HCl (pH 7.6)-500 mM NaCl-1 mM EDTA (TNE; 37°C; 10 min). Sections were then treated with 10 pg/ml ribonuclease-A in TNE (37 C; 30 min). After being washed with TNE, sections were incubated once with 2 X SSC (50 C; 20 min) and twice with 0.2 X SSC (50 C; 20 min), dehydrated with increasing concentrations of ethanol, and air-dried.

## REFERENCES

- Adams, M., M.J. Reginato, D. Shao, M.A. Lazar, and V.K. Chatterjee. 1997. Transcriptional activation by peroxisome proliferator-activated receptor gamma is inhibited by phosphorylation at a consensus mitogen-activated protein kinase site. *J Biol Chem.* 272:5128-32.
- Chen, C., A.J. Koh, N.S. Datta, J. Zhang, E.T. Keller, G. Xiao, R.T. Franceschi, N.J. D'Silva, and L.K. McCauley. 2004. Impact of the mitogen-activated protein kinase pathway on parathyroid hormone-related protein actions in osteoblasts. *J Biol Chem.* 279:29121-9.
- Chung, U.I., B. Lanske, K. Lee, E. Li, and H. Kronenberg. 1998. The parathyroid hormone/parathyroid hormone-related peptide receptor coordinates endochondral bone development by directly controlling chondrocyte differentiation. *Proc Natl Acad Sci U S A.* 95:13030-5.
- Elefteriou, F., M.D. Benson, H. Sowa, M. Starbuck, X. Liu, D. Ron, L.F. Parada, and G. Karsenty. 2006. ATF4 mediation of NF1 functions in osteoblast reveals a nutritional basis for congenital skeletal dysplasias. *Cell Metab.* 4:441-51.
- Ge, C., G. Xiao, D. Jiang, and R.T. Franceschi. 2007. Critical role of the extracellular signal-regulated kinase-MAPK pathway in osteoblast differentiation and skeletal development. *J Cell Biol.* 176:709-18.
- Gossen, M., and H. Bujard. 1992. Tight control of gene expression in mammalian cells by tetracycline-responsive promoters. *Proc Natl Acad Sci U S A.* 89:5547-51.
- Greenblatt, M.B., J.H. Shim, W. Zou, D. Sitara, M. Schweitzer, D. Hu, S. Lotinun, Y. Sano, R. Baron, J.M. Park, S. Arthur, M. Xie, M.D. Schneider, B. Zhai, S. Gygi, R. Davis, and L.H. Glimcher. 2010. The p38 MAPK pathway is essential for skeletogenesis and bone homeostasis in mice. *J Clin Invest.* 120:2457-73.
- Hurley, M.M., K. Marcello, C. Abreu, and M. Kessler. 1996. Signal transduction by basic fibroblast growth factor in rat osteoblastic Py1a cells. *J Bone Miner Res.* 11:1256-63.
- Ikeda, S., H. Sumii, K. Akiyama, S. Watanabe, S. Ito, H. Inoue, H. Takechi, G. Tanabe, and T. Oda. 1989. Amplification of both c-myc and c-raf-1 oncogenes in a human osteosarcoma. *Jpn J Cancer Res.* 80:6-9.
- Karsenty, G., H.M. Kronenberg, and C. Settembre. 2009. Genetic control of bone formation. *Annu Rev Cell Dev Biol.* 25:629-48.

- Kistner, A., M. Gossen, F. Zimmermann, J. Jerecic, C. Ullmer, H. Lubbert, and H. Bujard. 1996. Doxycycline-mediated quantitative and tissue-specific control of gene expression in transgenic mice. *Proc Natl Acad Sci U S A.* 93:10933-8.
- Maes, C., T. Kobayashi, M.K. Selig, S. Torrekens, S.I. Roth, S. Mackem, G. Carmeliet, and H.M. Kronenberg. 2010. Osteoblast precursors, but not mature osteoblasts, move into developing and fractured bones along with invading blood vessels. *Dev Cell.* 19:329-44.
- Matsushita, T., Y.Y. Chan, A. Kawanami, G. Balmes, G.E. Landreth, and S. Murakami. 2009. Extracellular signal-regulated kinase 1 (ERK1) and ERK2 play essential roles in osteoblast differentiation and in supporting osteoclastogenesis. *Mol Cell Biol.* 29:5843-57.
- Murtaugh, L.C., L. Zeng, J.H. Chyung, and A.B. Lassar. 2001. The chick transcriptional repressor Nkx3.2 acts downstream of Shh to promote BMP-dependent axial chondrogenesis. *Dev Cell.* 1:411-22.
- Nakashima, K., X. Zhou, G. Kunkel, Z. Zhang, J.M. Deng, R.R. Behringer, and B. de Crombrughe. 2002. The novel zinc finger-containing transcription factor osterix is required for osteoblast differentiation and bone formation. *Cell.* 108:17-29.
- Parisi, T., T.L. Yuan, A.M. Faust, A.M. Caron, R. Bronson, and J.A. Lees. 2007. Selective requirements for E2f3 in the development and tumorigenicity of Rb-deficient chimeric tissues. *Mol Cell Biol.* 27:2283-93.
- Rodda, S.J., and A.P. McMahon. 2006. Distinct roles for Hedgehog and canonical Wnt signaling in specification, differentiation and maintenance of osteoblast progenitors. *Development.* 133:3231-44.
- Takeuchi, Y., M. Suzawa, T. Kikuchi, E. Nishida, T. Fujita, and T. Matsumoto. 1997. Differentiation and transforming growth factor-beta receptor down-regulation by collagen-alpha2beta1 integrin interaction is mediated by focal adhesion kinase and its downstream signals in murine osteoblastic cells. *J Biol Chem.* 272:29309-16.
- Urs, S., D. Venkatesh, Y. Tang, T. Henderson, X. Yang, R.E. Friesel, C.J. Rosen, and L. Liaw. 2010. Sprouty1 is a critical regulatory switch of mesenchymal stem cell lineage allocation. *FASEB J.* 24:3264-73.
- Wang, W., J.S. Nyman, K. Ono, D.A. Stevenson, X. Yang, and F. Elefteriou. 2011. Mice lacking Nf1 in osteochondroprogenitor cells display skeletal dysplasia similar to patients with neurofibromatosis type I. *Hum Mol Genet.* 20:3910-24.
- Wu, J.Y., P. Aarnisalo, M. Bastepe, P. Sinha, K. Fulzele, M.K. Selig, M. Chen, I.J. Poulton, L.E. Purton, N.A. Sims, L.S. Weinstein, and H.M. Kronenberg. 2011a. Galpha

- enhances commitment of mesenchymal progenitors to the osteoblast lineage but restrains osteoblast differentiation in mice. *J Clin Invest.* 121:3492-504.
- Wu, X., S. Chen, Y. He, S.D. Rhodes, K.S. Mohammad, X. Li, X. Yang, L. Jiang, G. Nalepa, P. Snider, A.G. Robling, D.W. Clapp, S.J. Conway, T.A. Guise, and F.C. Yang. 2011b. The haploinsufficient hematopoietic microenvironment is critical to the pathological fracture repair in murine models of neurofibromatosis type 1. *PLoS One.* 6:e24917.
- Xiao, G., D. Jiang, R. Gopalakrishnan, and R.T. Franceschi. 2002. Fibroblast growth factor 2 induction of the osteocalcin gene requires MAPK activity and phosphorylation of the osteoblast transcription factor, Cbfa1/Runx2. *J Biol Chem.* 277:36181-7.
- You, J., G.C. Reilly, X. Zhen, C.E. Yellowley, Q. Chen, H.J. Donahue, and C.R. Jacobs. 2001. Osteopontin gene regulation by oscillatory fluid flow via intracellular calcium mobilization and activation of mitogen-activated protein kinase in MC3T3-E1 osteoblasts. *J Biol Chem.* 276:13365-71.
- Zetser, A., D. Frank, and E. Bengal. 2001. MAP kinase converts MyoD into an instructive muscle differentiation factor in *Xenopus*. *Dev Biol.* 240:168-81.
- Zou, W., M.B. Greenblatt, J.H. Shim, S. Kant, B. Zhai, S. Lotinun, N. Brady, D.Z. Hu, S.P. Gygi, R. Baron, R.J. Davis, D. Jones, and L.H. Glimcher. 2011. MLK3 regulates bone development downstream of the faciogenital dysplasia protein FGD1 in mice. *J Clin Invest.* 121:4383-92.

## **ACKNOWLEDGEMENTS**

We thank Shigeki Nishimori and Tatsuya Kobayashi (MGH) for providing the *in situ* hybridization RNA probes for Col2, Col1 and OPN markers. We thank Tatsuya Kobayashi and Henry Kronenberg (MGH) for useful discussions regarding the experimental design of the studies presented in this chapter. We thank all members of the Lees and Kronenberg laboratory for valuable input during this study. This work was supported by an NCI/NIH grant to J.A.L. who is a Ludwig Scholar at MIT. S.N. was supported by a D.H. Koch Graduate Fellowship.

## **CHAPTER 4**

### **Discussion**

Mitogen-activated protein kinases (MAPKs) are well-characterized signal transducers that have been intensively studied for their ability to mediate neoplastic transformation (Greenblatt et al., 2013). In addition to the role of MAPK signaling in cancer, other studies have expanded our understanding of how members of this pathway function during development (Corson et al., 2003; Galabova-Kovacs et al., 2006). Many of these studies have focused on modeling developmental syndromes caused by aberrant Ras/MAPK signaling (Tidyman and Rauen, 2009). Importantly, there is considerable interest in understanding of how MAPK pathway functions during skeletal development. In this thesis, we have generated two novel mouse models to investigate the effects of aberrant MAPK signaling during bone development and understand how bone mass is regulated via MAPK control of osteoblast differentiation. Specifically, we expressed a hyperactive form of K-ras either in all mesenchymal lineages, including osteoblasts and chondrocytes, or specifically in osteoblasts.

When we express K-ras<sup>G12D</sup> in all mesenchymal lineages, using the Prx promoter, the *Prx1-Cre;K-ras<sup>G12D</sup>* mutant mice die at birth most of the time, and they all display abnormal skeletons. Their long bones are short and thick, and they have increased, abnormal cortical and trabecular mineralization. The bone defect becomes evident around embryonic day E14.5 when we observe a delay in the formation of the bone collar in the mutant mice. Importantly, if we treat these K-ras<sup>G12D</sup> expressing mutants with a MEK inhibitor from E10.5 to E14.5 then the bone phenotype is completely suppressed up to birth. Thus, by treatment with MEK inhibitors we identified a critical stage during development when aberrant K-ras

expression causes the mutant phenotype.

In parallel with analyzing the *Prx1-Cre;K-ras<sup>G12D</sup>* mutant mice, we expressed K-ras<sup>G12D</sup> specifically in osteoblast precursors, under the control of the *Osx* promoter. The *Osx1-Cre;K-ras<sup>G12D</sup>* mouse model also contains a Tet-Off regulatable system and therefore has the added advantage of allowing temporal control of Cre expression, and thus K-ras<sup>G12D</sup> induction, through doxycycline administration. In chapter 3 we show that by using doxycycline to inhibit Cre expression at various times during development, we identify the same critical time window during embryonic development (around day E14.5) when aberrant K-ras signaling is sufficient to cause the mutant phenotype. Despite the fact that the two mouse models converge on the same developmental time window when the phenotype first becomes visible and when aberrant K-ras signaling is absolutely required to cause the mutant phenotype, the defects we see in the two settings are drastically different. While *Prx1-Cre;K-ras<sup>G12D</sup>* mutant mice have short, thick bones, with increased mineralization, the *Osx1-Cre;K-ras<sup>G12D</sup>* mutant mice have short, fractured and under-mineralized limbs.

In chapter 3 we also show that when we express K-ras<sup>G12D</sup> under the control of the *Osx* promoter after birth, i.e. in the same population of cells but at a different time during the development of the organism, we obtain an increase in bone mass and in the mineralization of the limbs. Thus, we define a second time window, starting at birth, when aberrant K-ras signaling in osteoblasts leads to a distinct phenotype (increased bone mass) from the one observed when this pathway is activated during the first embryonic developmental time window (decreased bone

mass).

Taken together, our findings have raised the following interesting questions that will be discussed in greater detail in this chapter:

1. What are the events in bone development affected by aberrant K-ras/ MAPK signaling specifically at E14.5?
2. Why do we see distinct phenotypes when we express hyperactive K-ras in mesenchymal lineages versus osteoblast precursors?
3. Why do we see distinct phenotypes when constitutive K-ras expression is activated in *Osx* expressing osteoblast precursors in mid-gestation versus after birth?
4. What are the implications of our studies for human diseases in which there is a skeletal phenotype caused by hyperactive MAPK signaling?

#### **4.1. Identification of a critical developmental time period during bone development specifically affected by aberrant MAPK signaling**

In chapters 2 and 3 we describe a key critical period during embryonic development when aberrant MAPK signaling affects bone development. In both *Prx1-Cre;K-ras<sup>G12D</sup>* and *Osx1-Cre;K-ras<sup>G12D</sup>* mouse models we see that the defects become visible around embryonic day E14.5. In both mutants, if this restricted period is protected from K-ras<sup>G12D</sup> expression, either by treatment with MEK inhibitor (for the *Prx* model) or by inhibition with doxycycline (for the *Osx* model), the bone phenotype is rescued. Future studies should focus on how activated K-ras<sup>G12D</sup> signaling affects proper bone development specifically during this key

embryonic period around E14.5. What are events that occur during normal bone development at this stage and are affected by aberrant MAPK signaling?

In the *Prx1-Cre;K-ras<sup>G12D</sup>* mutants we identify a delay in the formation of the bone collar at E14.5. During bone development, the Col1 osteoblasts that form the bone collar originate from Col2 osteochondral progenitors (Maes et al., 2010). We hypothesize that there is a defect with the migration of the Col2 progenitors to the location of the future bone collar caused by K-ras<sup>G12D</sup> expression. This hypothesis is supported by other studies in literature, since aberrant MAPK signaling has been shown to affect cell migration in systems such as zebrafish development (Anastasaki et al., 2012) Lineage tracing experiments in *Col2-CreERT2;K-ras<sup>G12D</sup>;GFP* embryos could offer an answer to this question. For example, if we inject with tamoxifen into females carrying embryos with the above genotype at day E12.5 or E13.5 and analyze E14.5 limb sections, we could assess the migration of the GFP-labeled, Col2 cells to the location of the future bone collar to determine whether there is a defect. In *Osx1-Cre;K-ras<sup>G12D</sup>* mutants the defect is more subtle, but still visible at this E14.5 stage. In this model, we do see evidence of normal bone collar formation based on Col1 *in situ* hybridization. However, as seen in the H&E limb sections, osteoblasts from the perichondrium do not migrate into the center of the bone. At subsequent days in embryonic development, we notice a drastic reduction in the number of mineralizing osteoblasts in the long bones of the mutants. Since we observe the absence of osteoblasts later in the embryonic development of the limbs we hypothesize that expression of K-ras<sup>G12D</sup> in osterix expressing osteoblast progenitors does not impair migration of Col2 osteoprogenitors into the center of

the bone, but it affects their survival either by causing them to undergo apoptosis or by inducing a change in their cell fate. Unfortunately, immunohistochemistry (IHC) for cleaved caspase 3 in E14.5 limbs did not offer conclusive results. This could be due to the fact that the apoptosis and clearance of the *K-ras*<sup>G12D</sup> expressing osteoblasts occurs quickly and thus we cannot catch it by IHC staining. In many other settings, the ability of *K-ras*<sup>G12D</sup> to induce apoptosis, or cellular senescence, is p53 dependent. Thus, we generated *Osx1-Cre;p53<sup>c/c</sup>;K-ras<sup>G12D</sup>* mice to assess if indeed osteoblasts die due to programmed cell death. Embryos at E18.5 show a bone phenotype similar to the one seen in the *Osx1-Cre;K-ras<sup>G12D</sup>* embryos, more specifically the limbs are short and thin. This shows that p53 inactivation is not required for the bone phenotype in *Osx1-Cre;K-ras<sup>G12D</sup>* embryos, arguing that this defect is unlikely to be due to programmed cell death or senescence. In the section 4.4 of this chapter I will discuss in more detail our efforts trying to investigate a defect in cell fate specification of the mutant osteoblasts.

It is important to note that the embryonic developmental time window we have identified is approximate in both mouse models. In the *Osx1-Cre;K-ras<sup>G12D</sup>* mice treated with doxycycline we cannot be sure when doxycycline is completely eliminated from the system, and thus when Cre and *K-ras*<sup>G12D</sup> start to be expressed. Similarly, in the *Prx1-Cre;K-ras<sup>G12D</sup>* mice the injections with MEK inhibitor are also a source of variability in terms of both how quickly MAPK inhibition is achieved and released. However, experiments in both of these models converge on a similar developmental time window around E14.5, affected by aberrant MAPK signaling, which is consistent with when the phenotype becomes visible in these mice.

## **4.2. K-ras<sup>G12D</sup> activation leads to divergent bone phenotypes when expressed in all mesenchymal lineages versus exclusively in the osteoblast lineage**

In the *Prx1-Cre;K-ras<sup>G12D</sup>* mutant mice, K-ras<sup>G12D</sup> is expressed in early progenitors of the limb bud and thus affects all mesenchymal lineages, including osteoblast and cartilage lineages. As described in chapter 2, most of these mice die at birth and have short and thick long bones. In *Osx1-Cre;K-ras<sup>G12D</sup>* mutant mice, K-ras<sup>G12D</sup> is expressed in all osteoblast progenitors and affects the osteoblast lineage exclusively. As described in chapter 3, these mice have fragile and brittle bones, with reduced mineralization in both the long bones and in the calvaria.

The defect we see in the calvaria of the *Osx1-Cre;K-ras<sup>G12D</sup>* mice, a bone that develops through direct differentiation of mesenchymal progenitors to osteoblasts, suggests that expression of K-ras<sup>G12D</sup> in this setting directly impairs osteoblast differentiation. Interestingly, the expression of the same mutation in both the osteoblast and cartilage lineages in the *Prx1-Cre;K-ras<sup>G12D</sup>* mice does not impair the ability of osteoblasts to differentiate into functioning adult mineralizing osteocytes, since these mice display dense trabecular and cortical mineralization.

It is possible that the different phenotypes of our two mouse models could be due to different strengths of the K-ras signaling in the two settings. Since in the *Prx1-Cre;K-ras<sup>G12D</sup>* and *Osx1-Cre;K-ras<sup>G12D</sup>* mice mutant K-ras<sup>G12D</sup> is driven off different promoters, Prx versus Osx, it is possible that a difference in the promoter strength leads to the different phenotypes. Alternatively, and more interesting, it seems feasible that K-ras<sup>G12D</sup> affects different mesenchymal lineages and/or

different stages in the differentiation of mesenchymal progenitors to committed bone progenitors. Therefore, two possibilities, not mutually exclusive, emerge: a) defects in the chondrocyte – osteoblast crosstalk modulates the mutant osteoblast phenotype in *Prx1-Cre;K-ras<sup>G12D</sup>* mice and/or b) the expression of K-ras<sup>G12D</sup> in early versus late bone progenitors causes the distinct phenotypes in the *Prx1-Cre;K-ras<sup>G12D</sup>* versus *Osx1-Cre;K-ras<sup>G12D</sup>* models.

According to the first hypothesis it is possible that abnormal signaling between the mutant cartilage and osteoblasts in the *Prx1-Cre;K-ras<sup>G12D</sup>* mice is key in determining the differential phenotypes. To investigate this hypothesis, we wanted to exclusively express K-ras<sup>G12D</sup> in the cartilage and check the phenotype of the resulting mice. Unfortunately, there is no gene or Cre mouse strain that is specific exclusively for chondrocyte precursors. *Col2-Cre* is often used to target cartilage, but *Col2* it is expressed in osteo-chondral progenitors that differentiate into both bone and cartilage cells. Indeed, when we generated *Col2-Cre;K-ras<sup>G12D</sup>* mice we found the same phenotype as in *Prx1-Cre;K-ras<sup>G12D</sup>* mice. Thus, we cannot separate the functions of osteoblasts and chondrocytes completely using a mouse strategy. Instead, we need to test the possible involvement of chondrocytes in the *Prx1-Cre;K-ras<sup>G12D</sup>* mouse phenotype at a molecular level. Staining for factors important in cartilage – osteoblast signaling, such as *Ihh* or *Ptch*, would indicate whether defects in the crosstalk between osteoblasts and chondrocytes plays a role in the skeletal phenotype of the *Prx1-Cre;K-ras<sup>G12D</sup>* mice.

According to the second hypothesis, uncommitted multipotent progenitors (Prx expressing cells) and committed osteoprogenitors (Osx expressing osteoblasts)

respond differently to the same stimulus, hyperactive K-ras<sup>G12D</sup>, thereby explaining the differential phenotypes we observe in these mice. Notably, other scientists working in the bone field have observed such opposing phenotypes. For example, NF1 deletion in late stage osteoblasts (using the Col1-Cre mouse) results in an increase in bone mass, while deleting NF1 in osteochondral progenitors (using the Col2 promoter) causes reduced bone mass and impaired osteoblast differentiation (Elefteriou et al., 2006; Wang et al., 2011; Wu et al., 2011). Moreover, similar to the opposing phenotypes we see in the *Prx1-Cre;K-ras<sup>G12D</sup>* and *Osx1-Cre;K-ras<sup>G12D</sup>* mice, deletion of NF1 in Col2 uncommitted osteo-chondral progenitors versus committed Ocn osteoblasts also leads to distinct manifestations of phenotypes.

#### **4.3. K-ras<sup>G12D</sup> activation leads to divergent bone phenotypes when expressed in the osteoblast lineage during development versus after birth**

In chapter 3 we showed that when K-ras<sup>G12D</sup> is expressed exclusively in the osteoblast lineage, but starting at different times during the development of the organism, mice develop opposing bone phenotypes. We have observed this difference in phenotypes in two different mouse models. In the first model, generated in collaboration with Tatsuya Kobayashi from MGH, we injected tamoxifen in females carrying *Osx1-CreER<sup>T2</sup>;K-ras<sup>G12D</sup>* embryos at days E14.5 and E16.5 and analyzed the pups at 2 weeks of age (data not shown). In this setting, we noticed an increase in the mineralization of the long bones in the mutant *Osx1-CreER<sup>T2</sup>;K-ras<sup>G12D</sup>* mice (data not shown). In the second model (described in Chapter 3), using the Tet-Off doxycycline system specific to the *Osx-Cre* mouse, we activated

K-ras<sup>G12D</sup> starting at birth in *Osx1-Cre;K-ras<sup>G12D</sup>* mice and analyzed the mice at 6 weeks of age. We obtained a similar phenotype as above, an increase in the bone mass in the limbs.

Future studies should aim to understand at a molecular level why we see the divergent *Osx*-driven K-ras mutant phenotypes, *in utero* versus post birth. One hypothesis is that it could be an osteoblast cell autonomous effect due to a difference in the gene expression pattern that characterizes different developmental windows. Alternatively, the opposing phenotypes could be due to differential external cues that are different at various stages of mouse development.

One could investigate these hypotheses by isolating osteoblasts from *Osx1-Cre;K-ras<sup>G12D</sup>* mice, either the embryonic mutants that have the under-mineralized bone or the mutants who have the increase in bone mass caused by K-ras<sup>G12D</sup> activation after birth, and examining them *in vitro* where there can be no influence of external cues. However, the difficulty with performing this type of experiments will be to isolate osteoblasts from *Osx1-Cre;K-ras<sup>G12D</sup>* embryos. These mice have very few osteoblasts, both because they are very young and because they have under-mineralized, fractured bones with very few osteoblasts.

#### **4.4. K-ras<sup>G12D</sup> affects the fate of osteoblast differentiation in an *in vitro* setting**

In chapter 3 of this thesis we have shown that K-ras<sup>G12D</sup> has an effect on osteoblast differentiation in an *in vitro* setting. We have isolated osteoblasts from *Osx1-Cre;K-ras<sup>G12D</sup>* mutant calvaria and then cultured them in media that promotes either bone or fat differentiation. We found that osteoblasts from the *Osx1-Cre;K-*

*ras*<sup>G12D</sup> mutants, but not control animals, had acquired adipogenic capacity, while their osteogenic ability was impaired.

Two hypotheses to explain this observation are that osteoblasts expressing activated K-ras form more adipocytes either by changing their fate (trans-differentiation) or by de-differentiating to a more primitive cell, which is then is capable of forming either bone or fat. Either possibility would bring interesting insights into a novel function of K-ras<sup>G12D</sup> in modulating mesenchymal lineage specification. Future studies should investigate if this phenotype is also seen in an *in vivo* setting. We looked in our *Osx1-Cre;K-ras*<sup>G12D</sup> embryos for signs of fat in their limbs; however, at embryonic stages the deposits of fat surrounding the limbs are very reduced, and we could not see any signs of fat increase in the long bones. Thus, one would have to look for this phenotype in adult mice. Thus, future studies should investigate *Osx1-Cre;K-ras*<sup>G12D</sup> adults, in which K-ras<sup>G12D</sup> was activated later in development to avoid embryonic lethality. Interestingly, our collaborators from MGH, Tatsuya Kobayashi and Fay Papaioannou have performed a similar study where they injected tamoxifen in females carrying *Osx1-CreERT2;K-ras*<sup>G12D</sup> embryos at E18.5 and followed the pups into adulthood. In *Osx1-CreERT2;K-ras*<sup>G12D</sup> mice around 8 weeks of age they notice an increase in the amount of fat in the long bones.

Our analysis of the cultured osteoblasts also show that Sprouty2 (a member of the Sprouty family, and a negative regulator of the MAPK pathway) is over-expressed in the K-ras<sup>G12D</sup> mutant cells, and Sprouty2 expression goes down as they differentiate into bone. Development of bone versus adipose tissue from their common progenitors is a carefully coordinated process and studies have identified

Sprouty1 (Spry1) as a critical regulatory switch of mesenchymal stem cells fate choice (Urs et al., 2010). Specifically, conditional deletion of Spry1 results in 10% increase in body fat and decreased bone mass (Urs et al., 2010). By suppressing the Ras/MAPK pathway and generating a negative feedback loop during development, Sprouty regulates several signaling pathways and affects common signal mediators. Thus, one hypothesis is that deregulation of members of the Sprouty family might contribute to the altered *in vitro* differentiation capacity of the K-ras mutant osteoblasts. To investigate if K-ras<sup>G12D</sup> acts directly through Sprouty, one could knock down Sprouty in osteoblasts expressing oncogenic K-ras and then assay their ability to form bone and fat; a reduced ability to form fat would suggest that Sprouty is essential in determining the altered mesenchymal specification conferred by K-ras activation.

Future studies should also focus on studying the mechanism through which K-ras<sup>G12D</sup> affects the mesenchymal fate choice by looking at its ability to modulate known master regulators of bone differentiation (TAZ) and fat differentiation (C/EBP- $\beta$ , PPAR $\gamma$ ). Data from the literature have shown a decrease in PPAR $\gamma$  expression both at the transcript and protein levels in a mouse model that conditionally expresses Spry1 in adipocytes (Urs et al., 2010). Other studies have shown that phosphorylation of ERK1/2 (downstream members in the MAPK pathway) induces C/EBP- $\beta$ , which then activates PPAR $\gamma$ 's transcriptional activity (Prusty et al., 2002). These observations suggest that the MAPK signaling pathway and its negative regulators play an important role in adipocyte specification.

Future studies should be conducted in either osteoblasts isolated from *Osx1-Cre;K-ras<sup>G12D</sup>* mutants or in mesenchymal stromal cells (MSCs) isolated from *Prx1-Cre;K-ras<sup>G12D</sup>* mutant mice. We did initiate studies in MSCs isolated from *Prx1-Cre;K-ras<sup>G12D</sup>* mutant mice limbs, but found unfortunately that K-ras<sup>G12D</sup> expression affected cell viability. A new and improved method of MSC isolation should be developed to perform these experiments.

The studies described above will be instrumental in describing the role of K-ras<sup>G12D</sup> as a switch of mesenchymal lineage commitment. Understanding the role of K-ras in a context related to cellular differentiation is very relevant to both normal development as well as cancer, as many tumors have cells that are un-differentiated, either through blocking at progenitor stage or via cellular de-differentiation. Understanding how K-ras<sup>G12D</sup> modulates the differentiation of mesenchymal lineages in our *in vivo* and *in vitro* systems will thus yield insight into its role in derailing lineage commitment/ maintenance, and thereby affecting normal development or promoting tumorigenesis.

#### **4.5. Generation of novel mouse models to study Noonan Syndrome associated bone defects and potential treatment strategies**

In chapter 2 we discuss our efforts trying to investigate the bone defects associated with Noonan Syndrome (NS) in a novel mouse model we have generated. We describe the histology of the bone phenotype, determine when the problem appears during development and investigate the underlying mechanisms. Furthermore, we describe a treatment strategy that is sufficient to block the skeletal

phenotype, and identify a narrow developmental time window in which the treatment must be applied.

Importantly, our treatment strategy indicates that appropriate MAPK signaling is critical for normal bone development. However, we also need to consider how expression of negative regulators of the MAPK pathway is affected in our mutants upon treatment with MEK inhibitors. Other studies have shown that when MAPK is inhibited in K-ras driven tumors, the expression of negative regulators of the MAPK signaling is up-regulated (Nissan et al., 2013). Thus, it remains an open question whether the bone defects we observe are a direct result of elevated MAPK signaling or an indirect consequence of downstream effects, including the negative feedback loops, that result from MAPK activation.

We were not able to recover living *Prx1-Cre;K-ras<sup>G12D/+</sup>* mice that received treatment during embryonic development. Although the embryos were alive at E18.5 and present in Mendelian ratios, none of the rescued mutants survived after birth. Since we also fail to recover viable wild type mice, this is clearly independent of K-ras effect. It is possible that due to the daily injections, the mothers are stressed and thus fail to care for their litters. To test this possibility, one could transfer the newborns to another lactating mother and assess if *Prx1-Cre; K-ras<sup>G12D/+</sup>* mice can survive to adulthood in this setting. It would be interesting to know if such surviving animals live a normal lifespan and/or whether they might develop other bone defects, particularly the enhanced bone differentiation that is observed upon the osteoblast-specific activation of K-ras after birth in the *Osx1-Cre;K-ras<sup>G12D</sup>* mutants.

Our current state of knowledge regarding the role of MAPKs in the skeleton is at an exciting balance between its established importance during bone development and unexplored and poorly understood functions that are currently under investigation. Furthermore, concomitantly with understanding the role of normal MAPK signaling in the skeleton, we are starting to decipher the effects of aberrant signaling in the bone compartment. Understanding how pathological MAPK signaling affects bone development and regulates bone mass is very important for a multitude of diseases which are caused by mutations in the MAPK pathway (the RASopathies), as well as diseases in which there is an imbalance of the bone mass, such as osteoporosis or osteopetrosis.

## REFERENCES

- Anastasaki, C., K.A. Rauen, and E.E. Patton. 2012. Continual low-level MEK inhibition ameliorates cardio-facio-cutaneous phenotypes in zebrafish. *Dis Model Mech.* 5:546-52.
- Corson, L.B., Y. Yamanaka, K.M. Lai, and J. Rossant. 2003. Spatial and temporal patterns of ERK signaling during mouse embryogenesis. *Development.* 130:4527-37.
- Elefteriou, F., M.D. Benson, H. Sowa, M. Starbuck, X. Liu, D. Ron, L.F. Parada, and G. Karsenty. 2006. ATF4 mediation of NF1 functions in osteoblast reveals a nutritional basis for congenital skeletal dysplasiae. *Cell Metab.* 4:441-51.
- Galabova-Kovacs, G., D. Matzen, D. Piazzolla, K. Meissl, T. Plyushch, A.P. Chen, A. Silva, and M. Baccarini. 2006. Essential role of B-Raf in ERK activation during extraembryonic development. *Proc Natl Acad Sci U S A.* 103:1325-30.
- Greenblatt, M.B., J.H. Shim, and L.H. Glimcher. 2013. Mitogen-Activated Protein Kinase Pathways in Osteoblasts. *Annu Rev Cell Dev Biol.*
- Maes, C., T. Kobayashi, M.K. Selig, S. Torrekens, S.I. Roth, S. Mackem, G. Carmeliet, and H.M. Kronenberg. 2010. Osteoblast precursors, but not mature osteoblasts, move into developing and fractured bones along with invading blood vessels. *Dev Cell.* 19:329-44.
- Nissan, M.H., N. Rosen, and D.B. Solit. 2013. ERK Pathway Inhibitors: How Low Should We Go? *Cancer Discov.* 3:719-21.
- Prusty, D., B.H. Park, K.E. Davis, and S.R. Farmer. 2002. Activation of MEK/ERK signaling promotes adipogenesis by enhancing peroxisome proliferator-activated receptor gamma (PPARgamma) and C/EBPalpha gene expression during the differentiation of 3T3-L1 preadipocytes. *J Biol Chem.* 277:46226-32.
- Tidyman, W.E., and K.A. Rauen. 2009. The RASopathies: developmental syndromes of Ras/MAPK pathway dysregulation. *Curr Opin Genet Dev.* 19:230-6.
- Urs, S., D. Venkatesh, Y. Tang, T. Henderson, X. Yang, R.E. Friesel, C.J. Rosen, and L. Liaw. 2010. Sprouty1 is a critical regulatory switch of mesenchymal stem cell lineage allocation. *FASEB J.* 24:3264-73.
- Wang, W., J.S. Nyman, K. Ono, D.A. Stevenson, X. Yang, and F. Elefteriou. 2011. Mice lacking Nf1 in osteochondroprogenitor cells display skeletal dysplasia similar to patients with neurofibromatosis type I. *Hum Mol Genet.* 20:3910-24.

Wu, X., S. Chen, Y. He, S.D. Rhodes, K.S. Mohammad, X. Li, X. Yang, L. Jiang, G. Nalepa, P. Snider, A.G. Robling, D.W. Clapp, S.J. Conway, T.A. Guise, and F.C. Yang. 2011. The haploinsufficient hematopoietic microenvironment is critical to the pathological fracture repair in murine models of neurofibromatosis type 1. *PLoS One*. 6:e24917.

## **Appendix A**

### **Rb regulates fate choice and lineage commitment *in vivo***

Eliezer Calo, Jose A. Quintero-Estades, Paul S. Danielian, **Simona Nedelcu**, Seth D. Berman and Jacqueline A. Lees

The author contributed to Figure 1

**Published:** Nature. 2010 Aug 26; 466(7310):1110-4

## **Abstract**

Mutation of the RB-1 tumour suppressor occurs in one third of all human tumours and is particularly associated with retinoblastoma and osteosarcoma (Burkhart and Sage, 2008). Numerous functions have been ascribed to the product of the human RB-1 gene, pRB. The best known is pRB's ability to promote cell cycle exit through inhibition of the E2F transcription factors and the transcriptional repression of genes encoding cell cycle regulators (Burkhart and Sage, 2008). In addition, pRB has been shown *in vitro* to regulate several transcription factors that are master differentiation inducers (Korenjak and Brehm, 2005). Depending on the differentiation factor and cellular context, pRB can either suppress or promote their transcriptional activity. For example, pRB binds to Runx2 and potentiates its ability to promote osteogenic differentiation program *in vitro* (Thomas et al., 2001). In contrast, pRB acts together with E2F to suppress Pparg, the master activator of adipogenesis (Fajas et al., 2002a; Fajas et al., 2002b). Since osteoblasts and adipocytes can both arise from mesenchymal stem cells, these observations suggest that pRB might play a role in the choice between these two fates. However, to date, there is no evidence for this *in vivo*. Here we use mouse models to address this hypothesis in the context of mesenchymal tissue development and tumorigenesis. Our data show that Rb status plays a key role in establishing fate choice between bone and brown adipose tissue *in vivo*

Mutations in RB-1 (70-90% of cases) and TP53 (50-70% of cases) are strongly associated with human osteosarcoma (Kansara and Thomas, 2007; Clark et al., 2008). To model osteosarcoma in the mouse, we crossed *Rb<sup>fl/fl</sup>* (Sage et al., 2003) and *p53<sup>fl/fl</sup>* (Jonkers et al., 2001) conditional mutant mice with a transgenic line, *Prx1-Cre* (Logan et al., 2002), which expresses Cre recombinase in uncommitted mesenchymal cells that contribute to bone, muscle, and both white and brown adipose tissue (Figure 1a-c). The homozygous deletion of *Rb* and/or *p53* by *Prx1-Cre* yielded viable neonates with no detectable developmental defects (data not shown), allowing us to determine the affect of *Rb* and/or *p53* loss on sarcomagenesis (Figure 2a). The *Prx1-Cre; p53<sup>fl/fl</sup>* animals developed osteosarcoma (62%), rhabdomyosarcomas (15%) and/or undifferentiated sarcomas (12%). In contrast, deletion of *Rb* alone did not yield sarcomas. However, *Rb* mutation had a profound effect on the tumor spectrum of *Prx1-Cre; p53<sup>fl/fl</sup>* mice (Figure 2a,b): deletion of one *Rb* allele increased the frequency of osteosarcomas (to 92%), while mutation of both *Rb* alleles shifted the tumour spectrum away from osteosarcoma (now 18%) and towards hibernomas (91 %; Supplementary figure 2). This propensity for brown fat, as opposed to white fat, tumors fits with prior studies showing that *Rb* loss promotes brown fat over white fat differentiation (Hansen et al., 2004; Scime et al., 2005; Dali-Youcef et al., 2007). Genotyping confirmed that the tumor cells had undergone Cre-mediated recombination of *Rb* and/or *p53* (Figure 2c, data not shown). Moreover, it showed that the *Prx1-Cre; Rb<sup>+/fl</sup>; p53<sup>fl/fl</sup>* tumors consistently retained the wild type *Rb* allele (Figure 2c, data not shown). Thus *Rb* acts in a

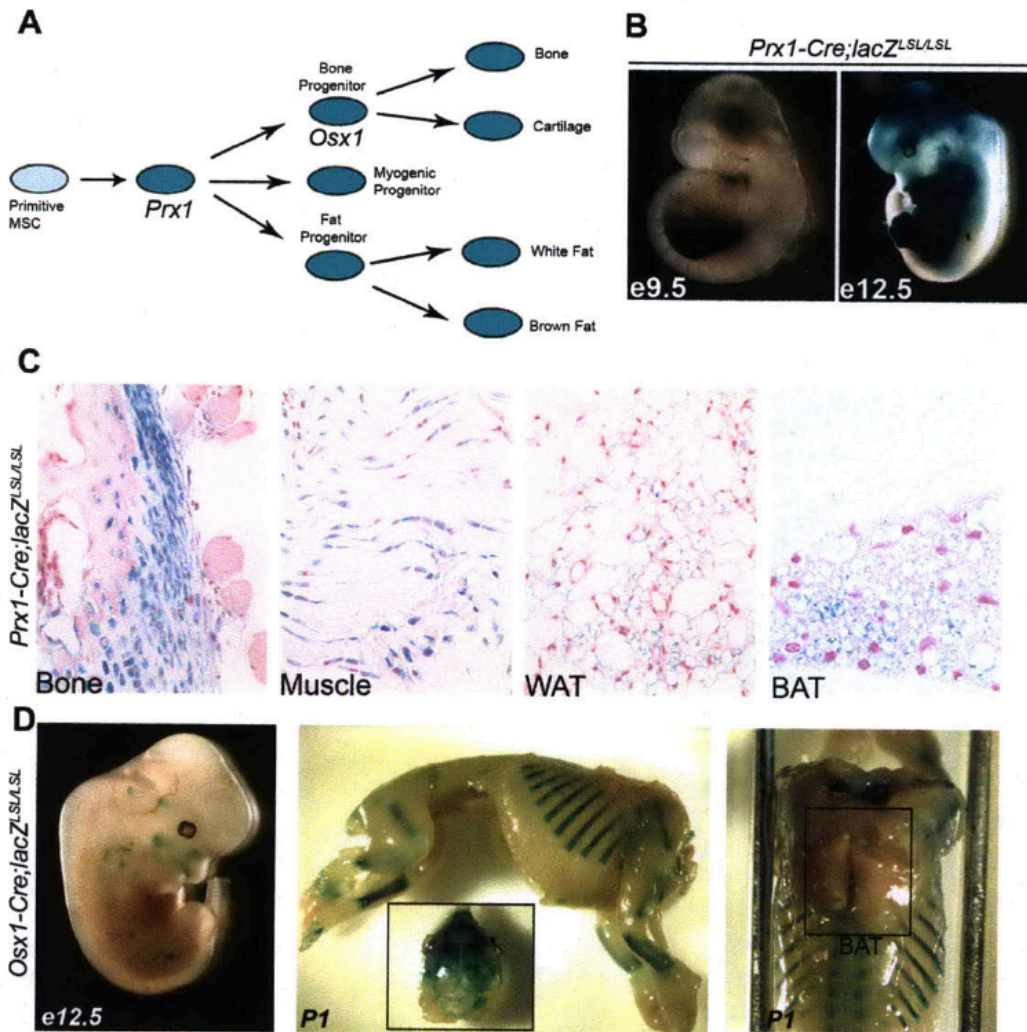


**Figure 1: Prx1-Cre is expressed in an uncommitted mesenchymal compartment that gives rise to bone, fat, and myogenic lineages in the adult.**

**a**, Diagram shows the onset of expression of *Prx1* versus *Osx1* in uncommitted mesenchymal stem cells versus committed osteoblast progenitors respectively. **b-c**, Intercrossing of *Prx1-Cre* with the *lox-stop-lox-LacZ* reporter mice and LacZ staining shows **(b)** that Prx-cre is expressed in the developing limb buds as early as e9.5 and is more evident at e12.5 as previously reported<sup>10</sup> and **(c)** it establishes extensive contribution of Cre-expressing cells to the bone, muscle, white and brown adipose tissues in 4-6 weeks old animals. **d**, Intercrossing of *Osx1-Cre* with the *lox-stop-lox-LacZ* reporter mice and staining for LacZ shows that unlike *Prx1-Cre*, *Osx1-Cre* is barely expressed at e12.5. In addition *Osx1-Cre* expression at postnatal day 1 is restricted to the bone tissue, and undetectable in the muscle and the brown fat compartments.

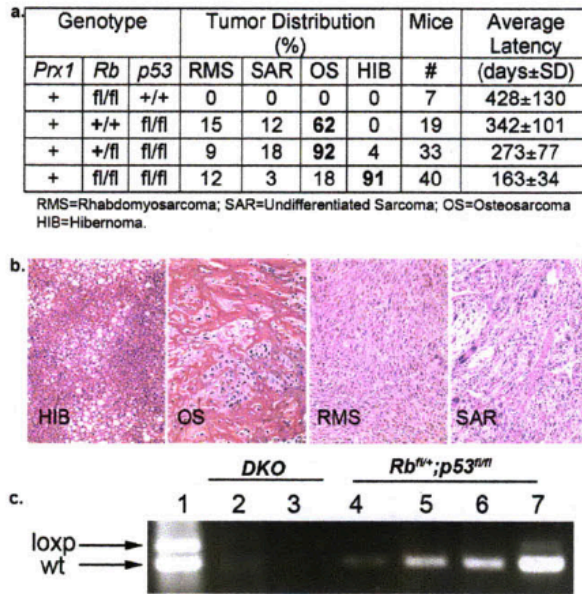


**Figure 2: *Rb* cooperates with *p53* and modulates mesenchymal tumor fate in a dosage-dependent manner.**

**a**, Mesenchymal tumor distribution (percentage of animals analyzed up to 24 months of age) for *Prx1-Cre;Rb* and/or *p53* compound mutant animals. **b**, H+E staining of representative sarcomas (20x magnification). **c**, PCR genotyping to detect *Rb* wildtype (wt) and recombined conditional mutant (*loxp*) alleles in control *Rb<sup>fl/+</sup>;p53<sup>fl/+</sup>* tissues (lane 1) or cell lines derived from *Prx1-Cre;Rb<sup>fl/fl</sup>;p53<sup>fl/fl</sup>* (DKO) or *Prx1-Cre;Rb<sup>fl/+</sup>;p53<sup>fl/fl</sup>* osteosarcomas. Cell lines were cultured for ≥20 passages prior to genotyping to eliminate stromal cell contribution.

dose dependent manner to modulate the spectrum of tumors arising from *p53*-deficient, uncommitted mesenchymal stem cells: osteosarcomas predominant in the presence of *Rb*, while *Rb* loss strongly favors hibernoma formation. Given that *Rb* loss in *p53* mutant uncommitted mesenchymal cells disfavors osteosarcoma formation, we also investigated the affect of *Rb* loss in a bone-committed progenitor. For this, we deleted *Rb* and/or *p53* using the *Osx-Cre* transgenic (Rodda and McMahon, 2006) which uses Osterix promoter sequences to express Cre in the pre-osteoblast (Figure 1d). In this model (Berman et al, 2008a), *Osx-Cre; p53<sup>fl/fl</sup>* mice specifically develop osteosarcoma (100%) while *Osx-Cre; Rb<sup>fl/fl</sup>; p53<sup>fl/fl</sup>* develop osteosarcoma (53%), hibernomas (46%) and sarcomas (2%). We established cell lines from multiple (3) independent *Osx-Cre; p53<sup>fl/fl</sup>* and *Osx-Cre; Rb<sup>fl/fl</sup>; p53<sup>fl/fl</sup>* osteosarcomas and discovered that the two genotypes have distinct differentiation properties (Figure 3, data not shown). The *Rb; p53 (DKO)* osteosarcoma (OS) cell lines expressed mRNAs that are characteristic of bone and fat differentiation (Figure 3a). Indeed, their expression pattern more closely resembled that of mesenchymal stem cells (MSCs) than primary osteoblasts (Supplementary Figure 2). Accordingly, culture in the appropriate differentiation media induced these DKO cells to adopt either the adipogenic or osteoblastic fate (Figure 3a). In contrast, the *p53KO* OS cell lines closely resembled pre-osteoblasts based on their gene expression patterns, but these cells were unable to differentiate into either bone or fat (Figure 3a and Supplementary Figure 2). Since this differentiation block occurs in the *p53*-null OS cell lines, but not *p53*-deficient primary osteoblasts (Lengner et al., 2006;

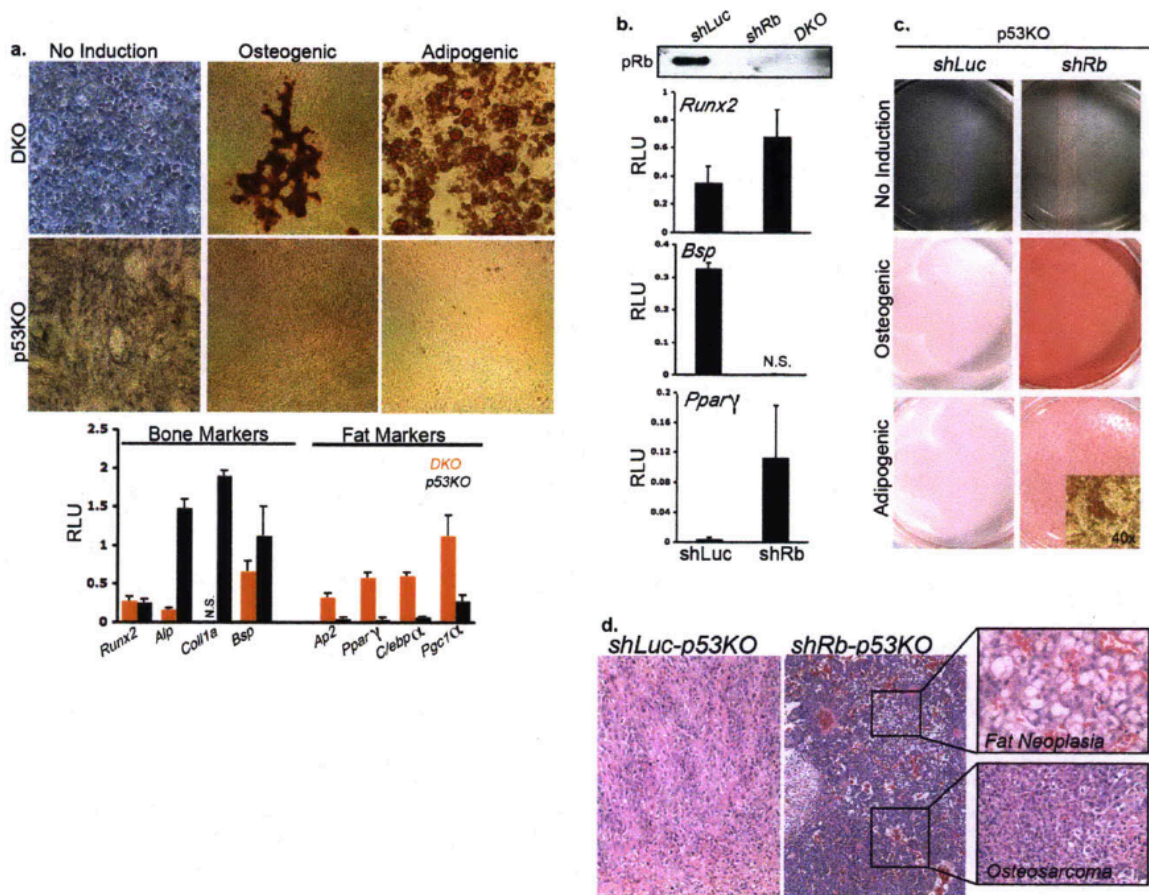


**Figure 3: *Rb* regulates osteosarcoma-cell lineage plasticity *in vitro* and *in vivo*.**

**a.** The differentiation potential of 3 different *DKO* and *p53KO* OS cell lines was assessed by addition of osteogenic or adipogenic differentiating media. Expression of bone and fat markers was assessed by qPCR of un-induced *DKO* (orange) and *p53KO* (black) OS cells. **b.** *Rb* or control (Luc) shRNAs were expressed in the *p53KO* cell lines. *Rb* knockdown was confirmed by immunoprecipitation and qPCR showed that this caused downregulation of the bone marker *Bsp* and upregulation of the fat marker *Ppar $\gamma$*  without culture in differentiating media. **c.** The osteogenic and adipogenic potential of *shLuc*- and *shRb-p53KO* cell lines was assessed. **d.** H+E staining of representative tumors derived from *shLuc*- and *shRb-p53KO* cell lines injected subcutaneously into immunocompromised mice. Moreover, the *shRb-p53KO* OS derived tumors were frequently mixed lineage (top inset shows fat neoplasm; bottom inset bone/undifferentiated sarcoma), while the control *shLuc-p53KO* tumors were uniformly. Bars represent the mean of three independent experiments (+/- SD). NS = not significantly expressed.

Figure 6a), it likely reflects their transformed state. We used these *p53KO OS* cells to determine whether *Rb* loss was sufficient to alter the differentiation potential of blocked pre-osteoblasts by introducing control (*shLuc*) or *Rb*-specific (*shRb*) shRNAs. pRb was readily detectable in *shLuc-p53KO*, but not *shRb-p53KO*, OS cells (Figure 3b). Strikingly, without addition of differentiation media, pRb knockdown downregulated the bone-specific mRNA *Bsp* and upregulated the fat regulator *Ppar $\gamma$*  (Figure 3b). Accordingly, these *shRb-p53KO* OS cells were now able to differentiate into either bone or fat *in vitro* (Figure 3c). Moreover, when transplanted into nude mice, the *shRb-p53KO* OS cells formed more aggressive tumors than the parental *p53KO* OS cells, and these were of mixed lineage (fat, bone and undifferentiated sarcomas), in stark contrast to the undifferentiated osteoblastic tumours arising from either control *shLuc-p53KO* or parental *p53KO* OS cell lines (Figure 3d, Supplementary Figure 3, and data not shown). Thus, pRB loss is sufficient to override the differentiation block of these p53-deficient, tumor cell lines and also expand their fate commitment to include the adipogenic state. We also examined the consequences of reintroducing *Rb* into the *DKO* OS cells. For this, we induced pRb in confluence-arrested *DKO* cells using a doxycycline-inducible expression system (*DKO-Rb Dox-ON*; Figure 4). Remarkably, pRb restoration caused the *DKO* OS cells to adopt the differentiation state of the *p53KO* OS cell lines within two days: it induced down-regulation of adipogenic markers and up-regulation of osteogenic markers, and the cells were unable to

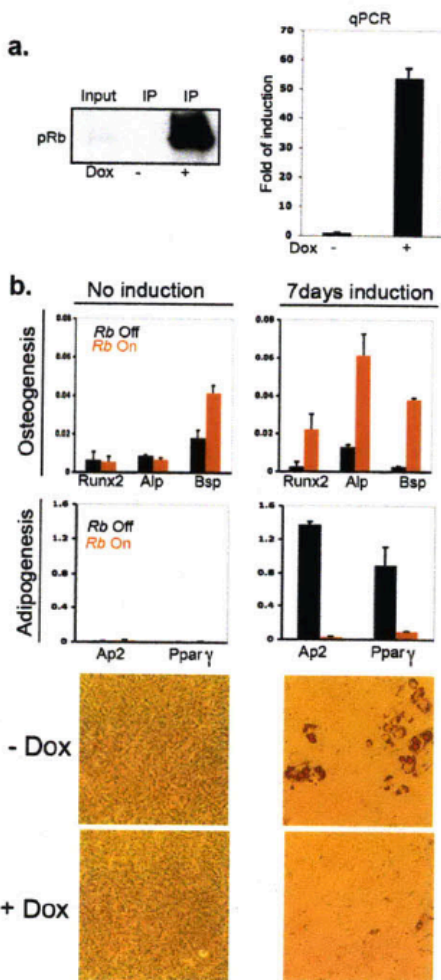


**Figure 4: Restoration of *Rb* function promotes lineage commitment in osteosarcoma cell lines.**

Immunoprecipitates of *DKO-Rb<sup>Dox-ON</sup>* OS cells showed pRb expression 48h after doxocycline (Dox) treatment (left, upper panel). *Rb* expression was also confirmed by qPCR (left, lower panel). OS cells were treated either with Dox (*Rb* On) or PBS (*Rb* Off) for 48h and then were induced to differentiate into the adipogenic and osteogenic lineages by addition of differentiation media. qPCR for osteogenic and adipogenic markers was used to analyzed the differentiation potential of these cells either prior to (-Diff. media) or 7 days after [+Diff. media (7d)] addition of differentiation media in the *Rb* On (orange) versus *Rb* Off (black) populations.

differentiate into fat (Figure 4). Thus removal or re-introduction of *Rb* appears sufficient to switch lineage specification between osteoblastic commitment and multipotency. *In vitro* studies have shown that pRB can act with E2F to enforce transcriptional repression of *Ppar $\gamma$*  (Fajas *et al.*, 2002a; Fajas *et al.*, 2002b), and also bind, and potentiate the transcriptional activity of, the osteogenic regulator RUNX2 (Thomas *et al.*, 2001). We hypothesized that pRb's role in these processes might underlie *Rb*'s affect on adipogenesis versus osteogenesis. Thus, we used our *DKO-RbDox-ON* cells to determine whether the presence or absence of pRb modulated these transcriptional regulators (Figure 5). First, we used chromatin-immunoprecipitation assays to investigate promoter regulation of *Ppar $\gamma$*  and representative Runx2-responsive genes *Coilla* (Figure 5a) and osteocalcin (*Oc*; data not shown). pRb-induction caused both pRb and E2f4, the predominant repressive E2f, to be recruited to the *Ppar $\gamma$*  promoter (Figure 5a) and this correlated with *Ppar $\gamma$*  mRNA downregulation (Figure 5a). Contemporaneously, pRb bound to *Col1 $\alpha$*  and *Oc* and this was accompanied by increased promoter occupancy of Runx2 and upregulation of *Col1 $\alpha$*  and *Oc* mRNAs (Figure 5a, data not shown). Importantly, these changes in *Ppar $\gamma$* , *Col1 $\alpha$*  and *Oc* regulation were all detected within 2 days of pRb induction and without addition of differentiation-inducing media. In addition, we found that Runx2 associated with pRb in the *p53KO*, but not the *DKO*, OS cells and its transcriptional activity was 8 fold higher in the former, versus the latter, population (Figure 5b). Thus the presence or absence of pRb directly modulates

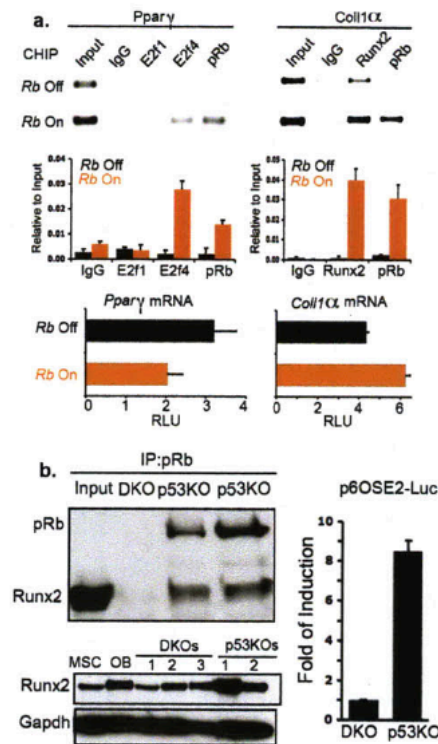


**Figure 5: pRb modulates the activity and the expression of the master lineage regulators Runx2 and Pparγ.**

**a**, *DKO-Rb<sup>Dox-ON</sup>* cells were cultured for two days in the absence (*Rb Off*) or presence (*Rb On*) of doxocycline and then analyzed. Results are representative of three independent experiments. Promoter occupancy was assessed by chromatin immunoprecipitation. Sequence analysis identified two potential E2f binding sites (-278 and -160) within the *Pparγ* promoter. pRb induction caused a dramatic upregulation of both pRb and E2F4 binding to the proximal site. (No binding was observed at the distal element.) Similarly, pRb induction allowed pRb to bind to the known Runx2 response element of *Col1a*<sup>16</sup> and also increased the binding of Runx2. These changes correlated with the downregulation of *Pparγ* mRNA and upregulation of *Col1a* mRNA as judged by qPCR. **b**, Western blotting detected Runx2 in pRb-immunoprecipitates from *p53KO-OS* cell lines (left, top panel). Western blotting of whole cell extracts confirmed that Runx2 was expressed in both DKO and *p53KO* OS cell lines (left, bottom panel). MSCs and osteoblasts were used as a positive control. Right panel: Runx2 transcriptional activity was shown to be higher in the *p53KO*- versus the DKO OS cell lines as judged by activation of the artificial Runx2-responsive reporter p6OSE2-Luc. Results are the average of six independent samples.

the levels and activity of *Ppar $\gamma$*  and *Runx2* in accordance with the preferential commitment of our OS cell lines to the osteogenic versus the adipogenic lineage. The preceding experiments establish a clear role for pRb in fate commitment bias *in vivo and in vitro*. However, since this analysis was conducted in p53-deficient cells, it is unclear whether *Rb* alone is sufficient to determine this plasticity or whether transformation is also required. To address this, we isolated primary osteoblasts from the calvaria of *Rb<sup>f/f</sup>*, *p53<sup>f/f</sup>* or *Rb<sup>f/f</sup>;p53<sup>f/f</sup>* e8.5 embryos. We brought these cells to confluence, to minimize the influence of altered proliferation, infected them with adenoviruses expressing Cre or a GFP control and then assayed differentiation. As expected, the control-infected osteoblasts were able to undergo osteogenesis but not adipogenesis (Figure 6a; data not shown). Similarly, p53 loss had no effect on this fate commitment (Lengner *et al.*, 2006; Figure 6a). In stark contrast, deletion of *Rb*, either alone or together with p53, allowed these cells to adopt either the bone or fat lineage (Figure 6a; data not shown). This switch to multipotency correlated with the significant upregulation of adipogenic markers prior to the induction of differentiation (Figure 6b). Thus, pRb-loss is sufficient to alter the fate commitment in otherwise wild type calvarial osteoblasts. *In vitro* culture can modulate the plasticity of cells. Thus, we wished to examine *Rb*'s role in fate choice *in vivo*. For this, we employed a third transgenic strain, *Meox2-Cre*, which expresses Cre in the embryo proper from e6.5 (Tallquist and Soriano, 2000). *Meox2-Cre; Rb<sup>f/f</sup>* embryos survive to birth

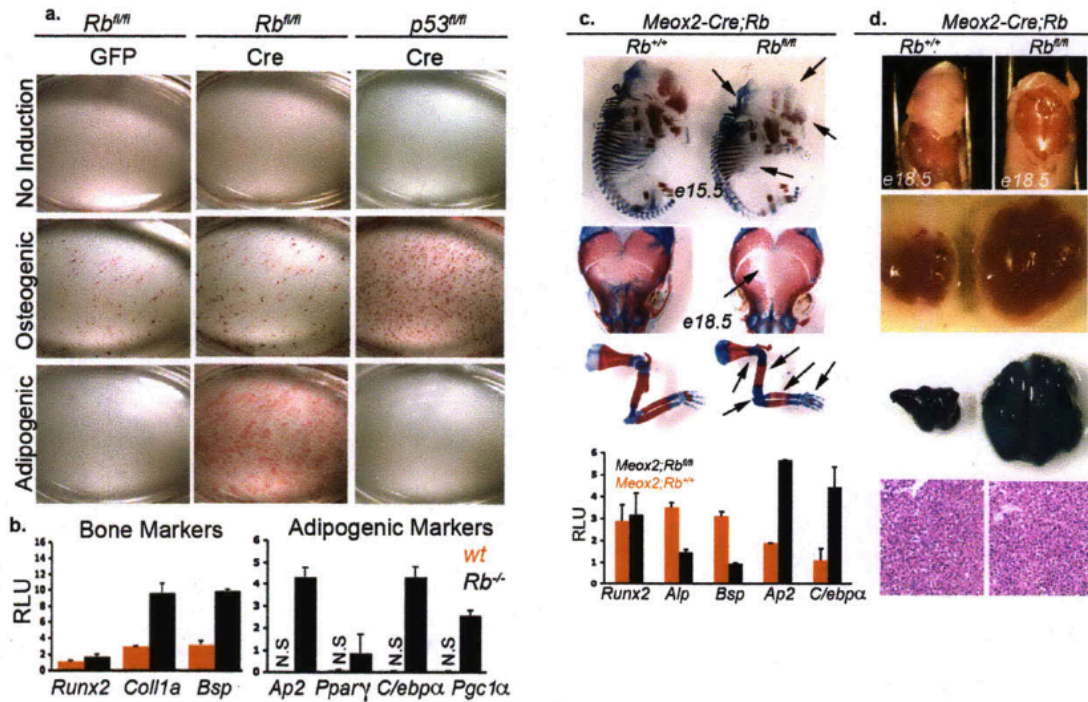
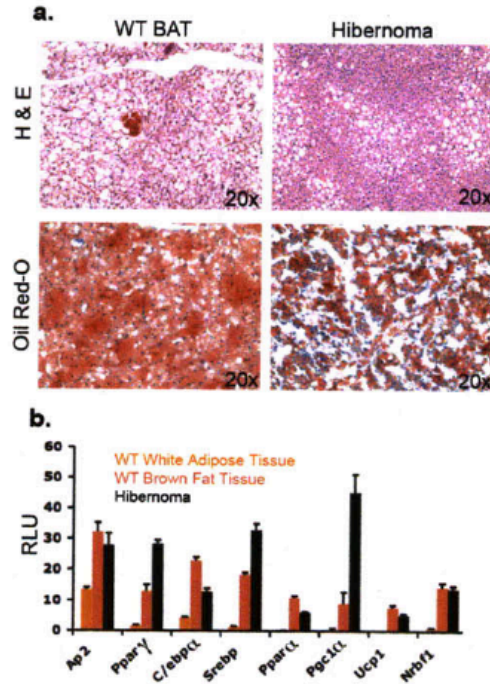


**Figure 6: *Rb* maintains the osteoblastic fate commitment in normal osteoblasts and regulates fate choice during normal development *in vivo*.**

**a**, Calvarial osteoblasts were prepared from e18.5 *Rb<sup>fl/fl</sup>* or *p53<sup>fl/fl</sup>* embryos and infected with Ad-GFP or Ad-Cre at P1. Five days later, the cells were induced with differentiation media and then assayed for osteogenesis and adipogenesis at 0, 14 and 25 days by staining with Alizarin Red and Oil-Red-O. A representative timepoint (25 days) is shown. **b**, qPCR was also used to assess osteogenic and adipogenic markers in the un-induced *Rb<sup>fl/fl</sup>* (*wt*) versus *Rb<sup>fl/fl</sup>*+Ad-Cre (*Rb<sup>-/-</sup>*) osteoblasts. Bars represent the mean of three independent experiments (+/- SD). **c**, Alizarian Red (bone mineralization) and Alcian Blue (cartilage) staining of e15.5 skeletons (top panel), e18.5 calvaria (middle panel) and e18.5 limbs (bottom panel) from *Meox2-Cre;Rb<sup>+/+</sup>* and *Meox2-Cre;Rb<sup>fl/fl</sup>* littermate embryos. Arrows mark visible skeletal defects. qPCR was used to assess osteogenic (*Runx2*, *Alp*, and *Bsp*) and adipogenic (*Ap2* and *C/ebp $\alpha$* ) markers in mRNA extracted from the calvarial bones of e18.5 *Meox2-Cre;Rb<sup>+/+</sup>* and *Meox2-Cre;Rb<sup>fl/fl</sup>* embryos. Bars show the mean of three embryos arising in two independent crosses (+/- SD). **d**, Brown adipose tissue (BAT) was dissected from the backs of *Meox2-Cre;Rb<sup>fl/fl</sup>* embryos (*n*=10) and their *Meox2-Cre;Rb<sup>+/+</sup>* littermate controls. All 10 showed a dramatic expansion of the brown fat compartment. A representative example is shown (upper two panels). Introduction of the LSL-LacZ reporter into this model, and LacZ staining confirmed equal, widespread expression of Cre in the control and *Rb* mutant BAT (third panel). H+E staining of BAT (bottom panel).

(Wu *et al.*, 2003). We isolated wildtype (*Meox2-Cre; Rb<sup>+/+</sup>*) and *Rb* mutant (*Meox2-Cre; Rb<sup>fl/fl</sup>*) littermates at e15.5 and e18.5 and examined both bone and brown fat development. First, there was a significant reduction in the level of calcified bone matrix in both the calvaria and long bones of *Rb* mutant versus wildtype embryos (Berman *et al.*, 2008b; Figure 6c). Moreover, qPCR analysis established that *Runx2* mRNA was present at appropriate levels in the *Rb* mutant e8.5 calvarial osteoblasts, but there was a downregulation of other bone markers and a clear upregulation of fat-associated mRNAs (Figure 6c). In parallel, we found that the level of brown fat was dramatically increased in the e8.5 *Rb* mutant versus the wildtype controls (Figure 6d and Supplementary Figure 4). Thus, *Rb* loss in an, otherwise wildtype, embryo impairs bone differentiation and expands the fat compartment. Our data establish a clear role for pRB in determining the fate choice of mesenchymal progenitors and the lineage commitment of pre-osteoblasts. This occurs both *in vitro* and *in vivo* and irrespective of whether these cells are transformed or otherwise wildtype. *In vivo*, *Rb*-loss favours adipogenesis over osteogenesis to the extent that it can reduce the levels of calcified bone and greatly increase the levels of brown fat. Moreover, *Rb*-loss in pre-osteoblasts is sufficient to disfavor commitment to the osteogenic state and restore multipotency. It is possible that *Rb* loss allows expansion of a rare multipotent progenitor population that exists within the pre-osteoblast compartment. Alternatively, *Rb* loss could be actively reprogramming the pre-osteoblasts by driving either trans-differentiation to the adipogenic lineage or true dedifferentiation to the multipotent progenitor stage. Between the two reprogramming models we favor de-differentiation based on both

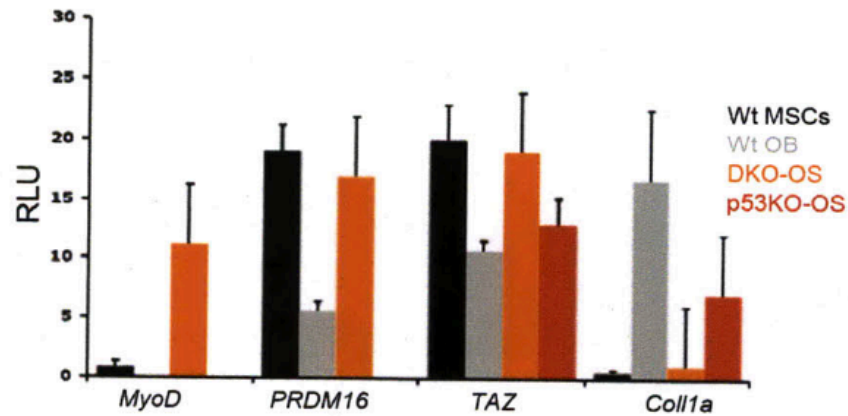
the expression of multi-lineage differentiation markers in the DKO OS cells (Supplementary Figure 4) and the broadening of the tumor spectrum from solely osteosarcomas in the *Osx-Cre;p53<sup>fl/fl</sup>* animals to include not only osteosarcomas and hibernomas but also sarcomas in the *Osx-Cre;Rb<sup>fl/fl</sup>;p53<sup>fl/fl</sup>* mice. Finally, our data offers potential insight into the cell of origin for osteosarcomas. Specifically, given the high frequency of *RB-1* mutations in human osteosarcoma, we were surprised to find that *Rb* mutation predisposes mesenchymal cells away from the osteoblastic state. Given this finding, we speculate that *RB-1* mutant osteosarcomas are likely to arise from more committed osteoblastic lineages than from uncommitted mesenchymal progenitors. In this setting, *RB-1* loss could enable de-differentiation and thereby synergize with other mutations to promote tumorigenesis.



**Supplementary Figure 1: Characterization of brown fat adipogenic sarcomas (Hibernomas).**

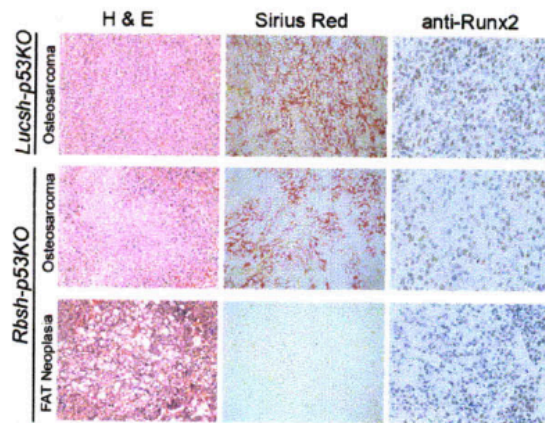
**a**, H&E staining of brown adipose tissue (WT BAT) and hibernoma (upper panel). To confirm the adipogenic nature of the HIB, frozen sections for both WT BAT and HIB were stained with Oil Red-O, which marks accumulation of lipid droplets.

**b**, The expression profile of HIB for different adipogenic marker was compared to that of white and brown adipose tissues. This data clearly shows that the adipogenic sarcomas observed in our mouse model are indeed from the brown fat compartment.



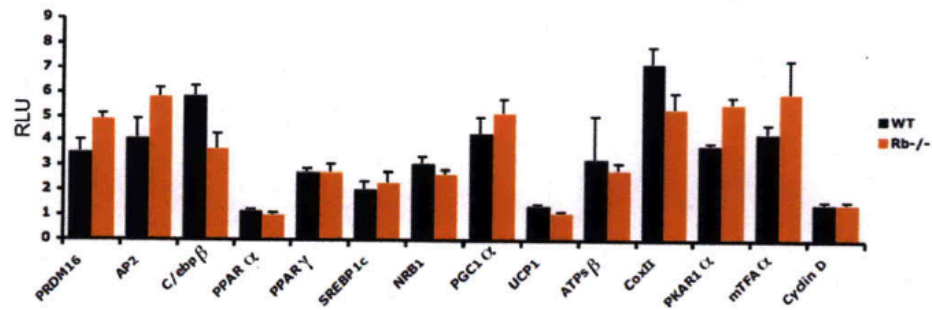
**Supplementary Figure 2: Expression of multilineage specific markers in DKO-OS cell lines.**

Different lineage specific markers for mesenchymal lineages were analyzed by qPCR in DKO-OS cell lines and compared to wt MSCs, wt osteoblasts and the p53KO OS cells. MyoD is a myogenic specific transcription factor, PRDM16 is a molecular determinant for the brown fat/skeletal muscle lineages, TAZ is a molecular determinant for the bone/fat lineages, and Coll1a is a bone specific factor. This expression analysis showed that the p53KO OS cells closely resemble the committed osteoblasts, consistent with the stage at which the Cre was expressed and therefore *p53* deleted. In contrast, the DKO OS cells more closely resembled the multipotent progenitors, consistent with the notion that these cells have undergone de-differentiation.



**Supplementary Figure 3: *Rb*-loss promotes tumor-cell plasticity *in vivo*.**

Tumors arising from *Lucsh-p53KO* and *Rbsh-p53KO* cell lines were stained with Sirius Red, which marks collagen fibers and immuno-stained for the bone-specific transcription factor Runx2. Both collagen and Runx2 were clearly detected in all *Lucsh-p53KO* cells, but low levels of collagen and Runx2 were present in *Rbsh-p53KO* cells. In addition, neither Runx2 nor Collagen staining was observed in the fat neoplasia observed in the *Rbsh-p53KO* tumors.



**Supplementary Figure 4: Expression profile of *Rb*-mutant and -wt brown adipogenic tissue.**

The brown fat compartment of e18.5 *Meox2-Cre;Rb<sup>+/+</sup>* and *Meox2-Cre;Rb<sup>fl/fl</sup>* embryos was collected and analysed for the expression of different adipogenic markers using qPCR. This confirms that the adipogenic nature of the tissues analyzed for this study.

## **Experimental Procedures**

### *Animal maintenance and histological analyses*

Animal procedures followed protocols approved by MIT's Committee on Animal Care. The *Rb<sup>fl/fl</sup>*, *p53<sup>fl/fl</sup>*, *Oxsl-GFP::Cre*, *Prxl-Cre*, *Rosa26-LSL-IacZ* (REF), and *Meox2-Cre* animals were maintained on a mixed genetic background. Skeletal stainings were conducted as described. The transplant assays were conducted in NOD/SCID mice using 10<sup>4</sup> cells. Tissues were fixed in PBS with 3.7% formaldehyde. Prior to paraffin sectioning, soft tissues were dehydrated via an ethanol series, while bone-containing tissue was decalcified in 0.46M EDTA, 2.5% Ammonium Hydroxide pH 7.2.

### *Mouse genotyping*

The *Rb* conditional band was detected using the primers 5'lox: 5'-CTCTAGATCCTCTCATTCTTC-3' and 3'lox: 5'-CCTTGACCATAGCCCAGCAC-3'. Primer Rbcre3.2 (5'-GGTTAATGAAGGACTGGG-3') was used in conjunction with primer 5'lox to detect the recombined band. To identify the p53 conditional allele we used primer p53A: 5'-CACAAAAACAGGTAAACCCAG-3' and primer p53B: 5'-AGCACATAGGAGGCAGAGAC-3'. The recombined allele was detected using primer p53A in conjunction with primer p53D: 5'-GAAGACAGAAAAGGGGAGGG-3'.

### *Tumor monitoring and analysis*

The criteria for euthanasia (by CO<sub>2</sub> inhalation) were a total tumor burden of 2cm<sup>3</sup>, tumor ulceration/bleeding, signs of infection, respiratory distress, impaired

mobility, 220% reduction in body weight or general cachexia. All tissues were collected and hip bones, femurs and tibias were separated and fixed overnight in PBS with 3.7% formaldehyde. Soft tissues were transferred into 70% ethanol and dehydrated via an ethanol series prior to embedding in paraffin for sectioning. Tissues containing bone was either decalcified in 0.46M EDTA, 2.5% Ammonium Hydroxide pH 7.2 for two weeks then processed for paraffin sectioning. All paraffin embedded sections were cut at 5µm, dewaxed and stained with H&E. Sirius red staining was performed by treating sections briefly stained with hematoxylin with 0.1 % Sirius red in saturated picric acid (Electron Microscopy Sciences) for one hour, washing in 5% v/v glacial acetic acid and then dehydration in ethanol/xylene prior to mounting.

#### *Generation of osteosarcoma cell lines*

Osteosarcomas were dissected, minced, filtered through a 70µm filter, and plated in normal growth medium (10% FBS in DME, 1% P/S, L-glutamine) to generate the OS cell lines. Cells were passaged as they reached confluence. For RNA purification, cells were rinsed 2x with PBS, and RNA extraction was performed using RNAeasy kit (Quiagen). First-strand cDNA was transcribed from 1 µg of RNA using Superscript III reverse transcriptase (Invitrogen) following the manufacturer's instructions.

Quantitative RT-PCR with 20 to 100 ng cDNA was done using SYBR Green (Applied Biosystems). Reactions were run on the ABI Prism 7000 Sequence Detection System and analyzed using the 7000 SDS software. Primers used for qPCR are shown in Supplementary Table 1. Knockdown of *Rb* in the *p53KO-OS* cells was achieved using

the pMLP-miR30-based shorthairpin (*Rb* targeted sequence: CACGGACGTGTGAACTTATATA). Adenoviruses expressing Cre or GFP were provided by the U. of Iowa Gene Transfer Vector Core. For immunoprecipitations and immunoblotting, proteins were extracted with a Triton X-100 based buffer and quantified by the BCA assay reagent (Pierce, Inc). Antibodies were from Santa Cruz Biotechnology [pRb (H-153), E2F1 (C-20), and E2F4 (C-20)], BD Pharmingen (pRb), Ambion (GAPDH) and MBL (Runx2). Dual luciferase assays were performed as described by the manufacturer (Promega). The Runx2 reporter p60SE2-Luc and control p4Luc were provided by Dr. Gerard Karsenty.

#### *Immunohistochemistry (IHC)*

Runx2 IHC was performed using a modified citric acid unmasking protocol. Briefly, slides were deparaffinized in xylene and rehydrated through ethanol. Slides were boiled for 30 min in citrate buffer, pH 6.0, and then cooled in running tap water. Slides were then washed in PBS for 5 min followed by inactivation of endogenous peroxidases by incubation 0.5% H<sub>2</sub>O<sub>2</sub> in methanol. Slides were blocked in 10% Goat Serum for 1 h at room temperature. Primary antibody (MBL anti-Runx2 Clone 8G5) was diluted 1:200 in PBS 0.15% Triton and incubated overnight at 4 °C. The following day, slides were washed three times in PBS. Secondary antibodies (Vectastatin ABC kits, Vector laboratories) were diluted 1:500 in PBS containing 0.4% Goat Serum and detected using a DAB substrate (Vector Laboratories). All samples were counterstained with hematoxylin.

### *Skeletal Staining*

Embryos were sacrificed, skinned and eviscerated. The remaining tissue was fixed in 95% ethanol for 4 days, transferred to acetone for 3 days, and subsequently transferred to staining solution of 0.015% Alcian blue 8GX (Sigma), 0.005% alizarin red S (Sigma), and 5% glacial acetic acid in ethanol at 37°C for 2 days and at room temperature for a one more day. Tissue was cleared in 1 % potassium hydroxide for several days and then stored in glycerol.

### *Calvarial Osteoblasts Preparation and Culture*

Calvaria from embryonic day 18.5 embryos were removed and carefully cleaned in sterile PBS from contaminating tissue. Then treated with several rounds of collagenase/trypsin digestion at 37°C, and plated onto six-well plates for 2 days in  $\alpha$ MEM with 10% fetal bovine serum and penicillin/streptomycin. For differentiation,  $3.5 \times 10^5$  cells were plated onto a well of a 6-well tissue culture plates. Upon reaching confluence, calvarial osteoblasts were treated with medium supplemented with 50  $\mu$ g/mL of ascorbic acid and 10 mmol/L of  $\beta$ -glycerol-phosphate. Adenovirus (University of Iowa Gene Transfer Vector Core) was added to the medium at 100 plaque-forming units per cell and washed away 24 h later. To assay for calcium deposits, plates were stained with 1 % alizarin red S solution (pH 5.0).

### *Chromatin Immunoprecipitation assay*

Protein complexes were cross-linked to DNA in living nuclei by adding

formaldehyde (Sigma, Inc.) to give a final concentration of 1 %. After incubation for 10 min at 37 °C, crosslinking was stopped by addition of glycine to a final concentration of 0.125 M for 5 min. Cross-linked cells were washed twice with PBS containing PMSF 1 mM (phenylmethylsulfonyl fluoride), scraped and pelleted. Nuclei were extracted with a 20mM Tris pH 8, 3mM MgCl<sub>2</sub>, 20 mM KCl buffer containing protease inhibitors, pelleted by microcentrifugation and lysed by incubation in SDS lysis buffer (1% sodium dodecyl sulfate, 10 mM EDTA, 50 mM Trischloride pH 8.1), containing protease inhibitors. The resulting chromatin solution was sonicated to generate 500-1000 bp DNA fragments. After microcentrifugation, the supernatant was diluted 1:10 with a dilution buffer (0.01% sodium dodecyl sulfate, 1.1% Triton X-100, 1.2 mM EDTA, 16.7 mM Trischloride pH 8.1, 167 mM NaCl, containing protease inhibitors), precleared with blocked protein A-positive Staph cells (Santa Cruz, Inc), and divided into aliquots. Five micrograms of the indicated antibodies was added to each aliquot and incubated for 12 to 16 hours at 4°C with rotation. Antibody-protein-DNA complexes were isolated by immunoprecipitation with blocked protein A-positive Staph A cells. Following extensive washing, bound DNA fragments were eluted and analyzed by Quantitative RT-PCR using primers shown in Supplementary Table 2.

**Supplementary Table 1: Real Time PCR Primers**

<b>Gene</b>	<b>Forward Primer</b>	<b>Reverse Primer</b>
Alkaline Phosph.	TCT CCA GAC CCT GCA ACC TC	CAT CCT GAG CAG ACC TGG TC
Collagen 1a1	CGA GTC ACA CCG GAA CTT GG	GCA GGC AGG GCC AAT GTC TA
Osteocalcin	CTC TGT CTC TCT GAC CTC ACA G	CAG GTC CTA AAT AGT GAT ACC G
Osteopontin	TGC TTT TGC CTG TTT GGC AT	TTC TGT GGC GCA AGG AGA TT
Runx2	TGA GAT TTG TGG GCC GGA	TCT GTG CCT TCT TGG TTC CC
Ap2	ATCCCTTTGTGGGAACCTGGAA	ACGCTGATGATCATGTTGGGCT
C/ebp $\alpha$	CAAGAACAGCAACGAGTACCG	GTCACTGGTCAACTCCAGCAC
Ppar $\gamma$	GAGCTGACCCAATGGTTGCTG	GCTTCAATCGGATGGTTCTTC
Srebp-1c	GGAGCCATGGATTGCACATT	GCTTCCAGAGAGGAGGCCAG
Ucp-1	AGCCGGCTTAATGACTGGAG	TCTGTAGGCTGCCCAATGAAC
Pgc-1	GTCTCACAGAGACTGGA	TGGTTCTGAGTGCTAAGACC
Nbrf-1	CGGCACCTAGCGCCCGG	CGGCACCTAGCGCCCGG
MyoD	CGCCACTCCGGGACATAG	GAAGTCGTCTGCTGTCTCAAAGG
Prdm16	GACCACGGTGAAGCCATTC	GCGTGCATCCGCTTGTG
Taz	GTCACCAACAGTAGCTCAGATC	AGTGATTACAGCCAGGTTAGAAAG
Gapdh	CAAGGTGGCAGAGGCCTTT	TCCAGCTGCTCAATGGACGCATTT

**Supplementary Table 2: CHIP Primers**

Promoter	Forward Primer	Reverse Primer
Ppar $\gamma$ ( E2f Proximal Site)	ACGCGGAAGAAGAGACCT	TCCTGTCAGAGTGTGACTTCTCCT
Ppar $\gamma$ (E2f Distal Site)	TCGCACTCAGAGCGGCAG	AGGTCTCTTCCGCGTCCCT
Coll1a1 (Runx2 site)	TGCTTCCACGTTTACAGCTCTAAAG	GTCAGGAAAGGGTCATCTGTAGTCC
Osteocalcin (Runx2 Site)	GAGAGCACACAGTAGGAGTGGTGGAG	TCCAGCATCCAGTAGCATTATATCG

## References

- Berman, S. D., Calo, E., Landman, A. S., Danielian, P. S., Miller, E. S., West, J.C., Fonhoue, B. D., Caron, A., Bronson, R., Bouxsein, M. L., Mukherjee, S. and Lees, J. A. (2008a) Metastatic osteosarcoma induced by inactivation of Rb and p53 in the osteoblast lineage. *Proc Natl Acad Sci U S A*, 105, 11851-11856.
- Berman, S. D., Yuan, T. L., Miller, E. S., Lee, E. Y., Caron, A. and Lees, J. A. (2008b) The retinoblastoma protein tumor suppressor is important for appropriate osteoblast differentiation and bone development. *Mol Cancer Res*, 6, 1440-1451.
- Burkhardt, D. L. and Sage, J. (2008) Cellular mechanisms of tumour suppression by the retinoblastoma gene. *Nat Rev Cancer*, 8, 671-682.
- Clark, J. C., Dass, C. R. and Choong, P. F. (2008) A review of clinical and molecular prognostic factors in osteosarcoma. *J Cancer Res Clin Oncol*, 134, 281-297.
- Dali-Youcef, N., Matakis, C., Coste, A., Messaddeq, N., Giroud, S., Blanc, S., Koehl, C., Champy, M. F., Chambon, P., Fajas, L., Metzger, D., Schoonjans, K. and Auwerx, J. (2007) Adipose tissue-specific inactivation of the retinoblastoma protein protects against diabesity because of increased energy expenditure. *Proc Natl Acad Sci U S A*, 104, 10703-10708.
- Fajas, L., Egler, V., Reiter, R., Hansen, J., Kristiansen, K., Debril, M. B., Miard, S. and Auwerx, J. (2002a) The retinoblastoma-histone deacetylase 3 complex inhibits *Ppar $\gamma$*  expression and adipocyte differentiation. *Dev Cell*, 3, 903-910.
- Fajas, L., Landsberg, R. L., Huss-Garcia, Y., Sardet, C., Lees, J. A. and Auwerx, J. (2002b) E2Fs regulate adipocyte differentiation. *Dev Cell*, 3, 39-49.
- Hansen, J. B., Jorgensen, C., Petersen, R. K., Hallenborg, P., De Matteis, R., Boye, H. A., Petrovic, N., Enerback, S., Nedergaard, J., Cinti, S., te Riele, H. and Kristiansen, K. (2004) Retinoblastoma protein functions as a molecular switch determining white versus brown adipocyte differentiation. *Proc Natl Acad Sci U S A*, 101, 4112-4117.
- Jonkers, J., Meuwissen, R., van der Gulden, H., Peterse, H., van der Valk, M. and Berns, A. (2001) Synergistic tumor suppressor activity of BRCA2 and p53 in a conditional mouse model for breast cancer. *Nat Genet*, 29, 418-425.
- Kansara, M. and Thomas, D. M. (2007) Molecular pathogenesis of osteosarcoma. *DNA Cell Biol*, 26, 1-18.
- Korenjak, M. and Brehm, A. (2005) E2F-Rb complexes regulating transcription of genes important for differentiation and development. *Curr Opin Genet Dev*, 15, 520-527.

Lengner, C. J., Steinman, H. A., Gagnon, J., Smith, T. W., Henderson, J. E., Kream, B. E., Stein, G. S., Lian, J. B. and Jones, S. N. (2006) Osteoblast differentiation and skeletal development are regulated by Mdm2-p53 signaling. *J Cell Biol*, 172, 909-921.

Logan, M., Martin, J. F., Nagy, A., Lobe, C., Olson, E. N. and Tabin, C. J. (2002) Expression of Cre Recombinase in the developing mouse limb bud driven by a Prxl enhancer. *Genesis*, 33, 77-80.

Rodda, S. J. and McMahon, A. P. (2006) Distinct roles for Hedgehog and canonical Wnt signaling in specification, differentiation and maintenance of osteoblast progenitors. *Development*, 133, 3231-3244.

Sage, J., Miller, A. L., Perez-Mancera, P. A., Wysocki, J. M. and Jacks, T. (2003) Acute mutation of retinoblastoma gene function is sufficient for cell cycle re-entry. *Nature*, 424, 223-228.

Scime, A., Grenier, G., Huh, M. S., Gillespie, M. A., Bevilacqua, L., Harper, M. E. and Rudnicki, M. A. (2005) Rb and p107 regulate preadipocyte differentiation into white versus brown fat through repression of PGClalpha. *Cell Metab*, 2, 283-295.

Tallquist, M. D. and Soriano, P. (2000) Epiblast-restricted Cre expression in MORE mice: a tool to distinguish embryonic vs. extra-embryonic gene function. *Genesis*, 26, 113-115.

Thomas, D. M., Carty, S. A., Piscopo, D. M., Lee, J. S., Wang, W. F., Forrester, W. C. and Hinds, P. W. (2001) The retinoblastoma protein acts as a transcriptional coactivator required for osteogenic differentiation. *Mol Cell*, 8, 303-316.

Wu, L., de Bruin, A., Saavedra, H. I., Starovic, M., Trimboli, A., Yang, Y., Opavska, J., Wilson, P., Thompson, J. C., Ostrowski, M. C., Rosol, T. J., Woolleft, L. A., Weinstein, M., Cross, J. C., Robinson, M. L. and Leone, G. (2003) Extra-embryonic function of Rb is essential for embryonic development and viability. *Nature*, 421, 942-947.

## **Acknowledgements**

We thank Tyler Jacks, Clifford Tabin and Andrew McMahon for providing key mutant mouse strains, Keara Lane for pCW22, Michael Hemann for the *Rb* shRNA, the U. of Iowa Gene Transfer Vector Core for the Adenoviral Cre and GFP vectors and Gerard Karsenty for p60SE2-Luc and p4Luc. We also thank Lees lab members, Siddhartha Mukherjee and Michael Hemann for input during this study. This work was supported by an NCI/NIH grant to J.A.L. who is a Ludwig Scholar at MIT.

## **Appendix B**

### **The retinoblastoma protein induces apoptosis directly at the mitochondria**

Keren I Hilgendorf, Elizaveta S Leshchiner, **Simona Nedelcu**, Mindy A Maynard, Eliezer Calo, Alessandra Ianari, Loren D Walensky, Jacqueline A Lees

The author contributed to Figure 9A

**Published:** Genes and Development. 2013. 27 (9), 1003-1015.

## Abstract

The retinoblastoma protein gene, *RB-1*, is mutated in one third of human tumors. Its protein product, pRB, functions as a transcriptional co-regulator in many fundamental cellular processes. Here, we report a non-nuclear role for pRB in apoptosis induction via pRB's direct participation in mitochondrial apoptosis. We uncovered this activity by finding that pRB potentiated TNF $\alpha$ -induced apoptosis, even when translation was blocked. This pro-apoptotic function was highly BAX-dependent, suggesting a role in mitochondrial apoptosis, and accordingly a fraction of endogenous pRB associated with mitochondria. Remarkably, we found that recombinant pRB was sufficient to trigger the BAX-dependent permeabilization of mitochondria or liposomes *in vitro*. Moreover, pRB interacted with BAX *in vivo*, and it could directly bind and conformationally activate BAX *in vitro*. Finally, by targeting pRB specifically to mitochondria we generated a mutant that lacked pRB's classic nuclear roles. This mito-tagged pRB retained the ability to promote apoptosis in response to TNF $\alpha$  and also additional apoptotic stimuli. Most importantly, induced expression of mito-tagged pRB in *Rb*<sup>-/-</sup>;*p53*<sup>-/-</sup> tumors was sufficient to block further tumor development. Together, these data establish a non-transcriptional role for pRB in direct activation of BAX and mitochondrial apoptosis in response to diverse stimuli, which is profoundly tumor suppressive.

## Introduction

Regulation of pRB is perturbed in most, if not all, cancers (Sherr and McCormick, 2002). pRB functions in many cellular processes and is a key regulator of the cell cycle by interacting with and inhibiting E2F transcription factors (van den Heuvel and Dyson, 2008). Upon mitogenic signaling, cdk/cyclin complexes phosphorylate pRB, resulting in release of E2Fs and cell cycle progression (van den Heuvel and Dyson, 2008). Notably, the two thirds of human tumors that are *RB-1* wildtype typically carry mutations in upstream regulators of pRB (*p16<sup>Ink4</sup>*, *cyclinD* or *cdk4*) that promote cdk/cyclin activation and thus pRB phosphorylation (Sherr and McCormick, 2002). Since these mutations all inactivate pRB's anti-proliferative function, little attention has been paid to the status of *RB-1* in considering tumor treatment. However, we note that pRB also functions as a transcriptional co-regulator of differentiation, senescence, and apoptosis genes (Calo et al., 2010; Gordon and Du, 2011; Ianari et al., 2009; Viatour and Sage, 2011). In addition, a portion of the pRB protein exists in the cytoplasm (Fulcher et al., 2010; Jiao et al., 2006; Jiao et al., 2008; Roth et al., 2009) and even at mitochondria (Ferecatu et al., 2009), but no known roles have been assigned to these species.

This current study concerns the role of pRB in the regulation of apoptosis. It is already well established that pRB can either promote or suppress apoptosis through both direct and indirect transcriptional mechanisms (Gordon and Du, 2011; Ianari et al., 2009). Earliest evidence for the anti-apoptotic role of pRB emerged from the characterization of the *Rb*-null mouse, which exhibits increased levels of apoptosis in the nervous system, lens, and skeletal muscle (Jacks et al., 1992). Subsequent studies showed that this phenotype is mostly non-cell autonomous, resulting from the deregulation of cell cycle genes and the

consequent over-proliferation of placental tissues that disrupts its normal architecture and vascularization, and causes hypoxia in embryonic tissues (de Bruin et al., 2003; Wenzel et al., 2007; Wu et al., 2003). Loss of pRB in mouse embryonic fibroblasts (MEFs) results in increased sensitivity to genotoxic stress (Knudsen and Knudsen, 2008). However, this is thought to be an indirect consequence of failure to prevent cell cycle entry in the absence of pRB, as well as increased chromosomal instability (Bosco et al., 2004; Burkhardt and Sage, 2008; Knudsen et al., 2000; Manning and Dyson, 2012). In contrast, and more consistent with a tumor suppressor role, pRB can also act in a pro-apoptotic manner in highly proliferative cells (Araki et al., 2008; Carnevale et al., 2012; Ianari et al., 2009; Knudsen et al., 1999; Milet et al., 2010). In this context, pRB and also hyperphosphorylated pRB contributes directly to apoptosis by functioning in a transcriptionally active pRB:E2F1 complex that promotes expression of pro-apoptotic genes, such as caspase 7 and p73, in response to DNA damage (Ianari et al., 2009). Taken together, these studies suggest that the ability of pRB to promote or repress apoptosis, at least in response to genotoxic stress, may be dictated by the cellular context.

The pro-apoptotic role of pRB has been primarily investigated in the context of DNA damage. The findings in this current study followed from our analysis of pRB's apoptotic function in response to another apoptotic stimulus, TNF $\alpha$ . TNF $\alpha$  can promote apoptosis via both the extrinsic and mitochondrial/intrinsic pathways (Jin and El-Deiry, 2005). The extrinsic pathway involves direct activation of the caspase cascade. In contrast, the intrinsic pathway depends on activation of the Bcl-2 protein family members BAX and BAK, which trigger mitochondrial outer membrane permeabilization (MOMP) and release of pro-apoptotic factors, such as cytochrome *c*, that lead to effector caspase activation (Brunelle

and Letai, 2009; Chipuk et al., 2010; Jin and El-Deiry, 2005; Martinou and Youle, 2011; Wyllie, 2010). Notably, in addition to its pro-apoptotic response, TNF $\alpha$  also induces a NF $\kappa$ B-mediated, pro-inflammatory response, which inhibits apoptosis (Karin and Lin, 2002). Thus, to study its apoptotic function, TNF $\alpha$  is commonly used in conjunction with a factor that abrogates the pro-inflammatory response such as the proteasome inhibitor MG-132 or the translational inhibitor cycloheximide (Karin and Lin, 2002; Traenckner et al., 1994).

In this current study, we show that pRB enhances apoptosis in response to TNF $\alpha$ , and can exert this effect in the presence of translation inhibition. This finding led us to discover a novel, non-nuclear function for the pRB protein. Specifically, pRB is associated with mitochondria and it can induce MOMP by directly binding and activating BAX. By localizing pRB specifically to the mitochondria, we showed that this mitochondrial apoptosis function is capable of yielding potent tumor suppression in the absence of pRB's canonical nuclear functions. Importantly, mitochondrial pRB can respond to a wide variety of pro-apoptotic signals, suggesting that this represents a general and potent tumor suppressive mechanism. Additionally, we find that cdk-phosphorylated pRB is present at the mitochondria and pRB's mitochondrial apoptosis function remains intact in the presence of tumorigenic events, such as p16 inactivation, that promote pRB phosphorylation. Thus, we believe that it may be possible to exploit pRB's mitochondrial apoptosis role as a therapeutic treatment in the majority of human tumors that retain wildtype *Rb-1*.

## Results

### **pRB is pro-apoptotic in response to TNF $\alpha$ treatment even in the presence of an inhibitor of translation.**

Our initial interest in exploring pRB's role in TNF $\alpha$ -induced apoptosis stemmed from prior reports that a phosphorylation-site mutant version of pRB played a pro-apoptotic role in the TNF $\alpha$  response (Masselli and Wang, 2006). We began our studies using a stable variant of an immortalized rat embryonic fibroblast cell line, RAT16, in which doxycycline withdrawal induces ectopic pRB expression. RAT16 cells with basal or induced pRB expression were treated with TNF $\alpha$  in concert with the proteasome inhibitor MG132 to block the TNF $\alpha$ -induced activation of NF $\kappa$ B and its pro-inflammatory response. We found that ectopic pRB expression significantly enhanced TNF $\alpha$ -induced apoptosis as measured by AnnexinV staining (Fig. 1A). Additionally, we note that pRB also caused a subtle increase in apoptosis even in the absence of TNF $\alpha$  treatment (Fig. 1A). We further confirmed these data by analysis of cleaved effector caspases 3 and 7 protein levels (Fig. 1B). We wanted to confirm that this was not simply a consequence of pRB overexpression, and thus also assessed the role of the endogenous pRB using knockdown cell lines. Notably, even partial knockdown of endogenous pRB in RAT16 cells was sufficient to significantly impair TNF $\alpha$ -induced apoptosis (Fig. 1C), without any detectable disruption of cell cycle phasing (Fig. 1D). Similar results were observed in a second cell line, human primary IMR90 fibroblasts, in which pRB knockdown also suppressed TNF $\alpha$ -induced

apoptosis (Fig. 1E). Thus, modulation of pRB levels by either overexpression or knockdown is sufficient to enhance or depress the apoptotic response to TNF $\alpha$ .

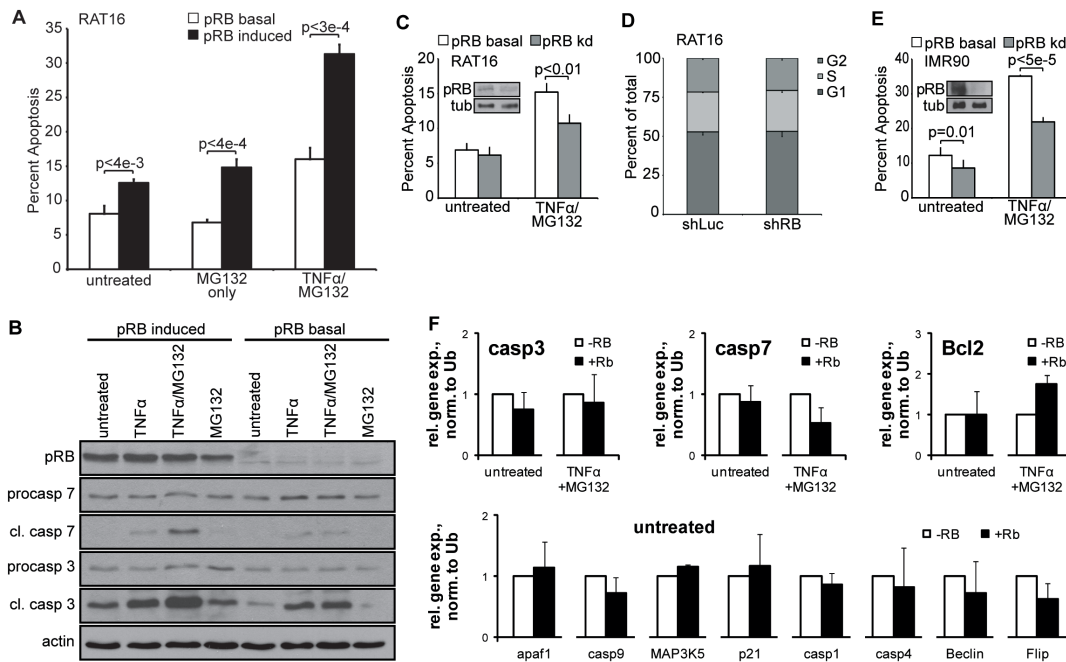


**Figure 1. pRB is pro-apoptotic in response to TNF $\alpha$  and MG132.** (A) RAT16 cells with and without induced expression of pRB for 24 hours were treated with TNF $\alpha$  and MG132 for 48 hours and analyzed for apoptosis by AnnexinV staining. Induced expression of pRB resulted in increased levels of apoptosis without TNF $\alpha$  treatment and greatly enhanced TNF $\alpha$ /MG132-induced apoptosis. (B) Western blot showing induction of pRB expression in RAT16 cells and procaspase 3, cleaved caspase 3, procaspase 7, and cleaved caspase 7 protein levels. Induced expression of pRB for 24 hours resulted in increased levels of cleaved caspase 3 and 7 protein levels in response to 48 hours of TNF $\alpha$ /MG132 treatment. (C) Stable pRB knockdown in RAT16 cells decreased levels of apoptosis in response to treatment with TNF $\alpha$ /MG132 for 48 hours and (D) did not affect cell cycle phasing. Western blot verifying knockdown of pRB in inset. (E) Stable pRB knockdown in IMR90 cells decreased TNF $\alpha$ /MG132-induced. Western blot verifying knockdown of pRB in inset. (F) Induced expression of pRB does not significantly change expression levels of apoptotic, inflammatory, or autophagic genes with or without TNF $\alpha$ /MG132 treatment as assessed by RT-qPCR and normalized to ubiquitin. (A-F) Bars, average of at least three independent experiments ( $\pm$ SD).

We anticipated that pRB's contribution to the pro-apoptotic TNF $\alpha$  response would reflect its ability to transcriptionally activate pro-apoptotic genes, as observed in our prior DNA damage studies (Ianari et al., 2009). However, we did not detect any significant changes in the levels of apoptotic, inflammatory, or autophagic mRNAs, including known pRB:E2F1 targets, in response to pRB induction in our RAT16-TNF $\alpha$  experiments (Fig. 1F). This led us to consider that perhaps pRB might be acting independently of transcription. To explore this possibility, we took advantage of the fact that cycloheximide (CHX) can be used instead of MG132 to block activation of NF $\kappa$ B (Karin and Lin, 2002; Traenckner et al., 1994). Since CHX acts to block translation, this would preclude any effects that required gene expression changes. Strikingly, induction of pRB in RAT16 cells was able to potentiate apoptosis in response to TNF $\alpha$  and CHX (Fig. 2A), with control experiments verifying translation inhibition by CHX (Fig. 2B). Moreover, pRB knockdown in IMR90s impaired TNF $\alpha$ /CHX-induced apoptosis (Fig. 2C). Thus, taken together, our data show that pRB synergizes with TNF $\alpha$  to promote apoptosis in both primary and immortalized human and rodent cell lines in the absence of translation. This strongly suggests that pRB can act through a previously unappreciated mechanism.

### **pRB activates mitochondrial apoptosis in a BAX-dependent manner.**

TNF $\alpha$  can induce apoptosis through both the extrinsic and mitochondrial pathways. To further pinpoint pRB's role, we exploited the fact that the mitochondrial pathway is highly dependent on BAX and/or BAK (Chipuk et al., 2010; Martinou and Youle, 2011). Specifically, we generated stable pools of immortalized wildtype, *Bak*<sup>-/-</sup>, *Bax*<sup>-/-</sup>, or *Bax*<sup>-/-</sup>;*Bak*

/- MEFs that would allow for doxycycline-inducible pRB expression (Fig. 3A) and assayed for apoptosis in the absence and presence of TNF $\alpha$ /CHX treatment. To ensure that we were assaying the

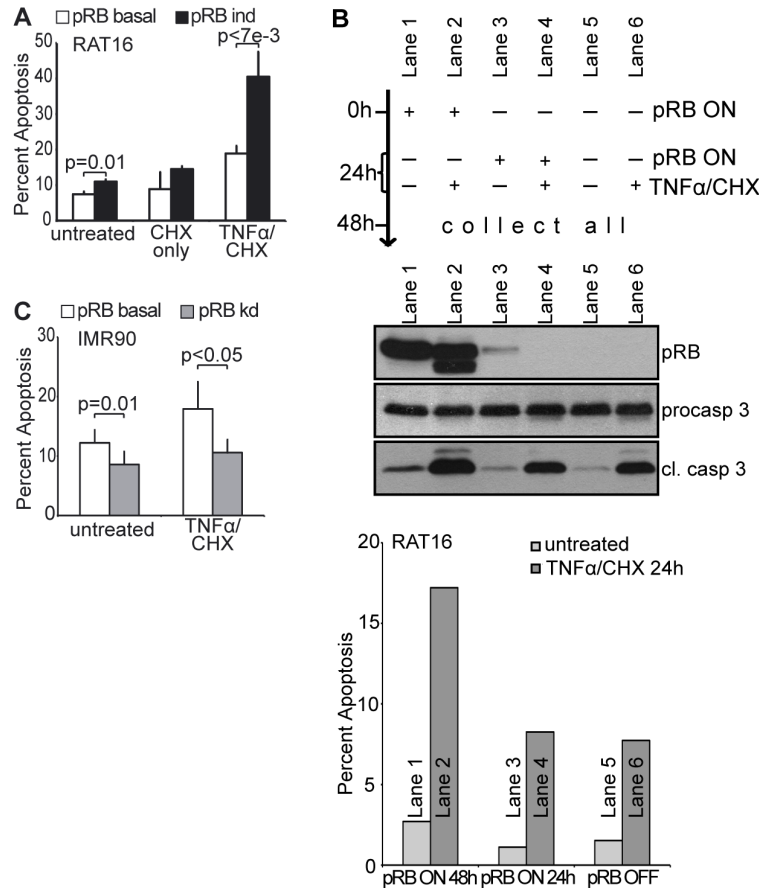


**Figure 2. pRB promotes TNF $\alpha$ -induced apoptosis in a transcription-independent manner.** (A) Induced expression of pRB for 24 hours in RAT16 cells increased apoptosis resulting from 24 hours of TNF $\alpha$  and CHX treatment. (B) Upper panel: Schematic of experiment. Lanes 1 and 2, pRB expression was induced for 24 hours and subsequently cells were left untreated and treated with TNF $\alpha$ /CHX, respectively. Lane 3 and 4, pRB expression was induced and concurrently cells were left untreated or treated with TNF $\alpha$ /CHX, respectively. Lane 5 and 6, pRB expression was never induced and cells were left untreated or treated with TNF $\alpha$ /CHX, respectively. Samples were collected after 24 hours of TNF $\alpha$ /CHX treatment and analyzed by western blotting (middle panel) and by FACS (lower panel). The addition of CHX concurrently to induction of pRB expression in Lane 4 resulted in no visible pRB protein, similar levels of apoptosis as no pRB expression (Lane 6) and less apoptosis than pRB expression for 24 hours prior to treatment (Lane 2). This suggests that CHX inhibited expression of pRB. (C) Stable knockdown of pRB in IMR90 cells decreased apoptosis induced by 24 hour treatment with TNF $\alpha$  and CHX. (A, C) Graph bars represent average of at least three independent experiments ( $\pm$ SD).

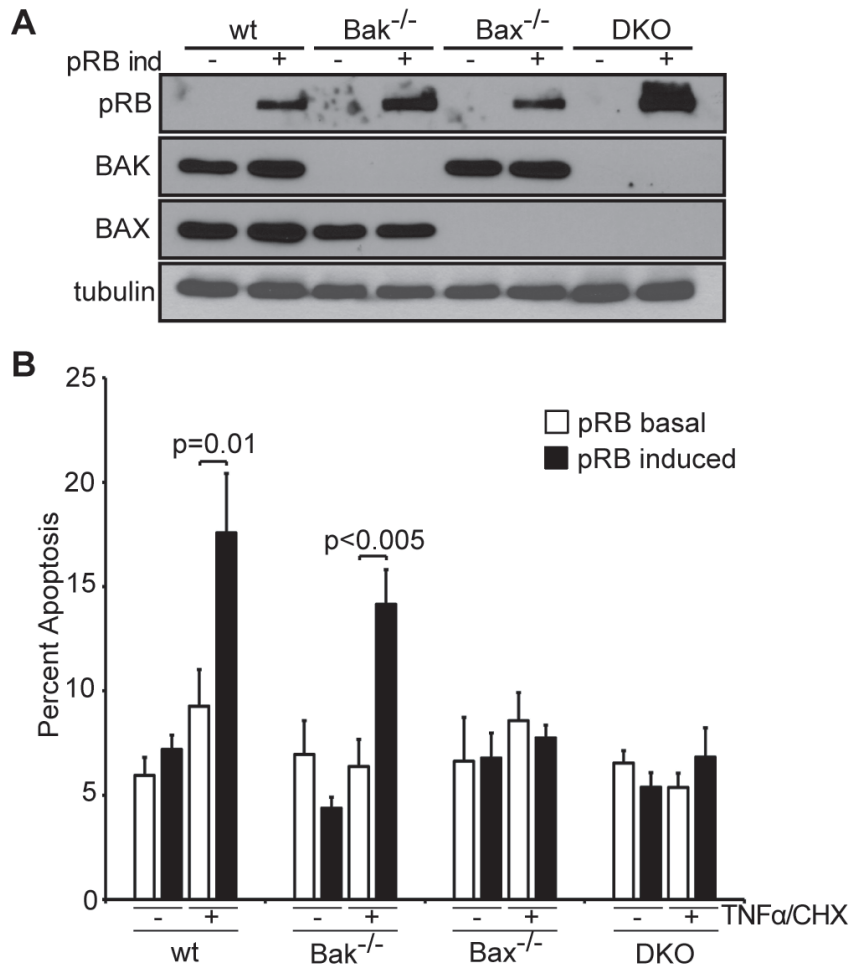


**Figure 3. pRB promotes mitochondrial apoptosis in a BAX-dependent manner.**

(A) pRB expression was induced for 24 hours in stable pools of wild-type, *Bak*<sup>-/-</sup>, *Bax*<sup>-/-</sup>, and *Bax*<sup>-/-</sup>;*Bak*<sup>-/-</sup> immortalized MEFs by doxycycline addition and confirmed by western blotting using antibodies against pRB, BAK, BAX, and tubulin. (B) Wild-type, *Bak*<sup>-/-</sup>, *Bax*<sup>-/-</sup>, and *Bax*<sup>-/-</sup>;*Bak*<sup>-/-</sup> immortalized MEFs with or without 24 hours of pRB expression were left untreated or treated with TNF $\alpha$  and CHX for 10 hours and analyzed for apoptosis by AnnexinV staining. Induction of pRB in wildtype and *Bak*<sup>-/-</sup>, but not *Bax*<sup>-/-</sup> or *Bax*<sup>-/-</sup>;*Bak*<sup>-/-</sup>, MEFs sensitized to TNF $\alpha$ /CHX-induced apoptosis. Each MEF variant was independently generated twice. Graph bars represent average of three representative, independent experiments ( $\pm$ SD).

BAX/BAK-dependence of any pRB effect, rather than a general difference in the apoptotic potential of the various *Bax/Bak* genotypes, we conducted these experiments using treatment conditions that yielded minimal response to TNF $\alpha$ /CHX in the uninduced (basal pRB) cells (Fig. 3B). Remarkably, pRB induction enhanced TNF $\alpha$ -induced apoptosis in both wildtype (p=0.01) and *Bak*<sup>-/-</sup> (p<0.005) MEFs, but had no effect in either *Bax*<sup>-/-</sup> or *Bax*<sup>-/-</sup>;*Bak*<sup>-/-</sup> MEFs (Fig. 3B). This analysis yielded two important conclusions. First, pRB exerts its effect on TNF $\alpha$ -induced apoptosis by acting specifically on the mitochondrial pathway. Second, pRB requires BAX, but not BAK, for this activity.

pRB is thought of primarily as a nuclear protein, but it also exists in the cytoplasm (Fulcher et al., 2010; Jiao et al., 2006; Jiao et al., 2008; Roth et al., 2009). Indeed, pRB has even been reported at mitochondria (Ferecatu et al., 2009), albeit without any known function. Thus, we speculated that pRB might act directly at mitochondria. To validate and further explore the mitochondrial localization of pRB, we first fractionated IMR90 cells. We note that our goal was not to necessarily recover all mitochondria, but rather to obtain a mitochondrial fraction free of nuclear and cytoplasmic contamination, as confirmed by western blotting for various nuclear, cytoplasmic and mitochondrial markers (Fig. 4). Intriguingly, we detected a portion of endogenous pRB in the isolated mitochondria, and found that this exists even in the absence of treatment with TNF $\alpha$  or genotoxic agents (Fig. 4A, B). Furthermore, using phospho-specific pRB antibodies, we showed that this mitochondrial pRB includes the cdk-phosphorylated species (Fig. 4A). Based on the relative loading and western blot signals, we estimate that about 5% of the total cellular pRB is present in the mitochondrial fraction. Since we optimized the mitochondrial

fractionation for purity, not completeness, this is likely a conservative estimate of the level of mitochondrial pRB.

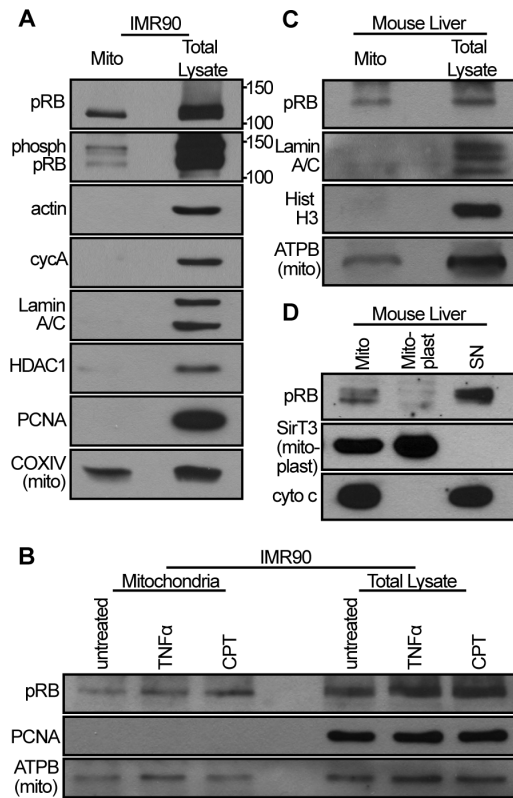


**Figure 4. A fraction of pRB localizes to mitochondria.** (A) IMR90 cell mitochondria were fractionated and equal amounts (in  $\mu$ g) of mitochondrial fraction (mito) versus total lysate were analyzed by western blotting using an antibody against pRB and a cocktail of antibodies against phosphorylated pRB. A fraction of pRB, including phospho-pRB localizes to mitochondria. The purity of the mitochondrial fraction was verified using control nuclear and cytoplasmic markers. (B) Mitochondria of IMR90 cells treated with camptothecin (CPT; 5 hours) or TNF $\alpha$  (24 hours) were isolated and analyzed by western blotting. The levels of mitochondrial pRB are unaffected by treatment with these drugs. (C) Mitochondria were isolated from mouse livers and analyzed by western blotting. A fraction of pRB is present at mouse liver mitochondria. (D) Mouse liver mitochondria were subfractionated into mitoplast and non-mitoplast (SN). Mitochondrial pRB localizes outside the mitoplast. (A-D) Data are representative of at least three independent experiments.

To further validate the mitochondrial localization of pRB *in vivo*, we next examined mitochondria from mouse livers. Again, western blotting showed that a fraction of pRB existed within the mitochondrial fraction (Fig. 4C). Finally, subfractionation of mouse liver mitochondria localized pRB outside of the mitoplast (inner mitochondrial membrane and enclosed matrix; Fig. 4D), consistent with the notion that it is associated with the outer mitochondrial membrane and therefore coincident with the site of BAX/BAK action.

### **pRB directly activates Bax and induces cytochrome c release from isolated mitochondria.**

Having established that pRB is associated with mitochondria *in vivo*, we hypothesized that pRB might act to trigger mitochondrial outer membrane permeabilization (MOMP). To test this, we performed *in vitro* cytochrome *c* release assays. First, we isolated mitochondria from wildtype mouse livers and added recombinant monomeric BAX, because BAX is not associated with mitochondria in unstressed conditions (Walensky et al., 2006). As expected, addition of BAX alone did not result in cytochrome *c* release (Fig. 5A). Remarkably, co-addition of purified, baculovirus-expressed human pRB and monomeric BAX was sufficient to induce cytochrome *c* release (Fig. 5A). This was comparable to the effect of cleaved BID, a BH3-only member of the BCL-2 family that is a physiologic trigger of MOMP. Thus, recombinant pRB can induce MOMP in isolated mitochondria supplemented with monomeric BAX.

Next, we wanted to investigate the BAX/BAK-dependence of this activity. As isolated mitochondria contain monomeric BAK, we repeated this assay using mitochondria

isolated from *Alb-cre<sup>pos</sup>;Bax<sup>f/-</sup>;Bak<sup>-/-</sup>* mouse livers (Walensky et al., 2006). Consistent with our cellular studies, pRB (up to 500nM) only induced cytochrome *c* release when these mitochondria were supplemented with BAX (Fig. 5B). Thus, pRB induces MOMP in a dose- and BAX-dependent manner.

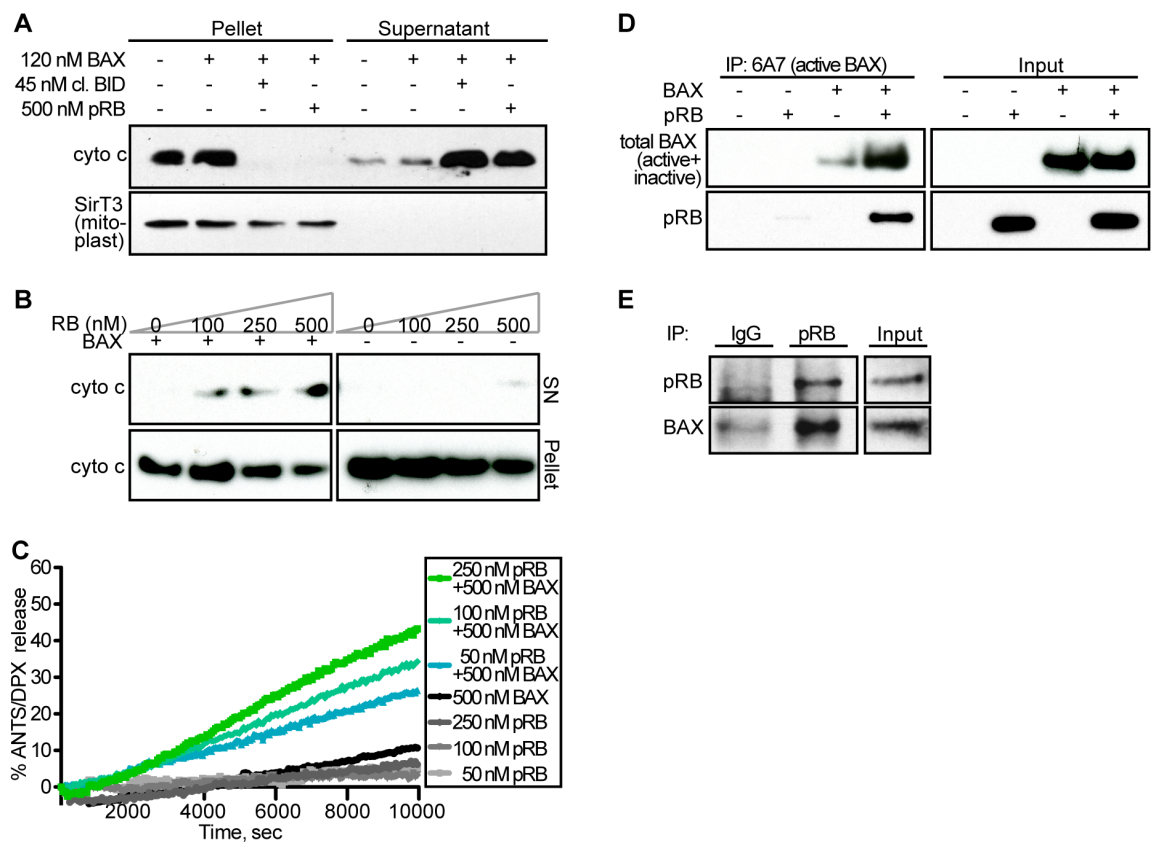


**Figure 5. pRB induces MOMP by directly activating BAX.** (A) Mouse liver mitochondria were isolated, supplemented with recombinant, monomeric BAX and incubated with and without recombinant cleaved BID (positive control) or baculovirus-expressed, recombinant human pRB. Cytochrome *c* release was assessed following incubation and centrifugation by western blotting of pellet versus supernatant. Addition of either pRB or cleaved BID was sufficient to release cytochrome *c* into the supernatant. (B) Mitochondria isolated from *Bax*<sup>-/-</sup>; *Bak*<sup>-/-</sup> mouse livers were incubated with indicated amounts of recombinant pRB only or recombinant pRB and monomeric BAX. Recombinant pRB promotes cytochrome *c* release in a dose-dependent and BAX-dependent manner. Data are representative of two independent experiments. (C) ANTS/DPX-loaded liposomes were incubated with 50, 100, and 250nM recombinant pRB in the presence or absence of recombinant, monomeric BAX. ANTS/DPX release was assessed over time. pRB yielded dose-dependent liposome permeabilization in a BAX-dependent manner. (D) *In vitro* binding assay using recombinant pRB and recombinant, monomeric BAX. Activated BAX was immunoprecipitated using an active-conformation specific BAX antibody (6A7) and binding was assessed by western blotting using an antibody against total BAX (inactive + active) and pRB. When co-incubated with inactive BAX, pRB bound to (lower panels) and stimulated formation of (upper panels) conformationally active BAX. (E) Co-immunoprecipitation experiment using IMR90 cells treated with TNF $\alpha$ /CHX for 3 hours. Endogenous pRB was immunoprecipitated from cell extracts and endogenous BAX association was assessed by western blotting. pRB and BAX form an endogenous complex *in vivo* in TNF $\alpha$ /CHX-treated cells. (A, C-E) Data are representative of at least three independent experiments.

To further explore this BAX specificity, we performed a liposome release assay in which freshly prepared ANTS/DPX-loaded liposomes were incubated with increasing concentrations of purified pRB in the absence or presence of recombinant, monomeric BAX (Fig. 5C). As expected, addition of either BAX or pRB (up to 250nM) alone was insufficient to yield ANTS/DPX release. In contrast, upon co-addition, pRB was sufficient to trigger BAX-dependent liposome permeabilization in a dose- and time-dependent manner.

We wanted to further investigate pRB's ability to directly activate BAX. It is well established that BAX undergoes a conformational change upon activation that can be detected using an antibody (6A7) specific for the active conformation of BAX (Hsu and Youle, 1997). Thus, we performed an *in vitro* binding assay in which recombinant pRB and/or monomeric BAX were incubated separately or together in the absence of mitochondria or liposomes. We then screened for BAX activation by immunoprecipitation with 6A7, and assayed pRB association by western blotting (Fig. 5D). Notably, we found that addition of pRB promoted formation of the active BAX conformation (Fig. 5D, upper panels). Moreover, pRB co-immunoprecipitated with this active BAX species (Fig. 5D, lower panels). Thus, pRB can both associate with BAX, and trigger its conformational activation. Since the liposome and co-immunoprecipitation assays were both conducted in the absence of any other proteins, we can conclude that pRB is sufficient to directly activate BAX and induce BAX-mediated membrane permeabilization.

We next sought to validate the pRB:BAX interaction in the *in vivo* context and with endogenous proteins. Endogenous interactions between BAX and pro-apoptotic proteins, including BH3-only proteins, are notoriously difficult to observe due to the dynamic, 'hit

and run' nature of these interactions (Eskes et al., 2000; Perez and White, 2000; Walensky and Gavathiotis, 2011). Thus, to enable detection of such transient interactions, we treated primary human IMR90 fibroblasts with TNF $\alpha$ /CHX and then crosslinked using the amine-reactive crosslinking agent DSP. Using this approach, we were able to detect BAX within immunoprecipitates of the endogenous pRB protein (Fig. 5E). Thus, taken together, our *in vitro* and *in vivo* experiments show that pRB can bind directly to BAX and induce it to adopt the active conformation that triggers MOMP and cytochrome *c* release.

### **The mitochondrial function of pRB induces apoptosis even in the absence of pRB's nuclear functions.**

Our data have identified a mitochondrial function for pRB. We next wanted to address how this function contributes to pRB's tumor suppressive activity. First, we asked which region of pRB is required for transcription-independent apoptosis. The tumor suppressor pRB is traditionally divided up into three domains (Fig. 6A): the N-terminus (residues 1-372), the small pocket domain (residues 373-766) and the C-terminus (residues 767-928). The small pocket is required for pRB's known biological functions and most of the mutations found in human tumors disrupt this domain. We expressed the three domains (RB\_N, RB\_SP, and RB\_C) in an inducible manner using stable RAT16 cell lines (Fig. 6A, B). Notably, expression of the small pocket of pRB, but not the N-terminal or C-terminal domains promoted apoptosis in response to TNF $\alpha$  and CHX (Fig. 6C). Thus, pRB's ability to induce transcription-independent apoptosis mapped to the small pocket domain. Since this domain is essential for pRB's tumor suppressive activity, these data are

consistent with functional significance. Unfortunately, the small pocket is also required for most other pRB functions.

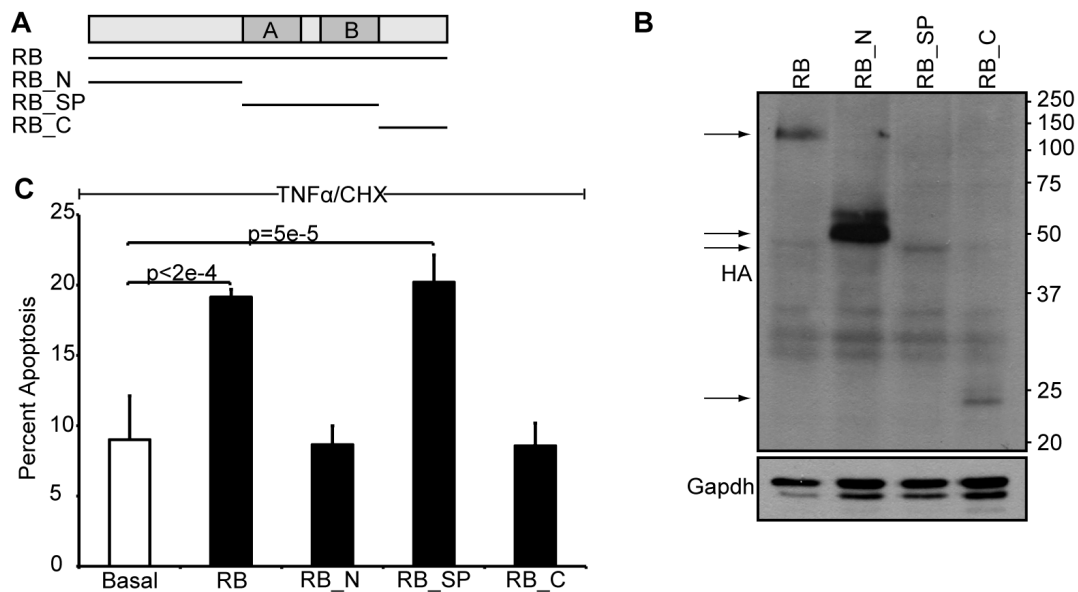


**Figure 6. The Small Pocket of pRB is sufficient to induce transcription-independent apoptosis.** (A) Schematic of pRB domains: the N-terminus (RB\_N; residues 1-372), the small pocket domain (RB\_SP; residues 373-766) and the C-terminus (RB\_C; residues 767-928). (B) Stable variants of RAT16 cells allowing for inducible expression of HA-tagged full-length pRB, RB\_N, RB\_SP, and RB\_C by doxycycline withdrawal were generated and expression was verified after 24 hours by western blotting using an HA-antibody. (C) RAT16 cells with and without expression of pRB, RB\_N, RB\_SP, and RB\_C for 24 hours were treated with TNF $\alpha$  and CHX for 24 hours and levels of apoptosis were assessed by AnnexinV staining. Induced expression of full-length pRB and RB\_SP, but not RB\_N or RB\_C, sensitized to TNF $\alpha$ /CHX-induced apoptosis. (B-C) Each RAT16 variant was independently generated three times. Graph bars represent average of three representative, independent experiments ( $\pm$ SD).

As an alternative approach, we sought to study the impact of the mitochondrial pRB activity in the absence of pRB's canonical nuclear functions by targeting pRB specifically to the mitochondria. Mutation of the NLS and direct targeting to the outside of the mitochondria using the transmembrane domain of Bcl2 proved insufficient for exclusive mitochondrial localization (data not shown), and instead we combined NLS mutation with fusion to the mitochondrial leader peptide of ornithine transcarbamylase (mitoRB $\Delta$ NLS; Fig. 7A). We note that this leader peptide targets to the matrix of mitochondria, but it has been used successfully to study protein function at the outer mitochondrial membrane, presumably by allowing resorting to other mitochondrial compartments (Marchenko et al., 2000). We confirmed that expression of mitoRB $\Delta$ NLS did not cause general mitochondrial cytotoxicity, as judged by the absence of increased ROS production (data not shown). We also localized a control protein, REL, to mitochondria to further control for any non-specific effect of mitochondrial targeting. Stable, inducible RAT16 cell lines were used to express mitoRB $\Delta$ NLS, wildtype pRB, or mitoREL upon doxycycline withdrawal. Importantly, we confirmed specific targeting of mitoRB $\Delta$ NLS and the control mitoREL protein to mitochondria (Fig. 7B, C). Consistent with its restricted localization, mitoRB $\Delta$ NLS was unable to perform nuclear pRB functions, as judged by its inability to mediate the transcriptional repression of cell cycle genes that are known pRB targets (*cdc2*, *mcm3*, *mcm5*, *mcm6*, *PCNA*, and *cyclinA2*) in stark contrast to the wildtype pRB protein (Fig 7D). Importantly, mitoRB $\Delta$ NLS retained the ability to enhance TNF $\alpha$ /CHX-induced apoptosis (Fig. 7E). This was not a non-specific effect of mitochondrial targeting, as the mitoREL control did not modulate apoptosis (Fig. 7E). We note that wildtype pRB was expressed at

much higher levels than the mitoRB $\Delta$ NLS protein, even when considering only the mitochondrially-localized fraction (Fig. 7C). Nevertheless, mitoRB $\Delta$ NLS was almost as efficient as wildtype pRB at promoting

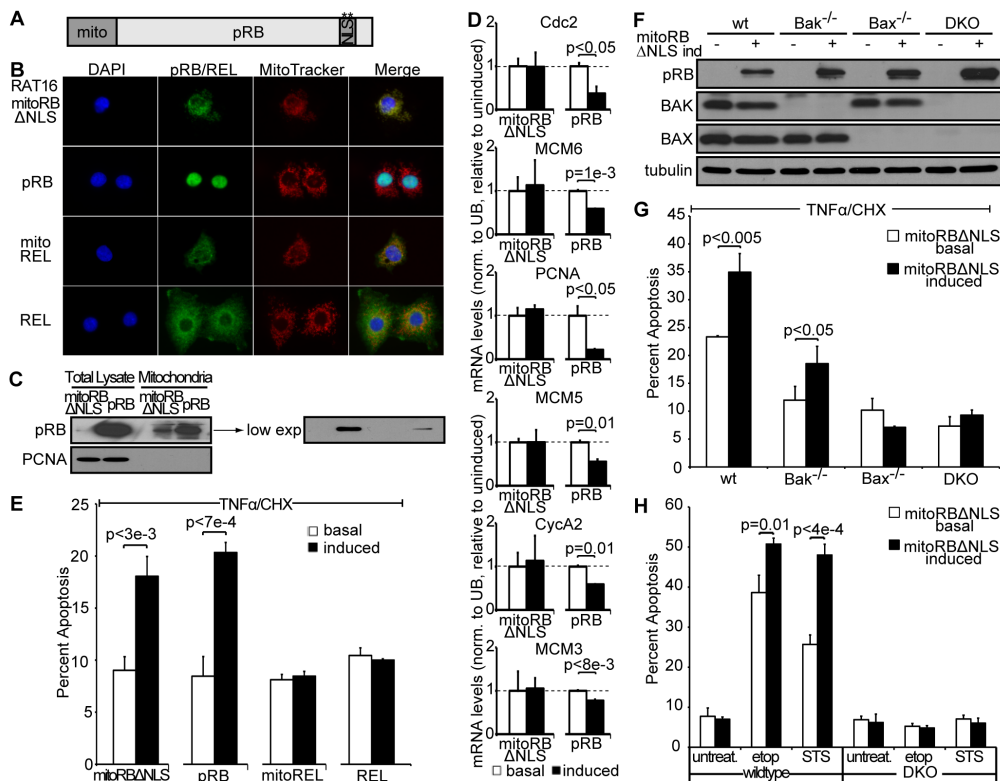


**Figure 7. Mitochondria-targeted pRB is deficient for pRB's nuclear function, but induces apoptosis in response to various apoptotic stimuli.** (A) Schematic of mitoRB $\Delta$ NLS construct. pRB was targeted to mitochondria by fusion to the mitochondrial leader peptide of ornithine transcarbamylase and mutation of the NLS. (B) Stable variants of RAT16 cells allowing for inducible expression of mitoRB $\Delta$ NLS, wildtype pRB, mitoREL, and wildtype REL were generated and cellular localization following 24 hours induction was assessed by immunofluorescence using antibodies against pRB and REL. Mitochondria were visualized using MitoTracker. mitoRB $\Delta$ NLS and mitoREL localized to mitochondria. (C) Western blotting showing induced expression levels of mitoRB $\Delta$ NLS and wildtype pRB at mitochondria and total lysate. mitoRB $\Delta$ NLS expressed at lower levels than wildtype pRB, even when considering the mitochondrial fraction. (D) pRB, but not mitoRB $\Delta$ NLS, repressed E2F target genes *cdc2*, *mcm3*, *mcm5*, *mcm6*, *PCNA*, *cycA2* as measured by RT-qPCR and normalized to ubiquitin. Average of two independent experiments ( $\pm$ SD). (E) Induced expression of mitoRB $\Delta$ NLS and wildtype pRB, but not mitoREL or REL, sensitized to apoptosis induced by 24 hour treatment with TNF $\alpha$  and CHX. (B-E) Each RAT16 variant was independently generated three times. Graph bars represent average of three representative, independent experiments ( $\pm$ SD). (F) mitoRB $\Delta$ NLS expression was induced

TNF $\alpha$ /CHX-induced apoptosis. As an additional control against non-specific mitochondrial cytotoxicity, we wanted to verify that mitoRB $\Delta$ NLS works through the same directed mechanism as wildtype pRB. Thus, we assessed the BAX/BAK dependence of this protein by generating stable variants of immortalized wildtype, *Bak*<sup>-/-</sup>, *Bax*<sup>-/-</sup>, or *Bax*<sup>-/-</sup>;*Bak*<sup>-/-</sup> MEFs to allow doxycycline-inducible mitoRB $\Delta$ NLS expression (Fig. 7F). Expression of mitoRB $\Delta$ NLS in wildtype and *Bak*<sup>-/-</sup>, but not *Bax*<sup>-/-</sup> or *Bax*<sup>-/-</sup>;*Bak*<sup>-/-</sup> MEFs, enhanced TNF $\alpha$ -induced apoptosis (Fig. 7G). Thus, mitoRB $\Delta$ NLS promotes apoptosis in a BAX-dependent manner, exactly like wildtype pRB. Targeting pRB directly to the mitochondria therefore successfully generates a separation of function mutant that is deficient for pRB's classic nuclear functions but retains the ability induce apoptosis in a transcription-independent, BAX-dependent manner in response to TNF $\alpha$ .

In our earlier experiments, induction of wildtype pRB and RB\_SP consistently yielded a small, but significant increase in apoptosis even in the absence of TNF $\alpha$  treatment. This led us to hypothesize that mitochondrial pRB may function in a broader manner in apoptosis. We therefore evaluated the effect of mitoRB $\Delta$ NLS expression on apoptosis induced by apoptotic factors other than TNF $\alpha$ . Immortalized wildtype or *Bax*<sup>-/-</sup>;*Bak*<sup>-/-</sup> MEFs with and without mitoRB $\Delta$ NLS expression were treated with two drugs, etoposide and staurosporine (STS), that work via distinct mechanisms. Notably, mitoRB $\Delta$ NLS expression enhanced both etoposide and STS-induced apoptosis (Fig. 7H).

Thus, mitochondrial pRB can be activated in response to a

---

by doxycycline addition for 24 hours in stable variants of wild-type, *Bak*<sup>-/-</sup>, *Bax*<sup>-/-</sup>, and *Bax*<sup>-/-</sup>;*Bak*<sup>-/-</sup> immortalized MEFs and confirmed by western blotting using antibodies against pRB, BAK, BAX, and tubulin. (G) Induction of mitoRB $\Delta$ NLS in wildtype and *Bak*<sup>-/-</sup>, but not *Bax*<sup>-/-</sup> or *Bax*<sup>-/-</sup>;*Bak*<sup>-/-</sup> MEFs sensitized to 10 hour treatment with TNF $\alpha$  and CHX. (H) Wildtype and *Bax*<sup>-/-</sup>;*Bak*<sup>-/-</sup> MEFs with and without induced expression of mitoRB $\Delta$ NLS were treated with staurosporine (STS; 1  $\mu$ M) for 6 hours or etoposide (25  $\mu$ M) for 12 hours.

variety of apoptotic stimuli, including both intrinsic and extrinsic stimuli. This argues that mitochondrial pRB function may contribute to pRB-induced apoptosis in various settings.

### **Mito-targeted pRB suppresses tumor growth *in vivo*.**

We next wanted to evaluate whether the mitochondrial function of pRB can contribute to tumor suppression *in vivo*. For this analysis, we used a murine *Rb*<sup>-/-</sup>;*p53*<sup>-/-</sup> osteosarcoma cell line (*DKO-OS*) that is capable of forming xenografts in mice. We generated stable variants of *DKO-OS* cells that would allow doxycycline inducible expression of mitoRBΔNLS or control proteins (Fig. 8A, B). Importantly, mitoRBΔNLS localized specifically to mitochondria in these tumor cells and it, but not mitoREL, promoted apoptosis in either the presence or absence of TNFα treatment (Fig. 8C and data not shown). We injected *DKO-OS-mitoRBΔNLS* or *DKO-OS-wtRb* cells into immunocompromised mice (12 injections/cell line) and switched half of the animals to doxycycline once the tumor volume reached approximately 0.05cm<sup>3</sup> to yield tumors without (herein referred to as basal) or with mitoRBΔNLS and wildtype pRB induction. We note that these tumor cells were not treated with apoptotic stimuli but presumably were subject to oncogenic stress. Control experiments (with parental *DKO-OS* cells) showed that the doxycycline treatment itself was not tumor suppressive (Fig. 8D). Strikingly, expression of wildtype pRB, versus mitoRBΔNLS, was similarly efficient in blocking further tumor expansion (Fig. 9A). Specifically, after 11 days, the tumor volume with basal expression was three fold greater than the tumor volume with either mitoRBΔNLS or pRB expression (Fig. 9A). Importantly, despite this equivalent impact on tumor growth, examination of

tumor sections confirmed that there were clear differences in the cellular response to mitoRB $\Delta$ NLS versus pRB expression (Fig. 9B). Ki67, a proliferation marker and pRB-repression target, was

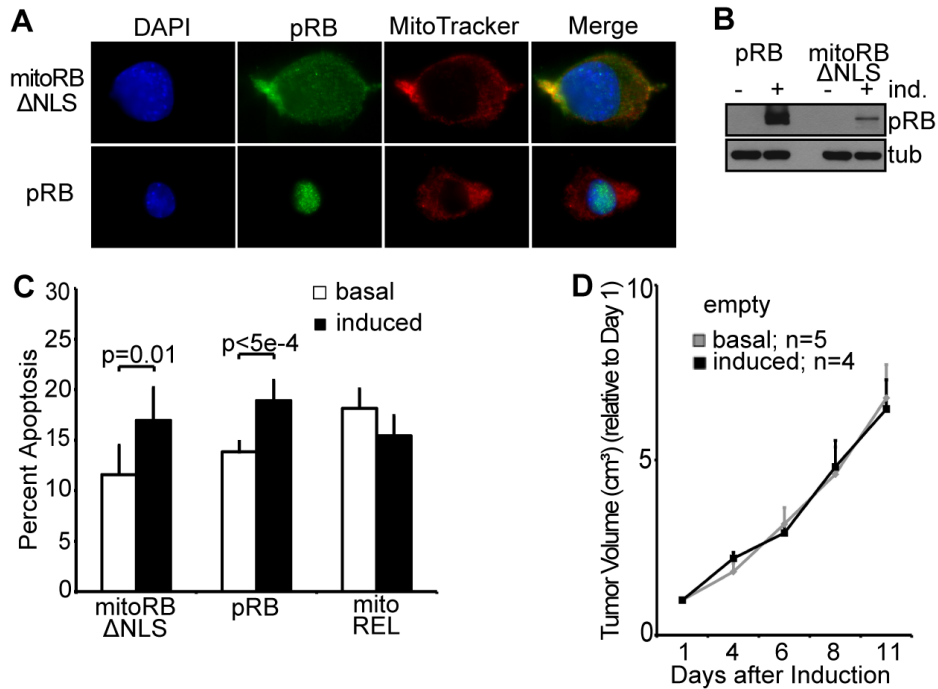


**Figure 8. Mitochondria-targeted pRB induces apoptosis in transformed  $Rb^{-/-};p53^{-/-}$  osteosarcoma cells.** (A) Representative image showing localization of mitoRB $\Delta$ NLS and pRB in transformed,  $Rb^{-/-};p53^{-/-}$  osteosarcoma cells by immunofluorescence. mitoRB $\Delta$ NLS localized to mitochondria and not the nucleus. (B) Western blot showing relative expression levels of mitoRB $\Delta$ NLS and pRB after 24 hours of induction. mitoRB $\Delta$ NLS expressed poorly compared to pRB. (C) Expression of mitoRB $\Delta$ NLS or pRB, but not mitoREL, in transformed,  $Rb^{-/-};p53^{-/-}$  osteosarcoma cells for 24 hours resulted in increased levels of apoptosis, even in the absence of TNF $\alpha$  treatment. Graph bars represent average of three independent experiments ( $\pm$ SD). (D)  $Rb^{-/-};p53^{-/-}$  osteosarcoma cells (parental) were injected into the flank of nude mice. Once a tumor volume of approximately 0.05 cm<sup>3</sup> was reached, half the mice were fed dox food and tumor volume was monitored for 11 days ( $\pm$ SEM). Doxycycline had no effect on the growth of xenografted tumors. Tumor volume normalized to Day 1.

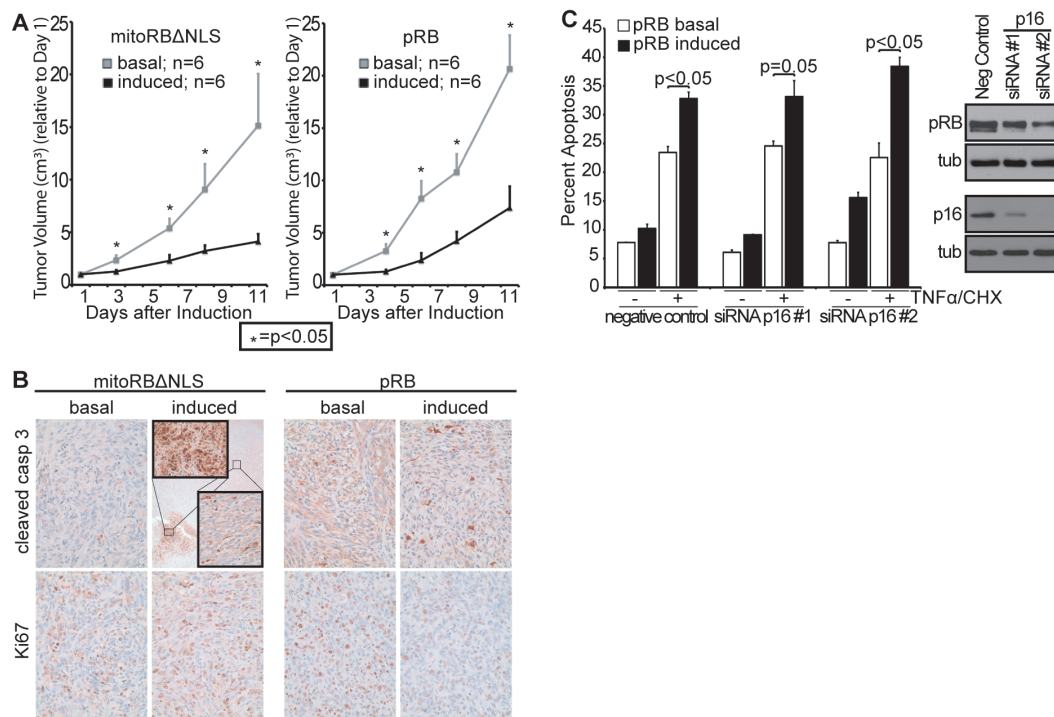


**Figure 9. Mitochondria-targeted pRB induces apoptosis *in vivo* and is tumor-suppressive.** (A) *Rb*<sup>-/-</sup>;*p53*<sup>-/-</sup> osteosarcoma cell variants allowing for doxycycline inducible expression of mitoRBΔNLS or wildtype pRB were injected into the flank of nude mice (2 injection sites per mouse; 12 injections per cell line variant). Once a tumor volume of approximately 0.05 cm<sup>3</sup> was reached, mitoRBΔNLS or wildtype pRB expression was induced in half the mice and tumor volume was monitored for 11 days (n=6/condition, ±SEM). Induced expression of mitoRBΔNLS or wildtype pRB suppressed growth of xenografted tumors. Tumor volume normalized to Day 1. (B) Induced expression of mitoRBΔNLS or wildtype pRB resulted in increased levels of apoptosis as measured by immunohistochemistry using a cleaved caspase 3 antibody (top). Tumors expressing mitoRBΔNLS also contained small areas with very high levels of apoptosis (inset). Induced expression of wildtype pRB, but not mitoRBΔNLS decreased proliferation as measured by Ki67 staining (bottom). Images representative of respective 6 tumor sections. (C) Murine p16 was knocked down in immortalized wildtype MEF variants that allow for doxycycline-inducible expression of pRB. Phosphorylation status of pRB (as judged by mobility) and knockdown of p16 using two distinct siRNAs was confirmed by western blotting. Induced expression of pRB enhances TNFα/CHX-induced apoptosis in the presence and absence of p16 and this activity is not inactivated by pRB phosphorylation. Bars, average of two independent experiments (±SD).

downregulated in tumors expressing wildtype pRB, but completely unaffected by mitoRB $\Delta$ NLS (Fig. 9B, lower panels), in accordance with mitoRB $\Delta$ NLS's inability to perform nuclear functions. Both pRB proteins promoted apoptosis, as judged by cleaved caspase 3 staining, but we observed qualitative differences in this response (Fig. 9B, upper panels). Tumors with wildtype pRB showed a uniform increase in apoptosis (2.5 fold increase relative to basal,  $p < 0.01$ ). Tumors with mitoRB $\Delta$ NLS had regions comparable to the wildtype pRB response (2.3 fold increase relative to basal,  $p < 0.001$ ), but also included smaller regions (Fig. 9B, insert box) that were profoundly apoptotic. Thus, wildtype pRB promotes both cell cycle arrest and apoptosis, while mitoRB $\Delta$ NLS is solely apoptotic. Importantly, despite its restricted biological activity, mitoRB $\Delta$ NLS was as efficient, if not more efficient, than wildtype pRB at mediating tumor suppression *in vivo*.

These observations raise the possibility that the mitochondrial function of pRB could be employed as a tumor suppressive mechanism, even in p53-deficient cells, at least when re-expressed in *Rb* null cells. This is very intriguing because approximately two thirds of human tumors are wildtype for the *Rb-1* gene, but instead carry alterations in upstream regulators of pRB (*p16<sup>Ink4A</sup>*, *cyclin D* or *cdk4*) that promote its cdk-phosphorylation. Thus, we wanted to determine whether pRB can mediate its mitochondrial apoptosis function in the presence of such tumorigenic changes. This question was further spurred by our finding that cdk-phosphorylated pRB is observed in the mitochondrial fractions (Fig. 4A). To address the influence of pRB phosphorylation on mitochondrial pRB function we used two distinct siRNAs to knockdown p16 in our immortalized MEF populations that allow for doxycycline-inducible expression of pRB. We

confirmed that these siRNAs yielded near complete p16 knockdown and promoted hyperphosphorylation of the doxycycline-induced pRB (Fig. 9C). Importantly, pRB enhanced TNF $\alpha$ /CHX-induced apoptosis with similar efficiency in MEFs with p16-knockdown versus those transfected with a negative control duplex (Fig. 9C). These data strongly suggest that cdk-phosphorylated pRB is competent to induce mitochondrial apoptosis and that this function will persist in the majority of human tumors that contain wildtype, constitutively phosphorylated pRB.

## Discussion

We have known for more than two decades that pRB is localized in both the nucleus and cytoplasm. However, prior studies have largely focused on pRB's nuclear functions, particularly its widespread transcriptional roles. To our knowledge, no biological function has been assigned to cytoplasmic pRB. In fact, it has been suggested that this species is essentially inactive, and its existence simply reflects the loss of nuclear tethering of cdk-phosphorylated pRB (Mittnacht and Weinberg, 1991; Templeton, 1992). By following the interplay between pRB and TNF $\alpha$ -induced apoptosis, we have uncovered clear evidence for a biological role for pRB at mitochondria in various cellular settings including normal, immortalized, and tumor cells. Initially, we found that pRB not only enhanced TNF $\alpha$ -induced apoptosis, but could do so even in the presence of cycloheximide. This argued that pRB could act in a novel manner to promote apoptosis. We then discovered that this pRB function was BAX-dependent, indicating crosstalk to the mitochondrial/intrinsic apoptotic pathway. Importantly, additional observations argue that pRB plays a direct, and broadly applicable, role in this pathway. First, a fraction of endogenous pRB, including some cdk-phosphorylated pRB, is localized on the outside of mitochondria. Second, recombinant pRB is able to induce MOMP and liposome permeabilization *in vitro*. Third, pRB can directly bind and activate BAX *in vitro* in the absence of any other proteins, and we confirm an interaction between the endogenous pRB and BAX proteins *in vivo*. Fourth, targeting pRB to mitochondria generates a separation of function mutant that is deficient for pRB's nuclear functions but able to induce apoptosis in response to various stimuli including TNF $\alpha$ , etoposide, staurosporine, and presumably (since it is active in tumor cells)

oncogenic stress. Finally, and most importantly, this mitochondrially-tethered pRB is sufficient to suppress tumorigenesis. Given these findings, we believe that endogenous, mitochondrial pRB acts non-transcriptionally, and in a broadly engaged manner, to promote apoptosis by activating BAX directly and inducing MOMP. To our knowledge, this is the first reported non-transcriptional and non-nuclear function for pRB.

Of course, we are not arguing that pRB is essential for mitochondrial apoptosis; this process is consistently impaired, but not ablated, by pRB-deficiency. Instead, we conclude that pRB is one of a growing list of proteins that are able to modulate the activity of core apoptotic regulators. We suspect that pRB acts at the mitochondria to fine-tune the apoptotic threshold, because its effects are dose-dependent (both *in vitro* and with overexpression/knockdown *in vivo*), it is localized to mitochondria both in the absence and presence of apoptotic stimuli, and it can potentiate many different pro-apoptotic signals. pRB's pro-apoptotic role is highly reproducible, but the fold change in our cell studies could be judged as relatively modest (often 2-3 fold). However, we note that these experiments sample only one snapshot in time. Indeed, in the context of the *in vivo* xenograft experiments, mitoRB $\Delta$ NLS yielded the same modest increase in the frequency of apoptotic cells within tumor sections (2-3 fold), but we can now see the cumulative effects of pRB action and it is profoundly tumor suppressive.

As described above, our data provide some insight into the underlying mechanism of mitochondrial pRB action; it requires BAX, but not BAK, both *in vivo* and *in vitro*, and pRB can directly bind to and activate formerly inactive monomeric BAX. Clearly, additional questions remain regarding this activity. The first concerns the precise nature of the pRB-BAX interaction. Given pRB's preference for BAX over BAK, we conclude that the pRB

binding site is either specific to BAX, and not BAK, or it represents a shared domain that is somehow masked in the BAK protein. We note that we have recently identified a novel, and unique, activation site on the BAX protein (Gavathiotis et al., 2010; Gavathiotis et al., 2008) and thus are interested to learn whether this might mediate pRB binding. In the case of pRB, we have shown here that the small pocket domain is both necessary and sufficient for transcription-independent apoptosis and thus likely contains sequences essential for BAX binding. This is gratifying, because the small pocket is essential for pRB's tumor suppressive activity. However, this region is still relatively large and mediates interactions with many other known pRB-associated proteins. Thus, additional analysis will be required to further define the critical BAX-interacting sequence(s) and determine how this might compete with the binding of other pRB targets. The second key question concerns the mechanisms by which pro-apoptotic signals trigger mitochondrial pRB to activate BAX. One obvious candidate is post-translational modifications. Our data show that cdk-phosphorylated pRB is present at mitochondria and capable of promoting mitochondrial apoptosis, based on the retention of mitochondrial pRB activity in p16 knockdown MEFs. However, we have yet to understand whether phosphorylation by cdk (or other kinases) is simply permissive for, or actively enables, pRB's mitochondrial apoptosis role. We also note that it has been previously reported that TNF $\alpha$  treatment induces cleavage of pRB at the C-terminus releasing a 5kDa fragment (Huang et al., 2007; Tan et al., 1997). We were intrigued by the possibility that this cleavage might be responsible for the activation of mitochondrial pRB function by TNF $\alpha$ , presumably by exposing/activating the required small pocket domain. However, our exploratory analyses of both pre-cleaved (i.e. delta 5kDa) and uncleavable forms of pRB in stable inducible cell

lines were inconsistent with the notion that cleavage is necessary and sufficient for pRB activation (data not shown). Thus, it remains an open question how pro-apoptotic signals including TNF $\alpha$  trigger the mitochondrial pRB response.

Regardless of the remaining mechanistic questions, our findings considerably expand our appreciation of pRB's role in apoptosis. It is already clear that pRB can either suppress apoptosis by enforcing cell cycle arrest, or promote DNA damage-induced apoptosis by transcriptionally co-activating pro-apoptotic genes (Ianari et al., 2009). Here, we show that in addition to these transcriptional mechanisms, pRB can also promote apoptosis directly at mitochondria. We believe that pRB's overall pro-apoptotic function is likely a result of the combined effect of nuclear and mitochondrial pRB. The relative extent to which these two functions contribute to apoptosis is likely context specific. However, our mito-tagged pRB experiments clearly showed that the mitochondrial function of pRB can contribute to apoptosis in response to a broad range of stimuli, including the oncogenic context of tumor cells. Most importantly, our *in vivo* xenograft studies establish the tumor suppressive potential of mitochondrial pRB in the absence of classic, nuclear pRB functions. Given these observations, we conclude that mitochondrial apoptosis represents a novel, and bona fide, mechanism of tumor suppression for pRB. This adds to a growing list of ways in which pRB has the potential to be tumor suppressive, including its classic cell cycle function (Burkhart and Sage, 2008), transcriptional co-regulation of apoptosis, autophagy, and metabolic genes (Blanchet et al., 2011; Ciavarra and Zacksenhaus, 2011; Takahashi et al., 2012; Tracy et al., 2007; Viatour and Sage, 2011), and its ability to control fate commitment by modulating the transcriptional activity of core differentiation regulators

(Calo et al., 2010; Viatour and Sage, 2011). The extent to which each of these mechanisms of pRB action contributes to overall tumor suppression remains to be fully elucidated. The ability to localize pRB specifically to the mitochondria allowed us to study pRB's mitochondrial role in the absence of all other known pRB functions. Remarkably, at least in this context, this mito-specific pRB was as efficient, if not more efficient, than wildtype pRB at suppressing tumorigenesis. This unequivocally establishes the potential potency of pRB's mitochondrial apoptosis function. However, it does not disavow the potential contribution of other pRB functions. It remains an open question whether the myriad roles of pRB collaborate consistently in tumor suppression or whether, in specific contexts, one or more functions have more physiological relevance than others. It is also interesting to note that the multiple functions of pRB are highly reminiscent of those of the p53 tumor suppressor. p53 was also initially linked to cell cycle arrest and then shown to play a central role in promoting apoptosis both through the transcriptional activation of pro-apoptotic genes and by directly inducing MOMP at the mitochondria in a transcription-independent manner (Chipuk et al., 2004; Leu et al., 2004; Mihara et al., 2003; Speidel, 2010; Vousden and Prives, 2009). Our data now suggest that the direct promotion of mitochondrial apoptosis is a general mechanism of tumor suppression.

Finally, we believe that our findings have significant implications for therapeutic treatment in the approximately two-thirds of human tumors that retain wildtype pRB but instead carry mutations that promote cdk/cyclin activation and pRB phosphorylation (Sherr and McCormick, 2002). Historically, little attention has been paid to *RB-1* status in chemotherapeutic response because the absence of pRB or the presence of phospho-pRB similarly inactivates pRB-mediated G1 arrest. However, we have previously found that

phospho-pRB can activate transcription of pro-apoptotic genes (Ianari et al., 2009). In this current study, we show that the endogenous mitochondrial pRB includes the cdk-phosphorylated form, and it retains its pro-apoptotic role in highly proliferative tumor cells and after inactivation of the cdk inhibitor p16. Moreover, both the transcriptional and the mitochondrial, pro-apoptotic functions of pRB occur independent of p53. Thus, we believe that it should be possible to develop chemotherapeutic strategies for the majority of human tumors that retain wildtype *RB-1*, which engage phospho-pRB and promote apoptosis through both transcriptional and mitochondrial mechanisms.

## Materials and Methods

### Cell Culture and Drug Treatment

RAT16 and IMR90 cells were grown in MEM with Earle's Salts and 10% FBS, Pen-Strep, L-Glutamine, Sodium Pyruvate, and NEAA. All other cell lines were grown in DMEM with 10% FBS and Pen-Strep. For TNF $\alpha$  treatments, 50ng/ml of recombinant mouse TNF $\alpha$  (Sigma) was used with 0.1 $\mu$ M MG132 (Calbiochem) for 48 hours or 0.5 $\mu$ g/ml CHX (Sigma) for 24 hours unless noted otherwise. MEFs were treated with TNF $\alpha$ /CHX for 10 hours, 1 $\mu$ M staurosporine (Sigma) for 6 hours, or 25 $\mu$ M etoposide (Sigma) for 12 hours. TET System approved FBS (Clontech) and 1 $\mu$ g/ml doxycycline (Clontech) were used for inducible cell lines unless noted otherwise. Overexpression was induced for 24 hours prior to TNF $\alpha$  treatment. 20 $\mu$ g/ml and 15 $\mu$ g/ml doxycycline were used in wildtype, *Bax*<sup>-/-</sup>, and *Bak*<sup>-/-</sup> MEFs to induce expression of pRB and mitoRB $\Delta$ NLS, respectively. 5 $\mu$ g/ml doxycycline was used in *Bax*<sup>-/-</sup>;*Bak*<sup>-/-</sup> MEFs to adjust for expression levels.

### FACS Apoptosis Analysis

Cell suspensions were stained with AnnexinV-FITC or APC (Becton Dickinson) and Propidium Iodide (Sigma) or 7AAD (Becton Dickinson). Total apoptotic cells were assessed by gating for AnnexinV positive using a FACScan or FACSCalibur System (Becton Dickinson). Similar trends were observed for all experiments when only early apoptotic (AnnexinV+;PI/7AAD-) cells were considered (data not shown). For cell cycle profiling, cell

suspensions were processed as previously described (Ianari et al., 2009) and analyzed by FACScan and FlowJo.

## **Plasmid and Stable Cell Line Generation**

Human pRB knockdown was performed as described previously (Chicas et al., 2010) and the rodent *Rb* target sequence was TATAATGGAATCAAACCTCCTC, Luc control GAGCTCCCGTGAATTGGAATCC. 10 $\mu$ M siRNAs (IDT, murine p16) were transfected into MEFs using RNAiMax (Invitrogen) according to manufacturer recommendations. The lentiviral vector pCW22 (tet-on) was used for expression studies. Since RAT16 cells already contained tTA (tet-off), the rtTA was removed by *AgeI* and *XmaI* digestion. mitoRB $\Delta$ NLS was generated by amplifying the mitochondrial leader peptide of ornithine transcarbamylase (caaaagcgctatgctgtttaatctgagga, ggaaggcgctgcactttattttgtag) and human RB (ctatggcgcccaaaaccccc, gattttaattaatcatttctcttctgt). The NLS was mutated using gcaaaactaagcttgatattgaagg, tatcaaagcttagtttgccagtgg, followed by HindIII digestion. mitoREL was generated by amplifying the mitochondrial leader peptide of ornithine transcarbamylase (caaagttaacatgctgtttaatctgagga, gtttccggaggcctgcactttattttgtag) and human REL (tggcctccggagcgtataaccc, caaattaattaacttataacttgaaaaattcatatg). pCW22 3HA was generated using 3HA peptide (IDT) and ligated to RB\_N (caaagtcgacatgccgccccaaac, gattttaattaatcagtgtggaggaattacattcacct), RB\_SP (caaagtcgacactccagtttagga, gattttaattaatcatgttttcagtctctgcatg), and RB\_C (caaagtcgacaatattttgcagtatgc, gattttaattaatcatttcttcttctgt). Cells infected with the inducible construct underwent

blastocidin (Invitrogen) selection. All RAT16 variants were independently generated three times and all MEF variants were independently generated twice.

### **Mitochondrial Fractionations**

IMR90 mitochondria were fractionated as follows: cells were resuspended in cold Buffer A [250mM Sucrose, 20mM Hepes pH 7.5, 10mM KCl, 1.5mM MgCl<sub>2</sub>, 1mM EDTA, 1mM EGTA, 1mM DTT, protease inhibitors (Roche)] and homogenized using 20 strokes in a ¼” cylinder cell homogenizer (H&Y Enterprises, Redwood City, CA), 0.1558” ball. Nuclei and unlysed cells were removed by low-speed centrifugation and mitochondria and 10% of initial cell suspension (for Total Lysate) were lysed using RIPA buffer (0.5% Sodium Deoxycholate, 50mM Tris HCl pH 7.6, 1% NP40, 0.1% SDS, 140mM NaCl, 5mM EDTA, 100mM NaF, 2mM NaPP<sub>i</sub>, protease inhibitors) and quantified using BCA Protein Assay reagent (Pierce).

Mitochondria were isolated from livers of 2-6 month old mice maintained on a mixed C57Bl/6 x129sv background as follows: Livers were minced in Buffer A (0.3M Mannitol, 10mM HEPES/K pH 7.4, 0.1% BSA, 0.2mM EDTA/Na pH 8.0) and homogenized using 3 strokes in a Teflon Dounce Homogenizer. A small fraction was removed for total lysate. Nuclei and unlysed cells were removed from the remaining supernatant by low-speed centrifugation and mitochondria were washed in Buffer B (0.3M Mannitol, 10mM HEPES/K pH 7.4, 0.1% BSA). For whole mitochondria analysis, mitochondria and total lysate were

lysed in RIPA buffer. For subfractionation, the mitochondrial pellet was resuspended at 2mg/ml in Hypotonic Buffer (10mM KCl, 2mM HEPES/K pH7.9), incubated on ice for 20 minutes and centrifuged at 14000rpm. The pellet was washed twice with Wash Buffer (150mM KCl, 2mM HEPES/K pH7.9) and all three supernatants combined yielded the non-mitoplast fraction. The mitoplast was resuspended in Hypotonic/Wash Buffer and equal fractions were analyzed by SDS-PAGE and western blotting. Mitochondria were isolated from livers of *Alb-cre<sup>pos</sup>;Bax<sup>f/-</sup>;Bak<sup>-/-</sup>* mice as reported previously (Walensky et al., 2006).

### ***In Vitro* Cytochrome C Release Assay**

The assay was performed as previously described (Chipuk et al., 2005). Briefly, wildtype mitochondria were resuspended in Mitochondrial Isolation Buffer (200mM Mannitol, 68mM Sucrose, 10mM HEPES/K pH 7.4, 100mM KCl, 1mM EDTA, 1mM EGTA, 0.1%BSA) to a concentration of 1µg/µl and incubated with pRB (Sigma), GST-Bax (Sigma), or cl. BID (R&D Systems) for 1 hour, 37°C. DKO mitochondria were resuspended in experimental buffer (125mM KCl, 10mM Tris-MOPS [pH 7.4], 5mM glutamate, 2.5mM malate, 1mM KPO<sub>4</sub>, 10µM EGTA-Tris [pH 7.4]) to a concentration of 1.5 mg/ml, and incubated with monomeric BAX (purified as previously described (Gavathiotis et al., 2008)) and pRB (ProteinOne) for 45 min, room temperature. Samples were centrifuged at 5500g and pellets versus supernatants were analyzed by SDS-PAGE and immunoblotting.

### **Liposomal Release Assay**

The liposomal release assay was performed as described previously (LaBelle et al., 2012; Lovell et al., 2008). Briefly, large unilamellar vesicles (LUVs) were generated from a lipid

mixture of 48% phosphatidylcholine, 28% phosphatidylethanolamine, 10% phosphatidylinositol, 10% dioleoyl phosphatidylserine and 4% tetraoleoyl cardiolipin as chloroform stocks (Avanti Polar Lipids). The lipid mixture was dried in glass test tubes under nitrogen gas and then under vacuum for 15 h. The fluorescent dye ANTS (6.3 mg) and the quencher DPX (19.1 mg) were added to 1 mg of dry lipid film, and the mixture resuspended in assay buffer (200mM KCl, 1mM MgCl<sub>2</sub>, 10mM HEPES, pH 7.0). After five freeze-thaw cycles, the lipid mixtures were extruded through a 100 nm nucleopore polycarbonate membrane (Whatman) using a mini extruder (Avanti). Liposomes were isolated by gravity flow SEC using a crosslinked Sepharose CL-2B column (Sigma Aldrich). LUVs (5  $\mu$ l) were treated with the indicated concentrations of BAX and pRB in 384-well format (Corning) in a total reaction volume of 30  $\mu$ l. After time-course fluorescence measurement on a Tecan Infinite M1000 spectrophotometer (excitation 355 nm, emission 520 nm), Triton X-100 was added to a final concentration of 0.2% (v/v) to determine maximal release.

### **Immunoprecipitation**

For the *in vitro* binding assay, recombinant, monomeric BAX (1  $\mu$ M) and pRB (1  $\mu$ M) were mixed in 10 $\mu$ l TBS (50 mM Tris, 150 mM NaCl) and pre-incubated for 30 minutes, room temperature. The samples were diluted with 1% BSA in TBS to 80 $\mu$ l, and incubated with pre-equilibrated Protein A/G-agarose beads (Santa Cruz) and 5 $\mu$ l 6A7 antibody (sc-23959, Santa Cruz) with rotation for 1 h, room temperature. Beads were collected and washed three times with 0.5 ml 1% (w/v) BSA/TBS buffer.

For the endogenous interaction study, IMR90 cells were treated with 50ng/ml TNF $\alpha$  and 0.5 $\mu$ g/ml CHX for 3 hours total and crosslinked with 1mg/ml DSP (Pierce) for 1 hour. Proteins were extracted using an NP40 based buffer (50mM HEPES pH7.9, 10% glycerol, 150mM NaCl, 1%NP40, 1mM NaF, 10mM B-Glycerophosphate, protease inhibitors). The following antibodies were used: pRB (Cell Signaling, 9309), normal rabbit IgG (Santa Cruz).

### **Western Blotting**

Samples were loaded in SDS Lysis Buffer (8% SDS, 250mM TrisHCl pH 6.6, 40 % glycerol, 5% 2-Mercaptoethanol, bromophenol blue), separated by SDS-PAGE, transferred to a nitrocellulose membrane, and blocked in 5% nonfat milk. The following antibodies were used in 2.5% nonfat milk: human pRB (Cell Signaling, 9309), rodent pRB (Becton Dickinson, 554136), phospho-pRB (Cell Signaling, 2181,9301,9307,9308), procaspase 7 (Cell Signaling, 9492), cleaved caspase 7 (Cell Signaling, 9491), procaspase 3 (Cell Signaling, 9662), cleaved caspase 3 (Cell Signaling, 9661), actin (Santa Cruz, SC1616 HRP), tubulin (Sigma, T9026), BAX (Cell Signaling, 2772; Santa Cruz, sc-493), BAK (Cell Signaling, 3814), cyclin A (Santa Cruz, sc594), HDAC1 (Upstate, 05-614), PCNA (Abcam, ab29), Lamin A/C (Cell Signaling, 2032), COXIV (Cell Signaling, 4850), Histone H3 (Santa Cruz, sc8654), ATPB (Abcam, ab5432), SirT3 (Cell Signaling, 5490), cytochrome c (Becton Dickinson, 556433), p16 (Santa Cruz, sc74401), HA.11 (Covance) and GAPDH (Ambion, 4300). Secondary HRP-conjugated antibodies (Santa Cruz) were used at 1:5000 in 1% nonfat milk.

### **RealTime PCR**

RNA was isolated using RNaseasy Kit (Qiagen) and reverse transcribed using Superscript III reverse transcriptase (Invitrogen). RealTime PCR reactions were performed with SYBR Green (Applied Biosystems) on the ABI Prism 7000 Sequence Detection System and analyzed using the 7000 SDS software. The following primers were used:

Cdc2 (CTGGCCAGTTCATGGATTCT, ATCAAACCTGGCAGATTTTCGG),  
Cyclin A2 (GAGAATGTCAACCCCGAAAA, ATAAACGATGAGCACGTCCC),  
Mcm3 (GTACGAGGAGTTCTACATAG, TCTTCTTAGTAGCAGGACAG),  
Mcm5 (GAGGACCAGGAGATGCTGAG, CTTTACCGCCTCAAGTGAGC),  
Mcm6 (CACGATTTGGAGGGAAAGAA, TCCACGGCAATGATGAAGTA),  
PCNA (TCCCAGACAAGCAATGTTGA, TTATTTGGCTCCCAAGATCG),  
UB (TTCGTGAAGACCCTGACC, ACTCTTTCTGGATGTTGTAGTC),  
Casp3 (ACTGCGGTATTGAGACAGAC, CGCAAAGTGACTGGATGAAC),  
Casp7 (GCTCCACCATCATCTCATCC, TGCCCATCTTCTCGAAGTCC),  
Bcl2 (AGTACCTGAACCGGCATCTG, AGGTCTGCTGACCTCACTTG),  
Apaf1 (CATGCCCTCCTAGAAGGTTG, GAACACGGAGACGGTCTTTG),  
Casp9 (GTAGTGAAGCTGGACCCATC, TTCCCTGGAGTACAGACATC),  
MAP3K5 (CGTTGGCCGAATCTACAAAG, ACTGTAGTGTTGGCTCAGAC),  
p21 (TGGCCTTGTCGCTGTCTTGC, AGACCAATCGGCGCTTGGAG),  
Casp1 (CTAAGGGAGGACATCCTTTC, CAGATAATGAGGGCAAGACG),  
Casp4 (AAGAGGAGCTTACGGCTGAG, CCTGCAATGTGCCATGAGAC),  
Beclin (TAGCTGAAGACCGGGCGATG, TGCTGCTGGACGCCTTAGAC),  
Flip (ATAAAGCAGCGGTGGAGGAC, TTGCCTCGGCCTGTGTAATC)

**Xenograft Model:** All animal procedures followed protocols approved by MIT's Committee on Animal Care. Nude/SCID mice (Taconic) were injected subcutaneously with  $10^7$  tumor cells per site, 2 sites per mouse. After euthanasia, tumors were removed, fixed overnight in formalin followed by overnight incubation in 70% ethanol, and subjected to histological processing.

### **Immunofluorescence and Immunohistochemistry**

Cells were plated at low density on coverslips and protein expression was induced for 48 hours. Mitochondria were labeled using MitoTracker Deep Red (Invitrogen) at 100nM for 45 minutes, 37°C. Cells were fixed in 4% Formaldehyde (Thermo Scientific), permeabilized with 0.25% TritonX-100/PBS, and blocked with 5% Goat Serum in 0.2% Tween20/PBS for 30 minutes, 37°C. The following antibodies were used at 1:200 for 1 hour, room temperature: pRB (Cell Signaling, 9309), c-REL (Cell Signaling, 4727). Alexa Fluor 488 (Invitrogen) was used at 1:1000 for 1 hour, room temperature and slides were mounted using SlowFade Gold Antifade Reagent with DAPI (Invitrogen) and observed under a fluorescence microscope (Zeiss).

Ki67 and cleaved caspase 3 immunohistochemistry was performed with a modified citric acid unmasking protocol. Briefly, paraffin was removed from slides, followed by incubation in 0.5%  $H_2O_2$ /methanol for 15 minutes and antigen retrieval using citrate buffer, pH 6.0 in a microwave for 15 minutes. Slides were blocked for 1 hour at room temperature in 2% normal horse serum (Ki67) or 10% goat serum (cc3) in PBS. Ki67 (Becton Dickinson, 550609, 1:50) and cleaved caspase 3 (Cell Signaling, 9661, 1:200) antibodies were used in 0.15% Triton/PBS overnight at 4°C. Secondary antibodies (Vector Laboratories) were used

at 1:200 in PBS with 0.4% normal horse serum (Ki67) or 2% goat serum (cc3), detected using a DAB Substrate Kit (Vector Laboratories), and counterstained with haematoxylin.

## Acknowledgments

We thank E. Knudsen for providing the RAT16 parental and LP-RB inducible cell lines, A. Letai for wildtype and *Bax*<sup>-/-</sup>/*Bak*<sup>-/-</sup> MEFs, S. Lowe for human *Rb* shRNA, and M. Hemann for rodent *Rb* shRNA. We also thank the members of the Lees laboratory for input during the study and manuscript preparation. This work was supported by an NCI/NIH grant to J.A.L. who is a Ludwig Scholar at MIT. K.I.H. was supported by an NSF pre-doctoral fellowship and D.H. Koch Graduate Fellowship.

## References

Araki, K., Ahmad, S.M., Li, G., Bray, D.A., Jr., Saito, K., Wang, D., Wirtz, U., Sreedharan, S., O'Malley, B.W., Jr., and Li, D. (2008). Retinoblastoma RB94 enhances radiation treatment of head and neck squamous cell carcinoma. *Clin Cancer Res* 14, 3514-3519.

Blanchet, E., Annicotte, J.-S.b., Lagarrigue, S., Aguilar, V., Clapé, C., Chavey, C., Fritz, V., Casas, F.o., Apparailly, F., Auwerx, J., *et al.* (2011). E2F transcription factor-1 regulates oxidative metabolism. *Nature cell biology* 13, 1146-1152.

Bosco, E.E., Mayhew, C.N., Hennigan, R.F., Sage, J., Jacks, T., and Knudsen, E.S. (2004). RB signaling prevents replication-dependent DNA double-strand breaks following genotoxic insult. *Nucleic Acids Res* 32, 25-34.

Brunelle, J., and Letai, A. (2009). Control of mitochondrial apoptosis by the Bcl-2 family. *Journal of cell science* 122, 437-478.

Burkhardt, D.L., and Sage, J. (2008). Cellular mechanisms of tumour suppression by the retinoblastoma gene. *Nat Rev Cancer* 8, 671-682.

Calo, E., Quintero-Estades, J.A., Danielian, P.S., Nedelcu, S., Berman, S.D., and Lees, J.A. (2010). Rb regulates fate choice and lineage commitment in vivo. *Nature* 466, 1110-1114.

Carnevale, J., Palander, O., Seifried, L.A., and Dick, F.A. (2012). DNA damage signals through differentially modified E2F1 molecules to induce apoptosis. *Mol Cell Biol* 32, 900-912.

Chicas, A., Wang, X., Zhang, C., McCurrach, M., Zhao, Z., Mert, O., Dickins, R., Narita, M., Zhang, M., and Lowe, S. (2010). Dissecting the unique role of the retinoblastoma tumor suppressor during cellular senescence. *Cancer Cell* 17, 376-463.

Chipuk, J., Bouchier-Hayes, L., Kuwana, T., Newmeyer, D., and Green, D. (2005). PUMA couples the nuclear and cytoplasmic proapoptotic function of p53. *Science (New York, NY)* 309, 1732-1737.

Chipuk, J., Kuwana, T., Bouchier-Hayes, L., Droin, N., Newmeyer, D., Schuler, M., and Green, D. (2004). Direct activation of Bax by p53 mediates mitochondrial membrane permeabilization and apoptosis. *Science (New York, NY)* *303*, 1010-1014.

Chipuk, J., Moldoveanu, T., Llambi, F., Parsons, M., and Green, D. (2010). The BCL-2 family reunion. *Molecular cell* *37*, 299-609.

Ciavarra, G., and Zacksenhaus, E. (2011). Direct and indirect effects of the pRb tumor suppressor on autophagy. *Autophagy* *7*, 544-546.

de Bruin, A., Wu, L., Saavedra, H.I., Wilson, P., Yang, Y., Rosol, T.J., Weinstein, M., Robinson, M.L., and Leone, G. (2003). Rb function in extraembryonic lineages suppresses apoptosis in the CNS of Rb-deficient mice. *Proc Natl Acad Sci U S A* *100*, 6546-6551.

Eskes, R., Desagher, S., Antonsson, B., and Martinou, J.C. (2000). Bid induces the oligomerization and insertion of Bax into the outer mitochondrial membrane. *Mol Cell Biol* *20*, 929-935.

Ferecatu, I., Le Floch, N., Bergeaud, M., Rodriguez-Enfedaque, A., Rincheval, V., Oliver, L., Vallette, F.M., Mignotte, B., and Vayssiere, J.L. (2009). Evidence for a mitochondrial localization of the retinoblastoma protein. *BMC Cell Biol* *10*, 50.

Fulcher, A., Dias, M., and Jans, D. (2010). Binding of p110 retinoblastoma protein inhibits nuclear import of simian virus SV40 large tumor antigen. *The Journal of biological chemistry* *285*, 17744-17797.

Gavathiotis, E., Reyna, D.E., Davis, M.L., Bird, G.H., and Walensky, L.D. (2010). BH3-triggered structural reorganization drives the activation of proapoptotic BAX. *Mol Cell* *40*, 481-492.

Gavathiotis, E., Suzuki, M., Davis, M.L., Pitter, K., Bird, G.H., Katz, S.G., Tu, H.C., Kim, H., Cheng, E.H., Tjandra, N., *et al.* (2008). BAX activation is initiated at a novel interaction site. *Nature* *455*, 1076-1081.

Gordon, G., and Du, W. (2011). Conserved RB functions in development and tumor suppression. *Protein & cell* *2*, 864-942.

Hsu, Y.T., and Youle, R.J. (1997). Nonionic detergents induce dimerization among members of the Bcl-2 family. *J Biol Chem* *272*, 13829-13834.

Huang, X., Masselli, A., Frisch, S.M., Hunton, I.C., Jiang, Y., and Wang, J.Y. (2007). Blockade of tumor necrosis factor-induced Bid cleavage by caspase-resistant Rb. *J Biol Chem* 282, 29401-29413.

Ianari, A., Natale, T., Calo, E., Ferretti, E., Alesse, E., Screpanti, I., Haigis, K., Gulino, A., and Lees, J.A. (2009). Proapoptotic function of the retinoblastoma tumor suppressor protein. *Cancer Cell* 15, 184-194.

Jacks, T., Fazeli, A., Schmitt, E.M., Bronson, R.T., Goodell, M.A., and Weinberg, R.A. (1992). Effects of an Rb mutation in the mouse. *Nature* 359, 295-300.

Jiao, W., Datta, J., Lin, H.-M., Dundr, M., and Rane, S. (2006). Nucleocytoplasmic shuttling of the retinoblastoma tumor suppressor protein via Cdk phosphorylation-dependent nuclear export. *The Journal of biological chemistry* 281, 38098-38206.

Jiao, W., Lin, H.M., Datta, J., Braunschweig, T., Chung, J.Y., Hewitt, S., and Rane, S. (2008). Aberrant nucleocytoplasmic localization of the retinoblastoma tumor suppressor protein in human cancer correlates with moderate/poor tumor differentiation. *Oncogene* 27, 3156-3220.

Jin, Z., and El-Deiry, W.S. (2005). Overview of cell death signaling pathways. *Cancer Biol Ther* 4, 139-163.

Karin, M., and Lin, A. (2002). NF-kappaB at the crossroads of life and death. *Nat Immunol* 3, 221-227.

Knudsen, E., and Knudsen, K. (2008). Tailoring to RB: tumour suppressor status and therapeutic response. *Nature reviews Cancer* 8, 714-738.

Knudsen, K.E., Booth, D., Naderi, S., Sever-Chroneos, Z., Fribourg, A.F., Hunton, I.C., Feramisco, J.R., Wang, J.Y., and Knudsen, E.S. (2000). RB-dependent S-phase response to DNA damage. *Mol Cell Biol* 20, 7751-7763.

Knudsen, K.E., Weber, E., Arden, K.C., Cavenee, W.K., Feramisco, J.R., and Knudsen, E.S. (1999). The retinoblastoma tumor suppressor inhibits cellular proliferation through two distinct mechanisms: inhibition of cell cycle progression and induction of cell death. *Oncogene* 18, 5239-5245.

LaBelle, J.L., Katz, S.G., Bird, G.H., Gavathiotis, E., Stewart, M.L., Lawrence, C., Fisher, J.K., Godes, M., Pitter, K., Kung, A.L., *et al.* (2012). A stapled BIM peptide overcomes apoptotic resistance in hematologic cancers. *J Clin Invest* 122, 2018-2031.

Leu, J., Dumont, P., Hafey, M., Murphy, M., and George, D. (2004). Mitochondrial p53 activates Bak and causes disruption of a Bak-Mcl1 complex. *Nature cell biology* 6, 443-493.

Lovell, J.F., Billen, L.P., Bindner, S., Shamas-Din, A., Fradin, C., Leber, B., and Andrews, D.W. (2008). Membrane binding by tBid initiates an ordered series of events culminating in membrane permeabilization by Bax. *Cell* 135, 1074-1084.

Manning, A., and Dyson, N. (2012). RB: mitotic implications of a tumour suppressor. *Nature reviews Cancer* 12, 220-226.

Marchenko, N., Zaika, A., and Moll, U. (2000). Death signal-induced localization of p53 protein to mitochondria. A potential role in apoptotic signaling. *The Journal of biological chemistry* 275, 16202-16214.

Martinou, J.-C., and Youle, R. (2011). Mitochondria in apoptosis: Bcl-2 family members and mitochondrial dynamics. *Developmental cell* 21, 92-193.

Masselli, A., and Wang, J.Y. (2006). Phosphorylation site mutated RB exerts contrasting effects on apoptotic response to different stimuli. *Oncogene* 25, 1290-1298.

Mihara, M., Erster, S., Zaika, A., Petrenko, O., Chittenden, T., Pancoska, P., and Moll, U.M. (2003). p53 has a direct apoptogenic role at the mitochondria. *Mol Cell* 11, 577-590.

Milet, C., Rincheval-Arnold, A., Mignotte, B., and Guenal, I. (2010). The Drosophila retinoblastoma protein induces apoptosis in proliferating but not in post-mitotic cells. *Cell Cycle* 9, 97-103.

Mittnacht, S., and Weinberg, R.A. (1991). G1/S phosphorylation of the retinoblastoma protein is associated with an altered affinity for the nuclear compartment. *Cell* 65, 381-393.

Perez, D., and White, E. (2000). TNF-alpha signals apoptosis through a bid-dependent conformational change in Bax that is inhibited by E1B 19K. *Mol Cell* 6, 53-63.

Roth, D., Harper, I., Pouton, C., and Jans, D. (2009). Modulation of nucleocytoplasmic trafficking by retention in cytoplasm or nucleus. *Journal of cellular biochemistry* 107, 1160-1167.

Sherr, C.J., and McCormick, F. (2002). The RB and p53 pathways in cancer. *Cancer Cell* 2, 103-112.

Speidel, D. (2010). Transcription-independent p53 apoptosis: an alternative route to death. *Trends in cell biology* 20, 14-38.

Takahashi, C., Sasaki, N., and Kitajima, S. (2012). Twists in views on RB functions in cellular signaling, metabolism and stem cells. *Cancer science*.

Tan, X., Martin, S.J., Green, D.R., and Wang, J.Y. (1997). Degradation of retinoblastoma protein in tumor necrosis factor- and CD95-induced cell death. *J Biol Chem* 272, 9613-9616.

Templeton, D.J. (1992). Nuclear binding of purified retinoblastoma gene product is determined by cell cycle-regulated phosphorylation. *Mol Cell Biol* 12, 435-443.

Tracy, K., Dibling, B.C., Spike, B.T., Knabb, J.R., Schumacker, P., and Macleod, K.F. (2007). BNIP3 is an RB/E2F target gene required for hypoxia-induced autophagy. *Mol Cell Biol* 27, 6229-6242.

Traenckner, E.B., Wilk, S., and Baeuerle, P.A. (1994). A proteasome inhibitor prevents activation of NF-kappa B and stabilizes a newly phosphorylated form of I kappa B-alpha that is still bound to NF-kappa B. *EMBO J* 13, 5433-5441.

van den Heuvel, S., and Dyson, N.J. (2008). Conserved functions of the pRB and E2F families. *Nat Rev Mol Cell Biol* 9, 713-724.

Viatour, P., and Sage, J. (2011). Newly identified aspects of tumor suppression by RB. *Disease models & mechanisms* 4, 581-586.

Vousden, K., and Prives, C. (2009). Blinded by the Light: The Growing Complexity of p53. *Cell* 137, 413-444.

Walensky, L.D., and Gavathiotis, E. (2011). BAX unleashed: the biochemical transformation of an inactive cytosolic monomer into a toxic mitochondrial pore. *Trends Biochem Sci* 36, 642-652.

Walensky, L.D., Pitter, K., Morash, J., Oh, K.J., Barbuto, S., Fisher, J., Smith, E., Verdine, G.L., and Korsmeyer, S.J. (2006). A stapled BID BH3 helix directly binds and activates BAX. *Mol Cell* 24, 199-210.

Wenzel, P.L., Wu, L., de Bruin, A., Chong, J.L., Chen, W.Y., Dureska, G., Sites, E., Pan, T., Sharma, A., Huang, K., *et al.* (2007). Rb is critical in a mammalian tissue stem cell population. *Genes Dev* 21, 85-97.

Wu, L., de Bruin, A., Saavedra, H.I., Starovic, M., Trimboli, A., Yang, Y., Opavska, J., Wilson, P., Thompson, J.C., Ostrowski, M.C., *et al.* (2003). Extra-embryonic function of Rb is essential for embryonic development and viability. *Nature* 421, 942-947.

Wyllie, A. (2010). "Where, O death, is thy sting?" A brief review of apoptosis biology. *Molecular neurobiology* 42, 4-13.